Study of Glucose Transporters in *C. elegans*

Ying Feng

A thesis submitted for the degree of Doctor of Philosophy

University of Bath

Department of Biology and Biochemistry

October 2010

Abstract

The calorie restriction (CR) and insulin/IGF-I-like signalling (IIS) are two pathways regulating the lifespan of *C. elegans*. Recent studies showed that glucose restriction extends the lifespan of *C. elegans* while excessive glucose shortens the lifespan of the worms. The first step of the glucose metabolism is the transport of glucose across the plasma membrane by the glucose transporters.

The work described in this thesis aims to identify glucose transporters in *C. elegans* and to provide a primary investigation of the in vitro and in vivo function of the identified glucose transporter.

Nine putative transporters have been cloned and expressed. Out of the nice cloned putative transporters in the *C. elegans* genome, H17B01.1 (H17) only is identified as a fully functional glucose transporter using an oocyte expression system in which glucose transport activity is directly measured. The two transcripts of H17 are both capable of transporting glucose with high affinity, as well as transporting trehalose. Heterologous expression of H17 in mammalian CHO-T cells suggests that the protein is localised both on the plasma membrane and in the cytosol. In vitro studies of H17 show that the protein does not respond to insulin stimulation when expressed in mammalian CHO-T cell and rat primary adipocyte systems.

In vivo functional studies using H17 RNAi indicate that the worm's lifespan is not affected by the H17 knockdown. However, glucose metabolism of *C. elegans* (as measured by glucose oxidation to CO2 and incorporation into fat reserves) is influenced by the decreased expression of H17, especially in the *daf-2* mutant strain, *e1370*. However, the increase of glucose metabolism caused by H17 knockdown observed in *daf-2* mutant is inhibited in the *age-1* and *akt-1* mutant strains.

The findings reported in this thesis suggest that the H17 glucose transporter may play an important role glucose metabolism in *C. elegans* and that this transport and metabolism is influenced by insulin receptor activity and serine kinase cascades.

Acknowledgements

I would like to express my deepest respect and gratitude to my supervisor Professor Geoffrey D. Holman (University of Bath) for his constant and selfless help, encouragement, patience and suggestions through out my research. This thesis would not have been possible without his great guidance. It has been my greatest pleasure and honour to be his student and work with him.

I would like to thank my second supervisor Dr. Adrian Wolstenholme (current in University of Georgia) for his kind guidance and help during the whole research. I would also like to thank my former internal examiner Dr. Barbara J. Reaves (current in University of Georgia) for her kind guidance and encouragement during my study. I wish to thank Dr. Andrew Chalmers, Dr Paul Whitley and Professor Keith Charnley for their great help during my research.

I wish to thank all the staffs and students (Francoise, Jing, Judith, Susan, Daniel, Sam, Sally et al) I have worked with in Lab 1.37 and Lab 0.47 for their selfless help and for sharing their knowledge and research experience with me. It is a great pleasure to work in this environment.

I owe my deepest gratitude to my parents for their firmest support. Without their love and encouragement throughout my study, I would never be able to finish this programme.

I wish to thank the Department of Biology and Biochemistry in the University of Bath for providing me the opportunity to study in a great research environment. I would also like to thank all the staff in the department for their help.

Table of content

Abbreviations

aa	Amino acid
AEBSF	[4-(2-aminoethyl)benzenesulfonylflouride, HCl]
AMP	AMP-Activated Protein
AMPK	AMP-Activated Protein Kinase
Approx.	Approximately
APS	Ammonium Persulphate
AraE	L–Arabinose/H^+ symporter
ATP	Adenosine-5'-triphosphate
BCA	Bicinchoninic Acid
Bp	Base pair
BSA	Bovine Serum Albumin
C35	C35A11.4
cDNA	Complementary DNA
C. elegans	*Caenorhabditis Elegans*
CGC	Caenorhabditis Genetics Center
CHO	Chinese Hamster Ovary
cm	Centimetre
CR	Calorie Restriction
cRNA	Complementary RNA
ddH_2O	Double Distilled H_2O
DEPC	Diethyl Pyrocarbonate
dH_2O	Distilled H_2O
DILP	*Drosophila* Insulin-Like Peptide
dINR	*Drosophila* Insulin Receptor
DMEM	Dulbecco's Modified Eagle's Medium
DMSO	Dimethylsulfoxide
DNA	Deoxyribonucleic Acid
DOG	2-Deoxy-D-Glucose
dsRNA	Double Stranded RNA
DTT	Dithiothreitol
E. coli	*Escherichia Coli*
EDTA	Ethylenediaminetetraacetic acid
EGFP	Enhanced Green Fluorescent Protein

F14	F14E5.1
F48	F48E5.2
FBS	Fetal Bovine Serum
FDG	Fluorescein di-β-D- galactopyranoside
FIRKO	Fat-specific Insulin Receptor Knockout
FMG	Fluorescein monogalactoside
FOXA	Forkhead Box A
FOXO	Forkhead Box O
FUDR	5-Fluoro-2'- Deoxyuridine
G	Gauge
G	Gram
G	Gravity
GAP	GTPase Activating Protein
GalP	D–Galactose/H^+ Symporter
GFP	Green Fluorescent Protein
GH	Growth Hormone
GlpT	Glycerol-3-phosphate transporter
GLUT	Facilitative glucose transporter
GO	Glucose Oxidase
GSK3β	Glycogen synthase kinase 3β
H	Hour
H17	H17B01.1
H17a	H17B01.1a
H17b	H17B01.1b
HA	Hemagglutinin
HEPES	4-(2-hydroxyethyl)-1-piperazineethanesulfonic acid
HMIT	H^+-Coupled *Myo-Inositol* Transporter
HPLC	High-performance liquid chromatography
HXT	Hexose transporter
IgG	Immunoglobulin G
IGF-1	Insulin-like growth factor-1
IIS	Insulin/IGF-1-like signalling
IPTG	Isopropyl β-D-1-thiogalactopyranoside
IR	Insulin Receptor
IRS	Insulin Receptor Substrate
K09	K09C4.1
K4.5	K09C4.5

Kb	Kilo base pair
KRH	Krebs-Ringer HEPES
LacY	Lactose transporter
LB	Luria Broth
M	Molar
MFS	Major Facilitator Superfamily
Mg	Microgram
Mg	Milligram
min	Minutes
Ml	Millilitre
Ml	Microlitre
mm	Millimetre
mM	Millimolar
µM	Micromolar
MNC	Median Neurosecretory Cell
miniprep	Mini-Preparation
MOPS	3-(N-morpholino)propanesulfonic acid
mRNA	Messenger RNA
Ms	Millisecond
mTOR	Mammalian Target Of Rapamycin
Ng	Nanogram
Nl	Nanolitre
nM	Nanomolar
Nm	Nanometre
NGM	Nematode Growth Medium
O.D.	Optical density
PCR	Polymerase Chain Reaction
PBS	Phosphate Buffered Saline
PFA	Paraformaldehyde
PI3K	Phosphoinositide-3-kinase
PIP_3	Phosphatidylinositol (3,4,5)-trisphosphate
PIP_2	Phosphatidylinositol (4,5)-bisphosphate
PKB	Protein Kinase B
PNK	Polynecleotide Kinase
PTS	Phosphotransferase System
QPCR	Quantitative PCR
R09	R09b5.11

RHEB	Ras Homolog Enriched In Brain
RNA	Ribonucleic acid
RNAi	RNA interference
ROS	Reactive Oxygen Species
rpm	Revolutions per minute
RT	Room Temperature
RT-PCR	Reverse transcription polymerase chain reaction
SDS	Sodium Dodecyl Sulfate
SDS-PAGE	Sodium Dodecyl Sulfate - Polyacrylamide Gel Electrophoresis
sec	Second
SGLT	Sodium Dependent Glucose Transporter
Sir 2	Silent information regulator 2
sod	Superoxide dismutase
T08	T08B1.1
TAE	Tris-acetate EDTA
TBS	Tris-Buffered Saline
TCA	Trichloroacetic Acid
TEMED	N,N,N,N'-Tetramethylethylenediamine
T_m	Melting temperature
TRET1	Trehalose transporter 1
Tris	Tris(hydroxymethyl)aminomethane
TSAP	Thermosensitive Alkaline Phosphatase
Tween-20	Polyoxyethylene (20) sorbitan monolaurate
U	Unit
UTRs	Untranslated Regions
UV	Ultraviolet light
V	Volts
w/v	Weight/Volume
WT	Wild Type
X-gal	Bromo-chloro-indolyl-galactopyranoside
XylE	D–xylose/H^+ symporter
Y39	Y39E4B.5

List of figures

List of tables

Chapter 1 Introduction

1.1 Regulation of lifespan

Aging, or organismal senescence, is defined as gradual changes in an organism that "adversely affect its vitality and function, but most importantly, increase the mortality rate as a function of time" (Finch 1990). Viewed within the framework of evolutionary theory, natural selection does not influence post-reproductive animals, therefore, there is no selection for mechanisms to maintain an organism past reproductive age. Hence, the aging process can be regarded as the byproduct of such lack of maintenance (Golden and Melov 2007). Many theories have been proposed to explain the aging phenotype within this evolutionary context. Among these, two are the most influential, the "disposable soma" theory (Kirkwood 1977; Kirkwood and Holliday 1979) and the "antagonistic pleiotropy" theory (Williams 1957). The disposable soma theory proposes that the organism must allocate resources between maintenance of somatic tissues and reproduction, resulting in a trade-off between reproductive fitness and life span (Partridge, Gems et al. 2005; Golden and Melov 2007). While the antagonistic pleiotropy theory suggests that genes that are actively selected because they increase reproductive fitness may have detrimental effects later in life and contribute to aging (Golden and Melov 2007). Consistent with the above theories, various types of damage have been proposed to accumulate with age, either because of an increased rate of production, or because of decreased repair or clearance of damage with time (Golden and Melov 2007). In humans, as a result, susceptibility to a wide variety of diseases increases with age, such as cancer, neuronal degeneration and type 2 diabetes. Therefore, understanding the mechanism of the regulation of lifespan will provide answers to the linkage between aging and age-related disease at a molecular level.

Numerous theories of aging and parameters have been suggested to influence the

regulation of lifespan, including genetic instability, telomerase activity and oxidative stress. Recent findings in several model organisms suggest that three mechanisms (insulin-like signalling, calorie restriction, and mitochondrial respiration) share conserved roles not only in the regulation of lifespan, but also in the timing and control of diverse functions such as reproduction, stress resistance and metabolism (Katic and Kahn 2005; Kloting and Bluher 2005). This introduction mainly focuses on insulin-like signalling and calorie restriction dependent regulation of lifespan.

1.1.1 Insulin/ IGF-1 signalling dependent regulation of aging

The insulin/IGF-1 (insulin-like growth factor-1)-like signalling (IIS) pathway plays a very important role in the mechanisms governing the ingestion, distribution, metabolism, and storage of nutrients in organisms ranging from worms to humans. Mutations in IIS can affect growth, development, metabolic homoeostasis, fecundity and stress resistance, as well as lifespan (Porte, Baskin et al. 2005; Broughton and Partridge 2009). Although alterations in IIS can have severely detrimental effects, for instance diabetes in mammals, lowered IIS has been reported as an evolutionarily conserved means of extending lifespan in the nematode *Caenorhabditis elegans*, the fruit fly *Drosophila melanogaster* and the mouse *Mus musculus* (Klass 1983; Friedman and Johnson 1988; Clancy, Gems et al. 2001; Tatar, Kopelman et al. 2001; Holzenberger, Dupont et al. 2003).

✧ *IIS dependent regulation of aging in C. elegans*

The IIS pathway is the most well-studied aging pathway in the worm. Single-gene mutations were discovered to lead to great extension of the *C. elegans* lifespan (Friedman and Johnson 1988; Kenyon, Chang et al. 1993). The first two genes identified were the key component of the IIS pathway, *daf-2* and *age-1*. DAF-2 (Kimura, Tissenbaum et al. 1997) is the sole insulin/IGF-1 receptor in the worm, and AGE-1 (Morris, Tissenbaum et al. 1996) is a conserved phosphoinositide-3-kinase

(PI3K). Although the full picture of the IIS pathway in *C. elegans* is yet to be unveiled, in the past 15 years, many of the key components of the signalling network were identified and found to be highly conserved in higher eukaryotes, adding piece by piece of the IIS jigsaw puzzle of the worm.

The life cycle of *C. elegans* comprises four larval stages (L1-L4), which are separated by moults (Figure 1.1). The embryonic development and hatching take about 1 day and the larva grows to a fertile adult in about 3 days. The adult worm can live on average 2-3 weeks when it is grown on a lawn of *E. coli* cells at 20-21°C. When encountering particular environmental stress, *C. elegans* larvae will enter a non-feeding, stress-resistant, dauer diapause larval stage to survive adverse conditions. After favourable environmental conditions arise, dauer larvae resume development and proceed to L4 larval stage and subsequently to adulthood. In the dauer state, worms can survive up to 6 months, which is much longer than the adult worm life span (2-3 weeks) (Braeckman, Houthoofd et al. 2001).

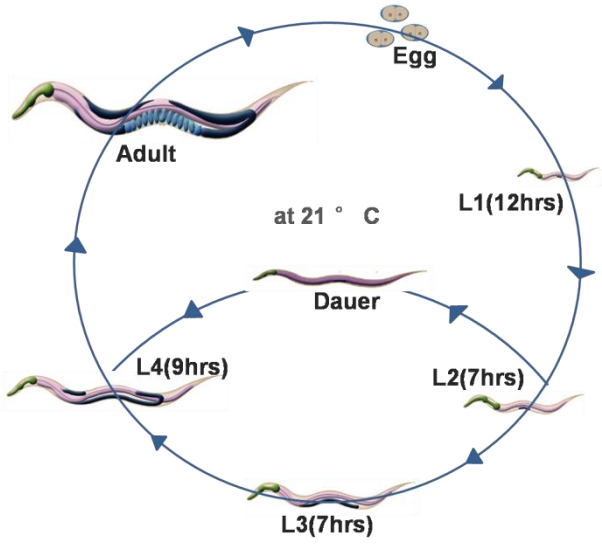

Figure 1.1 The life cycle of *C. elegans*. Adapted from (Braeckman, Houthoofd et al. 2001). After embryonic development and hatching, *C. elegans* (the worms) experience a series of four larval stages (L1-L4) before reaching adulthood. When encountering particular environmental stress, worms will enter the dauer larval stage, which allows worms to survive adverse conditions. After favourable environmental conditions arise, dauer larvae resume development and proceed to L4 larval stage and subsequently to adulthood. In the dauer state, worms can survive up to 6 months, which is much longer than the adult worm life span (2-3 weeks) (Braeckman, Houthoofd et al. 2001).

The *C. elegans* genome encodes 38 insulin-like genes, several of which (INS-1, *daf-28* and *ins-7*) can directly regulate the DAF-2 signalling and the function of the rest are unknown (Panowski and Dillin 2009) (Figure 1.2). Under normal conditions, in response to the taste and/or ingestion of food, one or more insulin-like ligands are secreted from neurosecretory cells in the worm central nervous system, activating DAF-2 and triggering the DAF-2 signalling (Porte, Baskin et al. 2005) (Figure 1.2). Active DAF-2 initiates a subsequent downstream cascade including the activation of AGE-1, production of second messenger phosphatidylinositol (3,4,5)-trisphosphate (PIP_3) and the activation of the AKT family kinases (AKT-1,2 and SGK-1 (Paradis and Ruvkun 1998; Hertweck, Gobel et al. 2004)) through a PDK-1 kinase ortholog (Paradis, Ailion et al. 1999). The activated AKT family kinases subsequently phosphorylate the Forkhead Box O (FOXO) transcription factor, DAF-16 (orthologous to mammalian FOXO1, FOXO3a and FOXO4) (Henderson and Johnson 2001; Lee, Hench et al. 2001). The phosphorylated DAF-16 then binds with the 14-3-3 protein FTT-2 (Wang, Oh et al. 2006; Li, Tewari et al. 2007), which prevents the transcription factor from entering the nucleus and thus, stopping it promoting or repressing transcription of genes required for DAF-2 dependent functions (Lin, Dorman et al. 1997; Ogg, Paradis et al. 1997). As a result, the worm will have a normal lifespan and normal reproduction rate. Inactivation of this pathway occurs in part via the activity of the PIP_3 phosphatase, DAF-18 (Ogg, Paradis et al. 1997). The absence of the insulin-like ligands or inactivation of cascade components reduces the phosphorylation of DAF-16. This allows the non-phosphorylated transcription factor to enter the nucleus and promote longevity. The DAF-16 dependent DAF-2 signalling function not only alters the lifespan of the worm but also is involved in other processes, including the response to many stressors, such as oxidative damage, heavy metals and heat, as well as the dauer development (Wolff and Dillin 2006). Weak loss-of-function mutations in *daf-2* lead to a dauer-constitutive phenotype (Daf-c) and allow the worms to enter dauer more readily (Gems, Sutton et al. 1998).

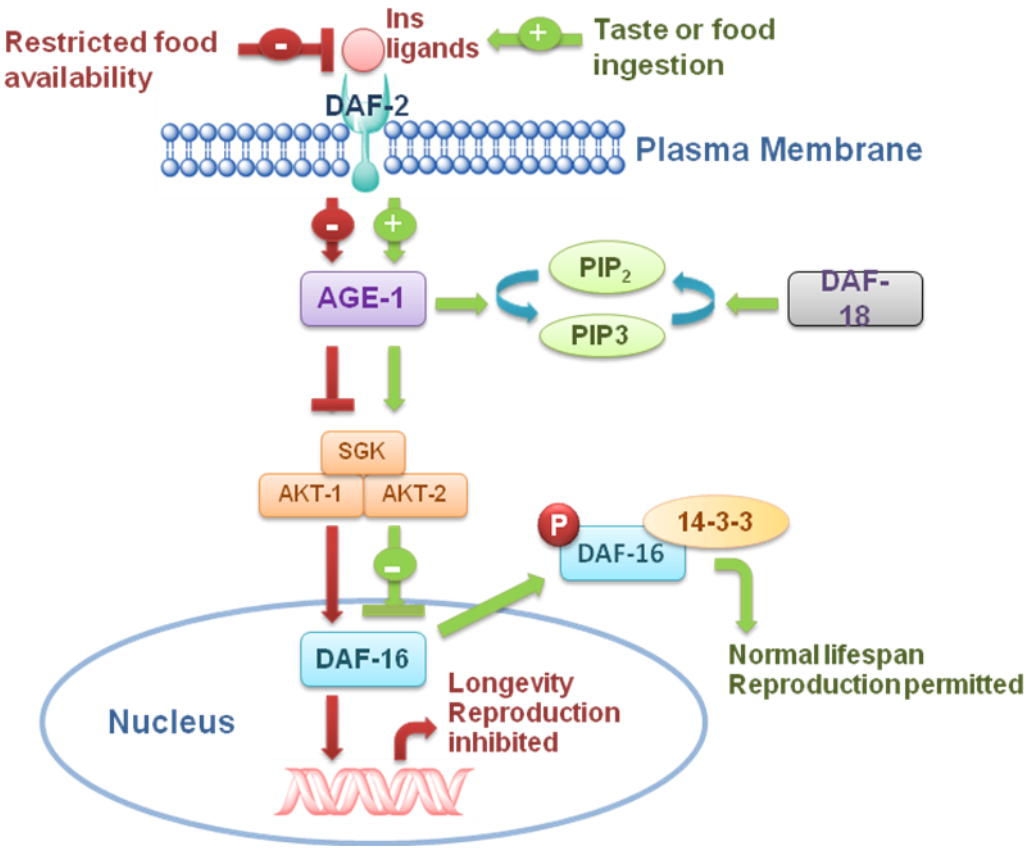

Figure 1.2 The putative role of IIS pathway in the control of lifespan, reproduction in *C. elegans*. Adapted from (Porte, Baskin et al. 2005). In response to the taste and/or ingestion of food, secretory cells will produce one or more insulin-like ligands to activate the insulin receptor ortholog, DAF-2. This in turn will activate the insulin-like signalling pathway. The activation of DAF-2 will trigger intracellular signalling via the PI3-kinase ortholog AGE-1. This consequently inactivates the forkhead transcription factor, DAF-16, by phosphorylation, which allows normal growth, aging, reproduction, and fat storage. The cascade can be interrupted by inadequate nutrient availability, leading to reduced insulin signalling, activation of DAF-16, and subsequently the worm enters into the dauer phase of development (Porte, Baskin et al. 2005).

✧ *IIS dependent regulation of aging in Drosophila*

Drosophila has endocrine tissues that resemble those of mammals. Three of the seven *Drosophila* insulin-like peptides (DILPs), DILP2, DILP3, and DILP5, are produced in large, specialized neurons of the central nervous system, the DILP-producing median neurosecretory cells (MNCs). The MNCs have been suggested to be functionally equivalent to pancreatic *β*-cells of mammals as producers of circulating insulin-like peptides for metabolic homoeostasis (Rulifson,

Kim et al. 2002; Wang, Tulina et al. 2007). DILPs produced by the MNCs activate *Drosophila* insulin receptor (dINR), starting the IIS cascade. The dINR transduces the signal, either directly or through insulin receptor substrate (CHICO), to the PI3-kinase. The conversion of phosphatidylinositol (4,5)-bisphosphate (PIP_2) to PIP_3 leads to the activation of dPDK-1 and AKT kinase. The AKT kinase then phosphorylates dFOXO and prevents its nuclear translocation. Down-regulation of IIS by mutations in dINR or CHICO (or by over-expression of IIS antagonist dPTEN) results in increased nuclear localization of dFOXO which regulates transcription of genes that increase longevity and stress resistance (Toivonen and Partridge 2009). (Figure 1.3A)

✧ *IIS dependent regulation of aging in mammals*

The IIS regulation of aging in mammals is much more complicated. Unlike worms and flies which have only one insulin/IGF-1-like signalling pathway, mammals have separate insulin and IGF signalling pathways controlling blood glucose metabolism, growth, stress resistance, reproduction and aging. Although the number of ligands is reduced to three (these are insulin, IGF-1 and IGF-2), compared with 7 for the flies and 38 for the worms, there are multiple receptors (separate insulin and IGF-1 receptors) with different ligand affinity and signalling output. Moreover, the mammalian IIS pathway is tightly linked with the actions of the growth hormone (GH) which has no counterpart in worms or flies (Bartke 2008). GH is the key regulator of IGF-1 biosynthesis and release and an important modulator of insulin actions in different organs (Bartke 2008).

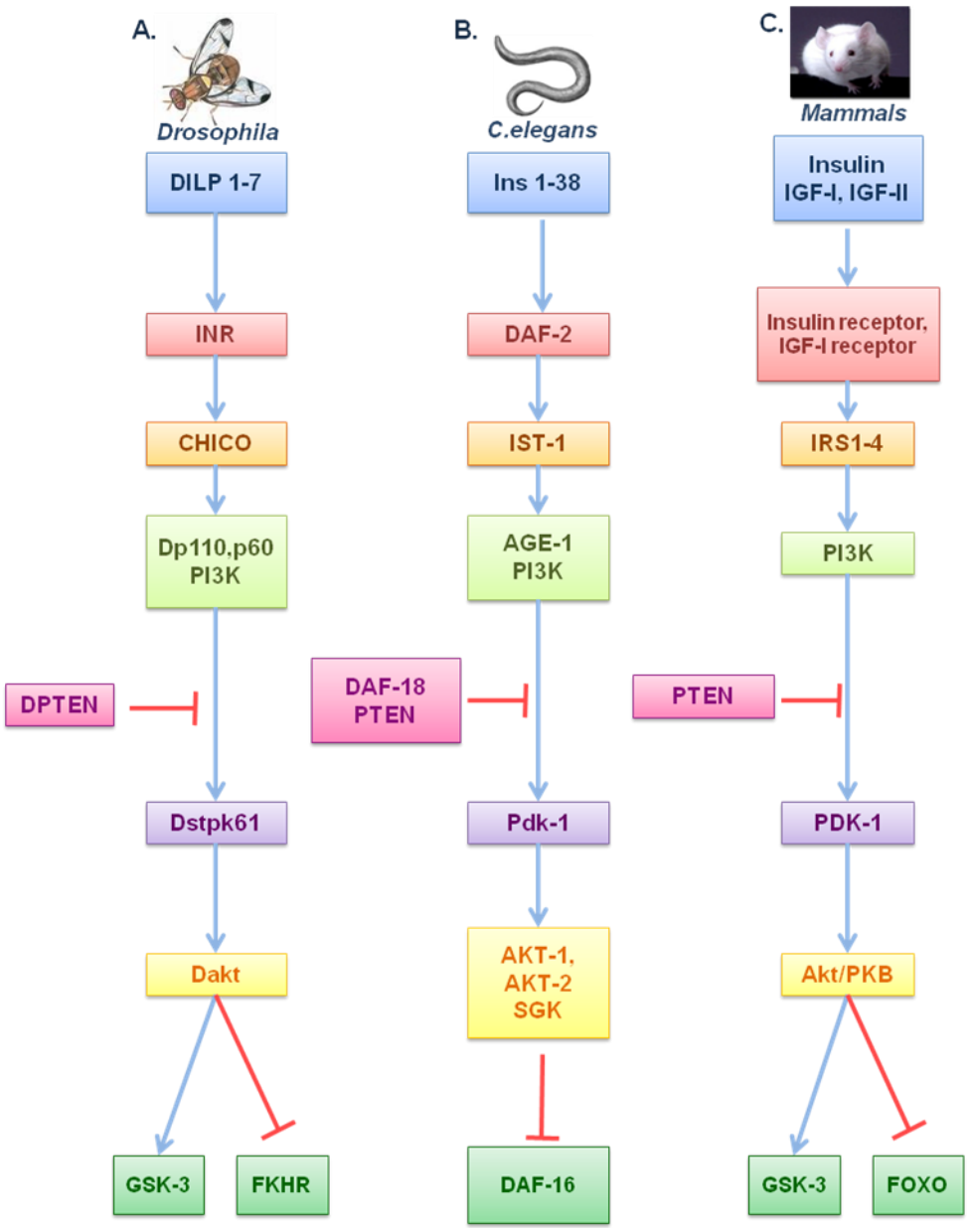

Figure 1.3 Comparison of the insulin-like signalling in *C. elegans*, *Drosophila*, and mammals. (Adapted from (Porte, Baskin et al. 2005; Broughton and Partridge 2009)) The signalling starts with binding of insulin-like peptides to an appropriate receptor. Mammals have three ligands to activate the signalling pathway (insulin, IGF-1 and IGF-2), whereas worms have 38 ligands and flies have seven ligands identified so far. On the contrary, worms and flies have one receptor, whereas mice have three. In worms and flies, the signal can be transduced to PI3K (or AGE-1 in worms) either directly or indirectly via the only IRS. In mice, the signal is transduced indirectly via four IRS (IRS1-IRS4). PI3K then converts PIP_2 into the second messenger PIP_3. The phosphorylation can be antagonized by the PTEN phosphatase (DAF-18 in worms). Elevated levels of PIP_3 lead to the activation of PKB and PDK. Flies have a single PKB, whereas worms have AKT-1, AKT-2 and SGK-1 and mice have Akt1, Akt2 and Akt3. The activated PKB phosphorylates the forkhead transcription factor leading to its exclusion from the nucleus, and thus inactivates it. Worms and flies contain a single forkhead transcription factor, whereas mice contain three. (Porte, Baskin et al. 2005; Broughton and Partridge 2009).

The best-studied insulin-like signalling in mammals is the PI3-kinase pathway (Figure 1.3C). The auto-phosphorylation of insulin receptor at several tyrosine residues upon binding with insulin results in the recruitment of the lipid kinase PI3-kinase to the plasma membrane of the cells. As the PI3-kinase becomes close to its physiological substrate PIP_2, it phosphorylates the substrate to generate the second messenger PIP_3. The binding of insulin to its receptor and the following events leads to a significant increase in the concentration of PIP_3. This causes the binding of PIP_3 to its key effector, AKT (also known as protein kinase B (PKB)), which subsequently causes the recruitment of AKT from cytosol to the plasma membrane. The recruitment of AKT makes it closer to another two enzymes that phosphorylate the protein and hence it is activated. The activated AKT will dissociate from plasma membrane and phosphorylate numerous substrates in both cytoplasm and nucleus, such as glycogen synthase kinase 3β (GSK3β) (hepatic glycogen synthesis) (Lizcano and Alessi 2002), AS160 (a rab GAP implicated in GLUT4 translocation) (Sakamoto and Holman 2008), the BAD·BCL2 heterodimer (antiapoptosis), and FOXO transcription factors (regulation of gene expression) (Taguchi and White 2008). AKT also phosphorylates tuberin (TSC2), which inhibits its GAP (GTPase Activating Protein) activity toward the small G protein RHEB. The inhibition causes the accumulation of the RHEB·GTP complex resulting in the activation of mammalian target of rapamycin (mTOR), which provides a direct link between insulin signalling and nutrient sensing (Watson and Pessin 2006).

The evidence supporting the IIS regulation of lifespan in mammals is abundant but largely indirect. The first evidence suggesting a major increase in average and maximal lifespan in mutant mice with reduced plasma levels of IGF-1 and insulin was reported in 1996 (Brown-Borg, Borg et al. 1996). The Snell and Ames dwarf mice both have mutations that result in lack of GH and other pituitary hormones leading to similar phenotypes including small size and female sterility, and both phenotypes are consistently long-lived (Brown-Borg, Borg et al. 1996). Later, other mutant mice with defects in GH function were found to be long-lived (Bartke 2008). However,

identifying the specific role of insulin and separating it from the effects of reduced GH and IGF-1 signalling in these mutants is very difficult. Mice with severely reduced insulin or IGF-1 signalling have short lifespan owing to developmental and metabolic defects (Accili, Drago et al. 1996). However, heterozygous deletion of the IGF1 receptor can extend the lifespan of female mice by up to 26% while no significant effect on male mice (Holzenberger, Dupont et al. 2003). In comparison of systemic deletion of the key components of the IIS pathway resulting in shortened lifespan, some tissue specific knockout mice were found to be long-lived. The fat-specific insulin receptor knockout (FIRKO) mice show 20% longer median and maximal lifespan than littermate controls (Bluher, Kahn et al. 2003). Mice with deletion of insulin receptor substrate-2 (IRS-2) only in the brain exhibit mild insulin resistance and show extended lifespan (Taguchi, Wartschow et al. 2007). Taken together, defining the role of IIS pathway in the control of mammalian aging is remaining a puzzle to be solved.

1.1.2 Calorie restriction dependent regulation of lifespan

The calorie restriction (CR) is usually defined as a dietary reduction in caloric intake (normally 20% ~ 40%) without compromising the maintenance of all essential nutrients (Piper and Bartke 2008). It is the most consistent non-pharmacological intervention increasing lifespan and protecting against the deterioration of biological functions. Since the first report of extending the lifespan in rats in 1935 (McCay, Crowell et al. 1989), evidence in multiple species (yeast, rotifers, spiders, worms, flies, fish, mice and rats) indicates that the effects of CR on lifespan extension are conserved all along the evolutionary scale (Koubova and Guarente 2003). Experiments with *C. elegans* and *Drosophila* show that CR extends their lifespan up to 50% or more (Clancy, Gems et al. 2002; Kenyon 2005). When subjected to CR, C57BL/6 or B6D2F1 mice postpone the accumulation of life-threatening tissue lesions and this extends the median and maximal lifespan by 35% (Forster, Morris et al. 2003). Studies on CR in Rhesus monkeys indicate that the CR monkeys are

protected from many age-associated pathophysiological changes, such as the development of insulin resistance and type 2 diabetes, atherosclerosis, and reductions in their basal metabolic rate, body temperature, oxidative damage and senescence of the immune system (Canto and Auwerx 2009).

Although the evidence of CR extending lifespan has been well documented for ~70 years the mechanism behind this remains largely unknown. The conventional mechanistic explanation of regulation of CR on lifespan was that reactive oxygen species produced during respiration would cause oxidative damage to DNA, RNA, protein, and lipids. And CR would decrease the load of reactive oxygen species, resulting in less damage and thus increased lifespan (Koubova and Guarente 2003). However, this theory was questioned by the findings of McCarter et al that, when normalized to body weight, metabolic rate was not slowed by calorie restriction (McCarter, Masoro et al. 1985).

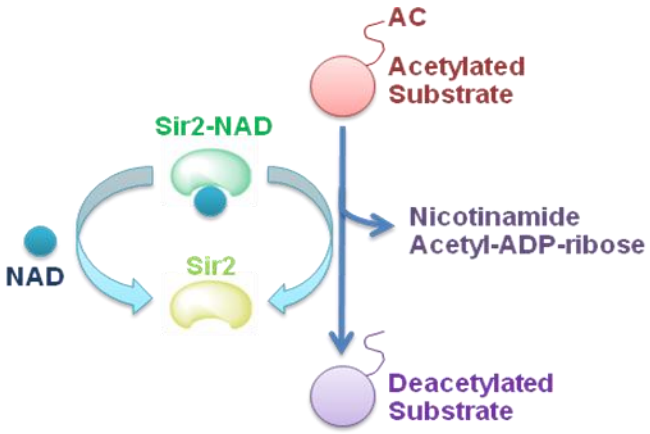

Figure 1.4 The schematic diagram of SIR2 activity. SIR2 deacetylates the acetyllysine group on histone, with NAD^+ as cofactor, forming the deacetylated histone, nicotinamide and ADP-ribose. Modified from (Wolf 2006)

More recently the gene, silent information regulator 2 (*Sir 2*), has been implicated in the response to CR (Wood, Rogina et al. 2004).The family of proteins coded by the *Sir2* gene function as histone deacetylases, removing the acetyl group from acetyllysine in histones, and require NAD^+ as a cofactor, forming O-acetyl-ADP-

ribose and nicotinamide (Figure 1.4) (Wolf 2006). The NAD^+/NADH ratio is critical for the Sir2 activity, as NADH is an inhibitor of Sir2 (Lin, Ford et al. 2004). In yeast, CR increases oxidative metabolism, shifting the NAD^+/NADH ratio in favour of NAD^+ and at the expense of NADH, therefore, Sir2 is activated resulting in an increased lifespan (Lin, Ford et al. 2004). In *Drosophila*, CR increase Sir2 mRNA level. The lifespan increase resulted from overexpression of Sir2 was not further increased by CR (Rogina and Helfand 2004), while the activation of Sir2 by resveratrol could not increase the flies already subjected to CR, either (Wood, Rogina et al. 2004). Furthermore, neither CR nor resveratrol were able to extend lifespan in Sir2 ablated flies (Rogina and Helfand 2004).

In *C. elegans*, however, the role of *Sir2* ortholog, *sir-2.1*, in CR remains ambiguous. The effect of overexpression of *sir-2.1* to induce extension of lifespan is dependent on *daf-16*, the master regulator of IIS in worms (Tissenbaum and Guarente 2001), while *daf-16* is not required for the long lifespan of *eat-2* mutant animals (a genetically modified mutant with slow pharynx pumping rate to mimic CR in worms) (Lakowski and Hekimi 1998). However, deletion of *sir-2.1* suppresses the extended lifespan of *eat-2* mutants but not *daf-2* mutant (Wang and Tissenbaum 2006). Similarly in mammals, the effect of CR in extending lifespan is blunted in mice lacking the mammalian *sir2* orthologue, SIRT1 (Boily, Seifert et al. 2008). Whereas the SIRT1 levels do not increase in all tissues in response to CR and it has been shown to be dispensable for proper adaptation to CR in liver (Chen, Bruno et al. 2008).

1.1.3 Links between CR and IIS in the regulation of lifespan

A possible explanation of CR increasing lifespan links it with the IIS pathway. Studies in rodents and humans show that CR consistently increases insulin sensitivity in the classic metabolic target tissues including liver, muscle, and adipose. As a result less insulin is needed to maintain glucose homeostasis leading to a dramatic decrease of circulating insulin concentrations. Therefore, all the tissues of the CR animal are

exposed to lower circulation insulin concentrations, which may lead to the increase of nuclear FOXO activity all over the body. In comparison, normal or excess nutrients increase the duration and concentration of circulating insulin. Thus, sustained activation of the insulin-like signalling cascades by high-calorie diet may expose animals to systemic stress due to reduced nuclear FOXO (Taguchi and White 2008).

However, this theory is challenged by findings in *C. elegans* because CR can increase the worm lifespan independently of DAF-16 activity (Antebi 2007). PHA-4, a forkhead transcription factor with similarity to the mammalian FOXA orthologs, was reported to play a role in the extension of lifespan by CR in worms independently of the IIS pathway (Panowski, Wolff et al. 2007). PHA-4 expression is increased under conditions of CR and overexpression of PHA-4 can increase the lifespan of the worms in the absence of DAF-16 (Panowski, Wolff et al. 2007). Whereas, in mammalian cells the FOXA activity can be inhibited by insulin (Friedman and Kaestner 2006).

On the other hand, work in both flies and worm suggests that IIS and CR share some of the mechanisms that can extend lifespan while different downstream effector mechanisms are involved (Taguchi and White 2008). As mentioned in 1.1.2, overexpression of sir2 leads to an increase in the lifespan in yeast, worms, and flies by mimicking the energy-depleted state (Longo and Kennedy 2006). However, sir2-induced lifespan extension is dependent upon *daf-16*, the master regulator of IIS (Tissenbaum and Guarente 2001); whereas, deletion of sir2 suppresses the extended lifespan of *eat-2* mutants, but not *daf-2* mutants (Wang and Tissenbaum 2006). These evidences from the work in worms suggest that sir2 may work through two parallel pathways to bridge the interaction between the CR and IIS pathways for the regulation of longevity (Wolff and Dillin 2006).

Studies in yeast, worms and flies also indicate the involvement of the TOR pathway in both CR and IIS regulated extension of lifespan (Wolff and Dillin 2006; Taguchi and White 2008). The TOR pathway is activated by nutrients and promotes protein

synthesis and growth (Wullschleger, Loewith et al. 2006). Mutations reducing TOR activity increase the lifespan of worms and flies (Giannakou and Partridge 2007). In mammalian cells, TOR inhibits signalling through the IRS protein and consequently inhibits the insulin signalling. Inhibition of TOR increases insulin sensitivity (Fisher and White 2004). In mammals, AMP-activated protein kinase (AMPK) is closely associated with IIS. It inhibits TOR activity and increases insulin sensitivity. The activator of AMPK, cellular AMP, increases during CR or energy depletion (Shaw, Lamia et al. 2005). In *C. elegans*, AMPK extends the lifespan of worm subjected to CR (Apfeld, O'Connor et al. 2004).

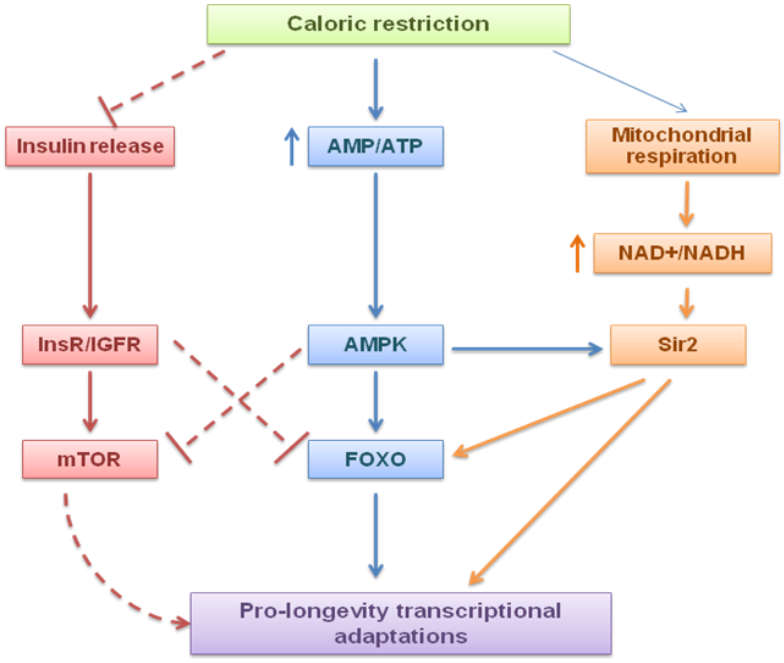

Figure 1.5 Integrative view of the signalling pathways involved in regulating the aging process. Different signalling cascades in the regulation of lifespan in both mammals and lower animals may act in a balanced interconnected network rather than in an independent manner. For instance, CR is not only sensed by SIR2 as a change in the NAD^+/NADH ratio but also by AMPK as a change in the AMP/ATP ratio. AMPK is involved in the regulation of mitochondrial respiration, which in turn can positively regulate SIRT2 activity. Both AMPK and SIRT2 have effects on the activity of FOXO transcription factors, which have been extensively linked to the regulation of metabolism and longevity. In addition, CR can promote the downregualtion of insulin-derived signals, which also interact with FOXO transcription factors. (Adapted from (Canto and Auwerx 2009))

Taken together, the failure to identify genetic components regulating CR that work independently of IIS suggests that IIS and CR increase lifespan via signalling

mechanisms that are genetically regulated and autonomous of one another. Different signalling cascades in the regulation of lifespan in both mammals and lower animals may act in a balanced interconnected network rather than in an independent manner (Figure 1.5).

1.2 Glucose homeostasis

Glucose occupies a central position in the metabolism of plants, animals, and many microorganisms. It acts not only as an essential fuel to supply essential energy for living organisms, but also as a versatile precursor that provides a huge array of metabolic intermediates for biosynthetic reactions. In mammals, glucose homeostasis is maintained by the coordinated regulation of three processes. First, glucose absorption via the small intestine; second, glucose production in the liver; and third, consumption of glucose by nearly all tissues (Kahn 1992). These three processes are mainly regulated by two hormones: insulin and glucagon which are both secreted by islet cells within the pancreas in response to blood sugar levels.

Insulin causes the glucose uptake from the blood by the cells in the liver, muscle and fat tissue and reduces the use of fat as an energy source. When insulin is low or absent, glucose uptake is stopped in the above cells and fat is used as an energy source (Chang, Chiang et al. 2004). On the contrary, glucagon, a 29-amino acid polypeptide, is synthesized and released by the alpha cells of the pancreas and acts as a counter-regulatory hormone of insulin. It can cause the liver to release stored glucose to raise the blood sugar level in response to insulin-induced hypoglycaemia (Jiang and Zhang 2003).

The blood glucose level is tightly regulated and is limited and maintained in a very narrow range. Normally, in mammals the blood glucose level is maintained at the range between approx. 3.6 and 5.8 mmol/l. Abnormal blood glucose level can cause severe health problems. A lower blood glucose level than the normal status

(hypoglycaemia) can cause seizures, unconsciousness, and irreversible cell damage. On the other hand, a higher blood glucose level than the normal concentration (hyperglycaemia) has a adverse effect defined as “glucotoxicity”, which can lead to blindness, renal failure, cardiac and peripheral vascular disease, and neuropathy (Scheepers, Joost et al. 2004). Furthermore, excessive amounts of glucose over a prolonged period have negative effects on pancreatic-cell function, leading to the increased sensitivity to glucose, increased basal insulin release, reduced maximal secretory response, and a gradual depletion of insulin stores (Kaiser, Leibowitz et al. 2003)

Recent studies in *C. elegans* showed that increased glucose availability decreases lifespan while impaired glucose metabolism (resulting from exposure of the worms to 2-deoxy-D-glucose (DOG) treatment) extends life expectancy by inducing mitochondrial respiration and increasing oxidative stress (Schulz, Zarse et al. 2007). A question that arises with this finding is: could this most important energy fuel and its catabolic pathway, glycolysis, be implicated in the aging process? A current explanation of the involvement of glucose in the aging process is that glucose can directly (through the glucose metabolism) or indirectly (by provoking insulin secretion from pancreatic β-cells) affect the main regulators of the aging process such as IIS pathway, sir2 and TOR signalling as well as increasing the oxidative stress (Kassi and Papavassiliou 2008).

The first and limiting step of glucose metabolism is the transport of glucose across the plasma membrane. Hence, the key components of these transport systems may also play a role in the mechanisms of CR directed lifespan extension. In yeast, an increase in lifespan can be achieved by mutations that reduce the metabolism of glucose (such as deletion of *hexokinase 2*) (Lin, Defossez et al. 2000). However, in the long-lived klotho mouse which genetically lacks *klotho* gene (encoding a β-glucosidase-like protein) expression, an associated increased expression of glucose transporter 4 and increased insulin sensitivity have been demonstrated

(Utsugi, Ohno et al. 2000).

1.3 The glucose transporter families

Being a very important nutrient for many types of cells, not only in mammals and other higher organisms but also in microbes, glucose, in the polymeric form of cellulose, is probably the most abundant biological molecule on earth. In parallel with the widespread utilisation of glucose as nutrient source, a variety of mechanisms have evolved to catalyse the cellular uptake of the hydrophilic molecules across the hydrophobic core of the plasma membrane (Baldwin 1993). In eukaryotic cells, glucose is transported across the plasma membrane by membrane associated carrier proteins, glucose transporters. There are two different types of transporter proteins, which mediate the transfer of glucose and other sugars through the lipid bilayer, a Na^+-coupled carrier system (SGLT) and the facilitative glucose transporters (GLUT) (Bell, Kayano et al. 1990; Carruthers 1990; Scheepers, Joost et al. 2004).

1.3.1 The SGLT family

The sodium dependent glucose transporter (SGLT) family comprises Na^+-dependent glucose co-transporters (SGLT1 and SGLT2), the glucose sensor SGLT3, the widely distributed inositol and multivitamin transporters SGLT4 and SGLT6, and the thyroid iodide transporter SGLT5 (Scheepers, Joost et al.). SGLT1 and SGLT2 are also known as co-transporters or symporters. They are integral membrane proteins that mediate the transport of glucose and, with much lower affinity, galactose across the plasma membrane by an active transport mechanism (Wright 2001). The transport process is a co-transport of glucose molecules and sodium ions. Human SGLT3 does not transport glucose when expressed in *Xenopus laevis* oocytes (Diez-Sampedro, Hirayama et al. 2003). It acts as a glucosensor by conveying information to the cell about external glucose concentration directly through the membrane potential or indirectly coupled through another molecule such as a G

protein (Scheepers, Joost et al. 2004) (Table 1.1).

Table 1.1 Properties of Na^+/glucose co-transporter family members (Zhao and Keating 2007)

Protein	K_m[1] (mM)	Major expression Tissue	Function
SGLT1	0.2	Kidney, intestine	Glucose re-absorption in intestine and kidney
SGLT2	10	Kidney	Low affinity and high selectivity for glucose
SGLT3	2	Small intestine, skeletal muscle	Glucose activated Na^+ channel

[1] Net influx for 2-deoxyglucose or glucose.

1.3.2 The GLUT family

The facilitative glucose transporters (GLUTs) are also called passive carriers which are specific for the D-enantiomer of glucose and are not coupled to any energy-requiring components, such as ATP hydrolysis or an H^+ gradient, and they can only transport their substrate down a concentration gradient (Gould and Holman 1993). These passive transporters are most effective when the cell is exposed to a relatively constant level of the substrate. Therefore, the passive carriers are mainly restricted to multicellular organisms that regulate the composition of their internal medium (Carruthers 1990; Baldwin 1993; Mueckler 1994). The primary function of the facilitative glucose carriers is to mediate the exchange of glucose between the blood and the cytoplasm of the cell. This may involve a net uptake or output of glucose from the cell, depending on the type of cell in question, its metabolic state, and the metabolic state of the organism (Mueckler 1994). Thus, the glucose transport in these organisms is mediated by a family of highly related transporters which are the products of distinct genes and are expressed in a highly controlled tissue-specific fashion (Gould and Holman 1993). Moreover, these transporters are also different in their functional characteristics, such as the substrate specificity, the K_m values, and their binding-affinities to the inhibitory ligands cytochalasin B and forskolin (Scheepers, Joost et al. 2004). The human genome contains 14 members of the

GLUT family (Figure 1.6). According to sequence similarities and characteristic elements, they are divided into three subfamilies (Table 1.2).

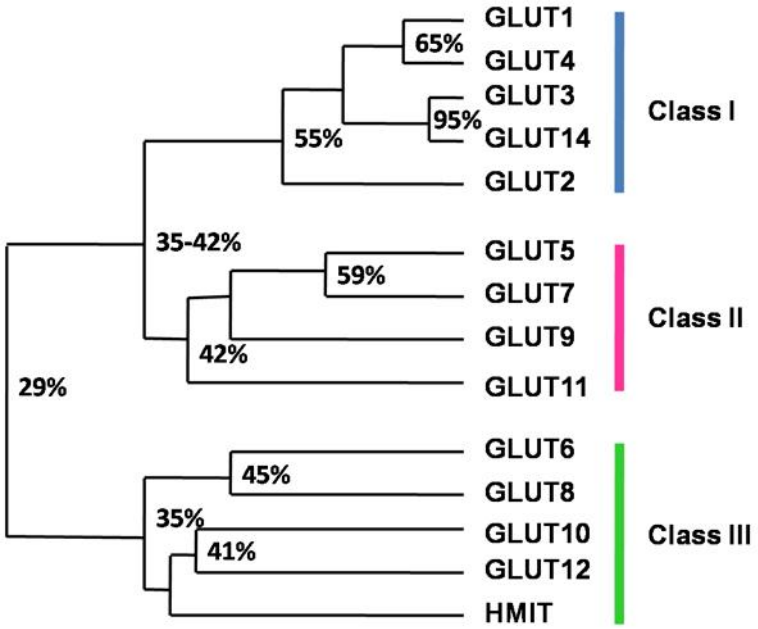

Figure 1.6 Dendrogram of the family of human sugar transporter facilitators. The alignment was performed with the CLUSTAL program. Numbers at the branches of the tree indicate percentage of identity. Adapted from (Scheepers, Joost et al. 2004).

✧ ***Class I facilitative transporters***

The class I facilitative transporters include the well characterized isoforms GLUT 1-4, plus the later identified isoform GLUT14. GLUT1 is the first identified protein in the mammalian glucose transporter family and is found to be responsible for the basic supply of cells with glucose (Baldwin, Baldwin et al. 1982; Mueckler, Caruso et al. 1985). It is ubiquitously expressed while having the highest expression levels in erythrocytes and endothelial cells of the brain. GLUT2 (Fukumoto, Seino et al. 1988) is a low-affinity glucose transporter. It can also transport fructose (Wood and Trayhurn 2003) and, with higher affinity, glucosamine (Uldry, Ibberson et al. 2002). It is found to have predominant expression in pancreatic beta-cells, liver, kidney, and the basolateral surface of proximal renal tubules and enterocytes. In β-cells, GLUT2 plays a role in the glucose-sensing mechanism, while in liver it allows for the

bi-directional transport of glucose under hormonal control. It also forms part of the transcellular pathway for glucose and fructose transport (Wood and Trayhurn 2003). GLUT3 (Kayano, Fukumoto et al. 1988) is a high-affinity glucose transporter, which is expressed predominantly by neurons and other tissues with high glucose requirement (e.g. sperm, preimplantation embryo, and white blood cells) (Simpson, Dwyer et al. 2008). The amino acid sequence of human GLUT14 shares 95% identity with GLUT3 (Wu and Freeze 2002) and it is exclusively expressed in testis; no ortholog of GLUT14 was found in mice (Scheepers, Joost et al. 2004).

GLUT4 (Fukumoto, Kayano et al. 1989) is the only insulin responsive glucose transporter which transports glucose with high affinity. It is found to be expressed in major insulin-sensitive tissues (heart, skeletal muscle, adipose tissue) (Gould and Holman 1993). In response to insulin stimulation, GLUT4 translocates from intracellular GLUT4-containing vesicles to the plasma membrane, leading to an immediate 2-10 fold (depending on tissue) increase in glucose transport (Bryant, Govers et al. 2002). In addition to insulin stimulation, muscle contraction and hypoxia can also induce the translocation of GLUT4 in skeletal muscle (Lund, Holman et al. 1995).

✧ ***Class II facilitative transporters***

The fructose-specific transporter GLUT5 and 3 related proteins, GLUT7, GLUT9 and GLUT11 comprise the class II facilitative glucose transporters. Among the 7 members of the GLUTs family that can transport fructose GLUT5 is the only fructose transporter with no ability to transport glucose and galactose, and is inhibitable by phloretin and cytochalasin B (Burant, Takeda et al. 1992). It is predominantly expressed in small intestine, testis, and kidney and is also found in fat, skeletal muscle, and brain with modest expression levels (Kayano, Burant et al. 1990; Douard and Ferraris 2008). Being the closest family member of GLUT5, GLUT7 (Li, Manolescu et al. 2004) is a high affinity glucose and fructose transporter which is

primarily expressed in the apical membrane of the small intestine and colon. The mRNA of GLUT7 can also be detected in the testis and prostate (Cheeseman 2008). The highest expression level of GLUT9 (Phay, Hussain et al. 2000) is found in kidney and liver while expression in small intestine, placenta, lung, heart, skeletal muscle, and leukocytes is also detected (Doblado and Moley 2009). The mRNA of GLUT9 has two alternative splice variants encoding two proteins which differ in the N-terminus (GLUT9a and GLUT9b). Although both forms of GLUT9 protein and mRNA are detected in the epithelia of the above tissues, in the polarized cells, GLUT9a was predominantly expressed on the basolateral surfaces while GLUT9b was expressed on apical surfaces (Augustin, Carayannopoulos et al. 2004). In addition to act as a high-affinity glucose and fructose transporter, GLUT9 is also a high-capacity uric acid transporter (Doblado and Moley 2009). The glucose transport of GLUT9 was not inhibited by cytochalasin B. The SLC2A11 gene of GLUT11 generates 3 alternatively spliced isoforms that differ in the N-terminal sequence (Sasaki, Minoshima et al. 2001). GLUT11 is expressed predominantly in pancreas, kidney, and placenta and is also detected in heart and skeletal muscle with moderate expression level (Scheepers, Joost et al. 2004). GLUT11 is suggested to be a fructose transporter with low glucose affinity because its glucose transport activity can be inhibited by fructose (Doege, Bocianski et al. 2001).

✧ ***Class III facilitative transporters***

The class III facilitative transporters (GLUT6, GLUT8, GLUT10, GLUT12 and HMIT), when comparing with the other two classes, are featured by the presence of the characteristic glycosylation motif on the larger extracellular loop 9, while having a shorter extracellular loop 1 (Joost and Thorens 2001). GLUT6 (Doege, Bocianski et al. 2000) is a low-affinity glucose transporter which is predominantly expressed in brain, spleen, and peripheral leukocytes. The high-affinity glucose transport activity of GLUT8 (Doege, Schurmann et al. 2000) is specifically inhibited by fructose and galactose, indicating that GLUT8 may be a multifunctional sugar transporter

(Scheepers, Joost et al. 2004). GLUT8 is predominantly expressed in testis, and lower expression level of GLUT8 is detected in most other tissues, including insulin-sensitive tissues like heart and skeletal muscle and adipocytes (Scheepers, Joost et al. 2004). The protein is also detected in preimplantation embryos, where it is reported to mediate insulin-stimulated glucose uptake (Carayannopoulos, Chi et al. 2000). The subcellular localization of GLUT8 is found to be associated with endosomes and lysosomes but also with the endoplasmic reticulum membranes (Schmidt, Joost et al. 2009). GLUT8, as well as GLUT6, has a dileucine motif at the N-terminus that directs the protein to intracellular storage compartments when expressed in isolated adipocytes and COS-7 cells (Lisinski, Schurmann et al. 2001). GLUT10 (McVie-Wylie, Lamson et al. 2001) is predominantly expressed in the liver and pancreas. The *SLC2A10* gene which codes for GLUT10 is localized on chromosome 20q13.1 which was previously linked to Type 2 diabetes. Recently, mutations in the *SLC2A10* gene are also found to be related to the arterial tortuosity syndrome (Cheng, Kikuchi et al. 2009; Zaidi, Meyer et al. 2009). When expressed in *Xenopus laevis* oocytes, the glucose transport ability of GLUT12 (Macheda, Kelly et al. 2002) can be competitively inhibited by D-galactose and to a lesser extent by D-fructose (Rogers, Chandler et al. 2003). The protein is predominantly expressed in heart and prostate. In addition, GLUT12 seems to sustain the increased glucose consumption in prostate carcinoma (Chandler, Williams et al. 2003), breast cancer (Rogers, Docherty et al. 2003), and in the late diabetic nephropathy (Linden, DeHaan et al. 2006). The H^+-coupled *myo-inositol* transporter (HMIT) (Uldry, Ibberson et al. 2001) does not have any sugar transport activity but specifically transports *myo-inositol* and related stereoisomers. HMIT is predominantly expressed in the brain.

Table 1.2 Properties of glucose transporter family members[1]

Protein	Km[2] (mM)	Substrate Specificity	Major expression Tissue	Function
GLUT1	5	Glucose/galactose	Ubiquitous; red cells	Basal glucose uptake, transport across blood tissue barriers
GLUT4	5	Glucose	Fat, muscle including heart	Insulin-regulated transport in muscle and fat
GLUT3 (GLUT14)	1	Glucose/galactose	Neurons	Neuronal transport
GLUT2	11	Glucose/galactose/ fructose	Intestine, kidney, liver, beta-cell	High-capacity low-affinity transport
GLUT5	6	Fructose	Intestine, kidney, sperm	Transport of fructose
GLUT7	0.3	Glucose/fructose not galactose	Intestine	Transport of fructose
GLUT9	0.3	Glucose/fructose not galactose	Kidney, liver	
GLUT11	0.2	Glucose/fructose not galactose	Muscle, heart, fat, placenta, kidney, and pancreas	Muscle-specific; fructose transporter
GLUT6	High Km	Glucose	Brain and spleen	
GLUT8	2.4 (2DG)	Glucose	Testis, brain, fat, liver, and spleen	Fuel supply of mature spermatozoa; insulin-responsive transport in blastocyst
GLUT10	0.3 (2DG)	Glucose/ galactose not fructose	Liver and pancreas	
GLUT12	4-5	Glucose, galactose, fructose	Heart and prostate	
HMIT	0.1	Myoinositol	Brain	H^+/myo-inositol co-transpoter

[1] adapted from (Manolescu, Witkowska et al. 2007; Zhao and Keating 2007)

[2]data collected when the proteins are expressed in *Xenopus* oocytes

* blue background: Class I facilitate transporters; pink background: Class II facilitate transporters; green background: Class III facilitate transporters.

1.3.3 Glucose transport in other organisms

The homologs of passive transporter family are found in *Escherichia coli (E. coli)*, yeast, *Drosophila* and other insects (Baldwin 1993; Escher and Rasmuson-Lestander 1999; Kikawada, Saito et al. 2007). The H^+-linked sugar

transporters in *E. coli* (D–galactose/H^+ symporter (GalP), L–arabinose/H^+ symporter (AraE) and the D–xylose/H^+ symporter (XylE)) are found to be homologous to human GLUT1 (Baldwin 1993). However, xylose is the only substrate of XylE while AraE is more tolerant of variations in sugar substrate (Henderson and Maiden 1990) but does not transport D–glucose. GalP is able to transport both galactose and glucose and, like the mammalian transporter, is inhibited by forskolin (Baldwin 1993). Different from the mammalian glucose transport system, the glucose transporter of *E. coli* acts by a mechanism that couples translocation with phosphorylation of the substrate. It belongs to the family of structurally and functionally related transporters known as enzymes II of the bacterial phosphotransferase system (PTS) (Buhr, Daniels et al. 1992). In yeast, the glucose induction of its own transport is similar to the mammalian transport system. In both cases, glucose increases the number of glucose transporters in the plasma membrane. However, unlike the indirectly regulation of glucose transporter translocation by insulin, glucose increase the cell surface glucose transporter directly by increasing expression of the HXT (yeast hexose transporter) genes (Ozcan and Johnston 1999). However, the characterization of glucose transporters in *C. elegans* and *Drosophila* is largely unknown.

1.4 Aims of the project

Being an experimental model organism, *C. elegans* has great advantage in the studying of ageing and lifespan because of its small size (1mm in length), relatively short lifespan (~3 weeks), rapid reproduction rate, well-characterized genetics, its transparency and the known location and fate of its 959 cells. Moreover, the somatic cells of the adult animal are post-mitotic, making it an attractive model for studying the aging process of non-dividing cells. Besides, aging in *C. elegans* shares many characteristics with aging in humans, such as muscle atrophy, reduced skin elasticity and increased susceptibility to infection. In addition, the entire genome of *C. elegans*

has been sequenced. The inactivation of almost any gene can be accomplished through RNA interference (RNAi) by feeding the worm with bacteria, its laboratory food source, which are expressing double-stranded RNA of the gene of interest.

Although aging research has strongly suggested that endocrine signalling has a key role in many of the pathways that alter the aging process in *C. elegans*, the biology of digestion and nutrient uptake in *C. elegans* remains largely unknown. The role of glucose transporters in *C. elegans* remains veiled. Identifying glucose transporters in the worm and studying of their function may lead to further understanding of the mechanisms of IIS and CR regulation of the lifespan.

The work described in this thesis is aimed at identifying the glucose transporter(s) in *C. elegans* by cloning the putative glucose transporters from the *C. elegans* total cDNA and carrying functional characterization in *in-vitro* systems by heterologous expression in model cell systems. Further *in-vivo* study is also carried out to assess the role of identified glucose transporter in the IIS and CR regulated lifespan extending process.

Chapter 2 Materials and methods

2.1. Materials

2.1.1. Laboratory chemicals and materials

Unless otherwise stated, all chemical reagents were purchased from Sigma or Fisher Scientific. All tissue culture medium and reagents were purchased from Cambrex or Gibco-Invitrogen. Plastic equipment for molecular biology was purchased from Eppendorf, Sterilin or Greiner Bio-One. Plastic equipment for tissue culture was purchased from Greiner Bio-One or Nunc.

Table 2.1 Laboratory Reagents

Reagents	Resources
Molecular biology grade agarose	Lonza
DNA molecular weight markers	Promega or Bioline
SuperSignal West Dura Extended Duration Substrate Kit	Thermo Fisher Scientific
Monocomponent porcine insulin	Calbiochem
Bovine Serum Albumin	Intergen Co.
Protein Molecular markers	Invitrogen
Acrylamide stock (30% acrylamide, 0.8% bis-acrylamide)	Flowgen
d-[U-^{14}C]Glucose (9.25 MBq, 250 µCi)	Amersham

2.1.2. Buffers

The buffer compositions are stated in the context of their use. A compiled full description of the buffers is listed in appendix).

2.1.3. Molecular biology reagents

General molecular biology reagents were purchased from Promega, Invitrogen or Novogen.

1) Oligonucleotide primers

DNA primers were synthesized by Sigma, MWG or Fisher Scientific. Primer sequences, where mentioned, are listed in the corresponding sections.

2) Vectors and constructs

Table 2.2 List of vectors and constructs

Vectors	Resources
pT7Blue	Novagen®
pcDNA3.1 (+)	Invitrogen
pT7TS	Gift from Dr. Adrian Wolstenholme
L4440	Gift from Dr. Adrian Wolstenholme
Constructs	**Resources**
pT7Blue-K09C4.1	Constructed by Anastasia Tsakmaki
pCIS-HA-GLUT4	Gift from Dr. Samuel W. Cushman
pUC19-GLUT1	Constructed by Edwards Lee
L4440-unc22	Gift from Dr. Adrian Wolstenholme

3) Restriction enzymes and ligase

All restriction enzymes and ligase were purchased from Promega. Detailed restriction enzymes used, when mentioned, are listed in the corresponding sections.

2.1.4. Antibodies

The source of antibodies and their appropriate dilutions for western blotting (section 2.2.3) and immunochemistry (section 2.2.6) are shown in the table below. All antibodies were diluted in Phosphate buffered saline (PBS) (154 mM NaCl, 12.5 mM Na_2HPO_4, pH 7.2).

Table 2.3 Sources and dilutions of antibodies used for Western Blot analysis and Immunochemistry

	Antibody	Polyclonal/Monoclonal Purified/Serum	Source	Dilution
Primary	Sheep anti-GLUT4 C-terminus	Polyclonal Purified	In House production	1:1000
	Mouse anti-HA.11 (16B12)	Monoclonal	Covance	1:1000
Secondary	Goat anti-sheep IgG HRP conjugate	-	Sigma	1:4000
	Goat anti-mouse IgG HRP conjugate	-	Sigma	1:4000
	Goat anti-mouse Alexa 633- conjugated	-	Molecular Probes, Invitrogen	1:1000

2.1.5. Protein inhibitors

Unless otherwise stated, protease inhibitors and the concentrations at which they were used are shown in table 2.4 below.

Table 2.4 Protease inhibitors

Inhibitor		Inhibits	Working concentration
Protease inhibitor cocktail	Antipain	Ser and Cys proteases	1 µg/ml (1.65 µM)
	Aprotinin	Ser proteases	1 µg/ml
	Pepstatin A	Ser and Cys proteases	1 µg/ml (1.46 µM)
	Leupeptin	Acid proteases	1 µg/ml (2.1 µM)
AEBSF		Ser proteases	100 µM

2.1.6. *C. elegans* strains

A list of *C. elegans* strain used in this thesis is list in table 2.5 below.

Table 2.5 List of *C. elegans* strains

Strains	Resources
wild type N2	Gift from Dr. Adrian Wolstenholme
CB1370 (*daf-2*)	Purchased from CGC
TJ1052 *(age-1)*	Purchased from CGC
GR1310 *(akt-1)*	Purchased from CGC

*CGC: Caenorhabditis Genetics Center

2.1.7. Cell line

The cell line used in the project was Chinese hamster ovary cells stably expressing insulin receptor (CHO-T cells).

2.2. Methods

2.2.1. *C. elegans* maintenance

1) Preparation of bacterial food source and seeding of NGM petri plates

A glycerol stock of *E. coli* OP50 (gift from Dr. Adrian Wolstenholme) was streaked on to the Luria Broth (LB) agar plate (1% [w/v] Bacto^{TM} Tryptone, 0.5% [w/v] Bacto^{TM} Yeast Extract, 0.5% NaCl, pH 7.5, 1.5% agar, autoclaved) using aseptic technique and incubated overnight at 37°C. On the next day, a single colony from the streak plate was inoculated aseptically in to 100 ml LB medium (1% [w/v] Bacto^{TM} Tryptone, 0.5% [w/v] Bacto^{TM} Yeast Extract, 0.5% NaCl, pH 7.5, autoclaved). The inoculated culture was left to grow overnight at 37°C with 250 *g* shaking. The *E. coli* OP50 solution was then stored at 4°C and ready for use in seeding.

When seeding, the appropriate amount of *E. coli* OP50 liquid culture (approximately 50 µl to small or medium plates or 100 µl to large plates) was applied to Nematode Growth Medium (NGM) plates (composition and preparation see appendix 1).) using sterile technique. The bacteria lawn was allowed to grow overnight at room temperature (RT) or at 37°C for 8 h (the plates were cooled to RT before adding worms).

2) Maintenance of *C. elegans*

C. elegans was maintained on the NGM plates pre-seeded with *E. coli* OP50 bacteria as food source. The general stock of all *C. elegans* strains except for CB1370 was maintained at 20°C. CB1370 was maintained at 15°C.

2.2.2. Molecular biology techniques

1) Total RNA Extraction and First-strand cDNA synthesis

C. elegans of mixed stages on a 9 cm NGM plate were washed 2 times with sterile M9 buffer (22 mM KH_2PO_4, 22 mM Na_2HPO_4, 85 mM NaCl, 1 mM $MgSO_4$) and transferred into 50 ml Falcon tubes. The worm pellet was collected by spinning at 1500 *g* for 5 min. The SV Total RNA Isolation System (Promega) was used for the total RNA extraction following the instructions in the technical manual supplied with the kit. The yield and quality of extracted RNA were determined using the Eppendorf® photometer.

First-strand cDNA was synthesised using SuperScript™ III First-Strand Synthesis for RT-PCR system (Invitrogen). The guideline provided with the kit was followed.

2) PCR amplification

The target gene was amplified by *Pfu Turbo* DNA polymerase (Stratagene) with the corresponding forward primer and reverse primer in the presence of 1X cloned *Pfu* reaction buffer (2 mM $MgCl_2$; Stratagene). The composition of each reaction is listed in Table 2.6 below. The final volume of each sample reaction is 50 µl.

Table 2.6 Reaction mixture for a single PCR reaction

Component	Amount per reaction	final concentration
DNA template	2 µl or 50 ng[a]	-
10 mM dNTP	1 µl	200 µM
10 µM forward primer	1 µl or 1.25 µl[a]	200 nM or 250 nM[a]
10 µM reverse primer	1 µl or 1.25 µl[a]	200 nM or 250 nM[a]
10X reaction buffer	5 µl	1X
DNA polymerase	1 µl	2.5 U
ddH_2O	Up to 50 µl	-

a When quick change site-directed mutagenesis is conducted, 50 ng of DNA template and 250 nM of the final concentration of primers were used.

The appropriate PCR condition was adopted according to the experiment purpose (see Table 2.7 and Table 2.8). PCR amplification was performed using a PTC-100TM programmable thermal controller (MJ Research, Inc).

Table 2.7 PCR cycling condition for general cloning

Segment	Number of cycles	Temperature	Duration
1	1	95°C	2 min
2	30 ~ 35	95°C	30 sec
		Primer T_m - 5°C	30 sec
		72°C	1 min for targets ≤ 1 kb 1 min per kb for targets > 1 kb
3	1	72°C	10min

Table 2.8 PCR cycling condition for quick change site-directed mutagenesis

Segment	Number of cycles	Temperature	Duration
1	1	95°C	30 sec
2	20	95°C	1 min
		55°C	1 min
		72°C	1 min per kb

3) Preparation of Competent XL-1 Blue Cells

A glycerol stock of XL-1 Blue cells (Stratagene) was streaked onto the LB agar plate (1% [w/v] Bacto^{TM} Tryptone, 0.5% [w/v] Bacto^{TM} Yeast Extract, 0.5% NaCl, pH 7.5, 1.5% agar, autoclaved) containing 12.5 μg/ml tetracycline and incubated overnight at 37°C. On the next day, a single colony of XL-1 Blue was inoculated into 2.5 ml LB medium (1% [w/v] Bacto^{TM} Tryptone, 0.5% [w/v] Bacto^{TM} Yeast Extract, 0.5% NaCl, pH 7.5, autoclaved) containing 12.5 μg/ml tetracycline and incubated overnight at 37°C with 250 *g* shaking. The entire overnight culture was inoculated into 250 ml LB medium (containing 20 mM $MgSO_4$ and 12.5 μg/ml tetracycline) incubating at 37°C with 250 *g* shaking. The growth of the culture was monitored by taking OD readings. Incubation was stopped until the OD A_{600} of the culture reached 0.4~0.6. XL-1 Blue cells were then pelleted by centrifuging at 2000 *g* for 10 mins at 4°C. Supernatant was discarded and the pellets of the XL-1 Blue were suspended in 100 ml ice cold TFB1 buffer (100 mM RbCl, 50 mM $MnCl_2$, 30 mM Potassium acetate, 10 mM $CaCl_2$, 15% glycerol [v/v], pH 5.8). The suspension was incubated at 4°C for 5 min. Cells were then pelleted at 2000 *g* for 10 min at 4°C. The supernatant was discarded. Pelleted cells were gently resuspended in 10 ml TFB2 (10 mM RbCl, 10 mM MOPS, 75 mM $CaCl_2$, 15% glycerol [v/v], pH 6.5) and incubate at 4°C for 15~60 mins. 100 μl of resuspended cells were then aliquoted into tubes on dry ice/isopropanol bath and stored at -80°C.

4) Transformation

One aliquot of competent XL-1 Blue cells for each sample was thawed at 4°C for 5 min. 10~100 pg of super-coiled DNA or 2 µl of ligation mixture (containing 100 ng of vector DNA) was added to the defrosted cells, mixed gently and then incubated at 4°C for 5 min. The cells were heat-shocked at 42°C for 1 min and returned to 4°C immediately. The mixture was then added to 500 µl LB medium and incubated at 37°C with 250 *g* shaking for 45 mins. The cells in LB medium were then scraped onto a LB agar plate containing the appropriate antibiotics. The plates were left to dry and then incubated overnight at 37°C.

5) Colony PCR

A single colony was picked by a fine yellow tip and suspended in 10.5 µl of dd H_2O. The suspension was then heated at 95°C for 10 minutes. A PCR mixture was prepared on ice during the heating. GoTaq® Green Master Mix (Promega) was used for the colony PCR reaction. The PCR reaction mixture for each colony is listed in Table 2.9 below.

Table 2.9 Reaction mixture for a single colony PCR reaction (25 µl reaction volume)

Component	Amount per reaction	final concentration
GoTaq® Green Master Mix, 2X	12.5 µl	1X
10 µM forward primer	1 µl	200 nM
10 µM reverse primer	1 µl	200 nM
Colony suspension	10.5 µl	-

PCR amplification was performed using a PTC-100TM programmable thermal controller (MJ Research, Inc). The colony PCR condition is listed in Table 2.10.

Table 2.10 PCR cycling condition for colony PCR

Segment	Number of cycles	Temperature	Duration
1	1	95°C	2 min
2	25	95°C	30 sec
		Primer T_m - 5°C	30 sec
		72°C	1 min for targets ≤ 1 kb 1 min per kb for targets > 1 kb
3	1	72°C	10min

6) Plasmid DNA preparation

One single *E. coli* colony was picked from LB agar plates with appropriate antibiotics, inoculated into 10 ml LB medium containing appropriate antibiotics and incubated overnight at 37°C with 250 *g* shaking. The overnight culture was pelleted at 2000 *g* for 5 mins. The DNA was prepared using the Wizard Plus SV Minipreps DNA purification system (Promega) Kit. The protocol provided with the kit was followed.

7) Restriction digests

Test digests were performed in a final volume of 7.5 µl and usually 1 µl of DNA was used. In cases that digested products were needed for further applications 2 µg of DNA were digested in final volume of 15 µl. The digest mixture was incubated at 37°C for hours or overnight depending on the efficiency of the enzyme.

Digest system:	10 × buffer	1.5 µl
	10 × BSA	1.5 µl
	Enzyme	1 µl
	DNA	2 µg
	double distilled H_2O (dd H_2O)	up to 15 µl

8) Agarose gel electrophoresis

Agarose solutions were prepared at a concentration appropriate for separating the at expected fragments in the DNA samples (Table 2.11) by melting the correct amount of powered agarose in certain volume of Tris-acetate EDTA (TAE) buffer (40 mM Tris-acetate, 1 mM EDTA, pH 8.5). The molten gel was cooled at RT to approx. 55°C. SYBR Safe™ DNA gel stain (Invitrogen) was added to the solution to a final concentration of 0.1% (v/v). The warm solution was then poured into a mold with appropriate comb for forming the sample slots in the gel. The gel was allowed to set completely at RT. The comb was then removed and the gel was mounted in the electrophoresis tank. TAE buffer was added to just cover the gel to a depth of approx. 1mm. DNA samples was mixed with 0.2 volume of gel-loading buffers (30% [v/v] glycerol, 0.25% [w/v] bromophenol blue, 0.25% [w/v] xylene cyanol). 1kb DNA ladder (Promega) was used as DNA marker. DNA samples and markers were loaded into the slots. A voltage of 1 ~ 5 V/cm was applied to separate the DNA samples. When the dyes had migrated a sufficient distance through the gel, the gel was examined by UV transillumination and photographed.

Table 2.11 Range of Separation in Different Amounts of Agarose

Agarose Concentration in Gel (% [w/v])	Range of Separation of Linear DNA Molecules (kb)
0.3	5-60
0.6	1-20
0.7	0.8-10
0.9	0.5-7
1.2	0.4-6
1.5	0.2-3
2.0	0.1-2

9) Gel band excision and purification

The desired DNA fragments were quickly separated from the gel by using a razor blade to make an incision in the gel directly with illumination by UV light. Each excised gel band was then placed into a weighed 1.5 ml Eppendorff® tube. Then a DNA purification procedure was carried out using the Wizard® SV Gel and PCR Clean-Up System (Promega). After DNA purification, the concentration of the DNA solution was measured using the Eppendorf® photometer.

10) Ligation

A LigaFast™ Rapid ligation system (Promega) was used to ligate DNA fragments. The amount of vector and insert DNA needed in the ligation was calculated using the following formula:

$$100 \quad ng \quad vector \times \frac{insert(kb)}{vector(kb)} \times \frac{2}{1} = ng \quad insert$$

A 10 µl system was used for the ligation reaction:

plasmid	100 ng
insert DNA	X ng
2 × buffer	5 µl
T4 DNA ligase	1 µl
ddH_2O	up to 15 µl

The ligation reaction was carried out at RT for 5~10 min. A negative control was conducted every time in which the insert DNA was replaced by the same volume of ddH_2O.

11) Phosphorylation of double-stranded oligos

In the presence of 1x Promega Buffer E, Plus and minus oligos were annealed in a 100 µl system (10 µM of each primer, 6 mM Tris-HCl, 6 mM $MgCl_2$, 100 mM NaCl, 1mM Dithiothreitol (DTT)) by heated at 95°C for 5 min in water bath and left cool to RT in the water bath.

The annealed oligos were then added to the phosphorylation mixture listed below and incubated at 37°C for 1 h. After the phosphorylation, 0.5 µl 0.5 M EDTA was added to the mixture, and the T4 Polynecleotide Kinase (T4 PNK) (Promega) was heat inactivated at 68°C for 10 min. The phosphorylation mixture was then diluted to 200 µl. 2 µl of the solution (100 nM phosphorylated oligos) was used in the ligation.

Phosphorylation system:	Annealed oligos	2 µl
	10 mM ATP	1 µl
	10 X T4 PNK buffer	0.5 µl
	T4 PNK	1 µl
	dd H_2O	up to 5 µl

12) Dephosphorylation of the vector

Linearized vector was gel-purified and freeze-dried to the appropriate concentration. 1 µg of the purified vector was added to a 20 µl dephosphorylation mixture system containing Promega MULTI-CORE^{TM} Buffer (25 mM Tris-Acetate, pH 7.5 (at 37°C) 100 mM potassium acetate, 10 mM magnesium acetate, 1 mM DTT) and 15 units of Thermosensitive Alkaline Phosphatase (TSAP) (Promega). The reaction mixture was incubated at 37°C for 15 min. The TSAP was then heat-inactivated at 74°C for 15 min. 40 ng of the dephosphorylated vector was used in the ligation reaction.

13) Sequencing

All the DNA sequencing was carried out using the service provided by either MWG Biotech or GATC Biotech.

2.2.3. Protein biochemistry techniques

1) Protein assay

Total protein concentration of the cell lysate was estimated using the bicinchoninic acid (BCA™) Protein Assay Kit (PIERCE). The procedure in the manual was followed. Briefly, a standard curve of BSA using a 1 mg/ml BSA (in 0.1 M NaOH solution) was prepared by adding 20 µl of 1 – 10 µg BSA to the Microtitre plate (Sterilin) in duplicate. The appropriate amount of cell lysate was either diluted with 0.1 M NaOH or undiluted to make the total volume 20 µl. The BCA working reagent was prepared by mixing Reagent A (1% BCA-NO_2, 2% $Na_2CO_3 \cdot H_2O$, 0.16% Na_2tartarate, 4% NaOH, 0.95% $NaHCO_3$) and Reagent B (4% [w/v] $CuSO_4 \cdot 5H_2O$) at the ratio of 50:1. 200 µl working reagent was then added to each of the 20 µl cell lysate samples and the standards in Microtitre plate wells. The mixtures were incubated at 37°C for 30 min with lid in place and then allowed to cool to RT. The absorbance of the reaction solution was measured at 565 nm on a microplate spectrophotometer (Tecan).

2) Sodium dodecyl sulfate - polyacrylamide gel electrophoresis (SDS-PAGE)

A concentrated SDS sample buffer (187.5 mM Tris-HCl, pH 6.8, 300 mM DTT, 6% [w/v] SDS, 0.03% [w/v] bromophenol blue, 30% [v/v] glycerol) was prepared and stored at RT. 1 M DTT stock solution was prepared in small aliquotes and stored at –20°C. At the time of use, reducing agent DTT was added freshly. Protein samples were solubilized in sample buffer (62.5 mM Tris-HCl, pH 6.8, 2% [w/v] SDS, 0.01% [w/v] bromophenol blue, 10% [v/v] glycerol) with 20 mM DTT added. The samples were then denatured at 95°C – 100°C for 5 - 10 min in a heating block.

The Laemmli discontinuous buffer system was used for the electrophoresis. Slab gels were prepared using the mini-Protean 3 system (Bio-rad). All gels were made to a thickness of 1.5 mm. 10% resolving gels and 6% stacking gels were prepared using the buffer system listed in Table 2.12. Polymerisation was initiated by the

addition of N,N,N,N'-tetramethylethylenediamine (TEMED) and ammonium persulphate (APS), both to 0.05% (v/v) final concentration. Gels were run at a constant 200 V in electrophoresis running buffer (25 mM Tris-HCl, pH6.3, 0.1% [w/v] SDS, 0.2 M Glycine) for approximately 1 h until the bromophenol blue dye just ran off the bottom of the gel. Novex® Sharp Protein Standard (3.5 – 260 kDa) (Invitrogen) was used as marker (Figure 2.1 A).

Table 2.12 SDS-PAGE gel solution composition

A. 10% Running gel solution (for 15 ml)	
H_2O	6.15 ml
Resolving gel Buffer (1.5 M Tris-HCl, pH 8.9, 0.4 % [w/v] SDS)	3.8 ml
Proto Gel® (30%[w/v] Acrylamide:0.8%[w/v] Bis-acrylamide 37.5:1)	5 ml
10% APS	56 µl
TEMED	12.6 µl
B. 6% Stacking gel solution (4% Acrylamide) (for 20 ml)	
H_2O	10.87 ml
Stacking gel Buffer (0.5 M Tris-HCl, pH6.8, 0.4% [w/v] SDS)	5 ml
Proto Gel® (30% [w/v] Acrylamide:0.8% [w/v] Bis-acrylamide 37.5:1)	3.99 ml
10% APS	73.3 µl
TEMED	16.8 Ml

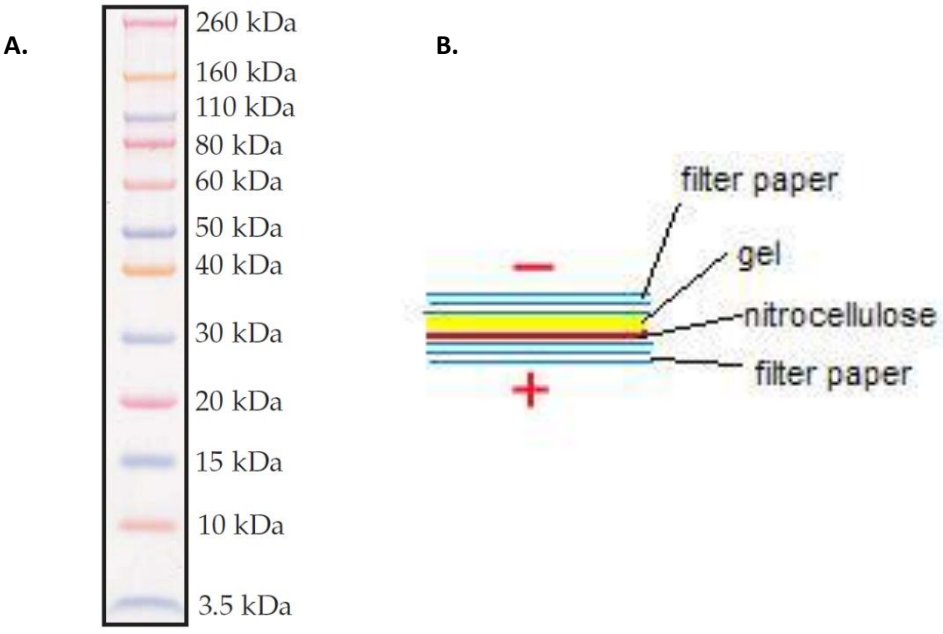

Figure 2.1 A. The molecular weights of the protein bands in the Novex® Sharp Proein Standard
B. Transfer schematic diagram

3) Electrophoretic transfer to nitrocellulose membrane

Proteins resolved in the SDS-gel were transferred onto nitrocellulose membrane using the Multiphor II Novablot electrophoretic transfer apparatus (Pharmacia) by the semi-dry transfer method. 18 pieces of 3mm Whatman filter paper and one piece of nitrocellulose were cut to the same size as the running gel and soaked in transfer buffer (48 mM Tris, 39 mM glycine, 0.0375% SDS [w/v], 20% [v/v] methanol, pH8.8 without adjusting) for 10 min. The stacking gel was removed from the running gel. The running gel was immersed in transfer buffer for 10 min. Nine sheets of filter paper were placed onto the anode electrode of the transfer apparatus, then the nitrocellulose membrane, the gel, and the other nine sheets of filter paper on the top (Fig. 2.1 B). Air bubbles were removed by rolling a 15 ml falcon tube over the blot. The cathode was dampened with transfer buffer and was placed above the blot on the anode. The transfer process was run for 1 h and 50 min at a constant current of 0.8 mA × the surface area of the gel in cm^2. After transfer, the nitrocellulose membrane was washed with double-distilled water and stained with Ponceau dye solution (0.1% [w/v] Ponceau, 3% [w/v] trichloroacetic acid (TCA)) for 2-3 min. Excess stain was washed off with distilled water so that the protein bands could be visualized. Markers were marked with a pencil after the membrane was dried.

4) Western blot analysis

The nitrocellulose membrane was washed with Tris-buffered Saline (TBS) - Tween washing buffer (9% [w/v] NaCl, 100 mM Tris, 0.1% [v/v] tween-20) to be re-hydrated and to remove the Ponceau S stain. The membrane was then blocked in blocking buffer (5% [w/v] dried skimmed milk (Marvel), 1 × TBS, 0.1% [v/v] tween-20) with gentle rocking either at RT for 30-60 min or at 4°C overnight to block non-specific protein binding sites. Blocking buffer was discarded. The membrane was washed with TBS-Tween washing buffer for couple of times followed by incubation with the primary antibody, at the required dilution (section 2.1.4) in TBS-Tween buffer

containing 1% (w/v) BSA, for 2 h at RT or overnight at 4°C with gentle rocking. The membrane was then washed with washing buffer for several quick wash and four long wash for 15 min with shaking. After washing, the membrane was immersed into the secondary antibody, at required dilution (section 2.1.4) in blocking buffer for 45 min to 2 h at RT with shaking. After the secondary binding, the membrane was washed with washing buffer by repeating the same wash after the primary binding.

The membrane was developed using SuperSignal® West Dura Extended Duration Substrate (Pierce) or AmershamTM ECL Advance (GE Healthcare) following the manufacturer's guideline. In brief the two reagents were mixed at a 1:1 ratio and the membrane was incubated the mixture for 5 min at RT. The chemiluminescent signals were detected with an EPI Chemi II darkroom imaging system (UVP). For experiments where protein bands were quantified by densitometry, multiple exposures of the blots were performed to ensure that the analysis was performed in the linear range of signal densities.

2.2.4. Maintenance of CHO-T cells

All the cell culture work was carried out in a class 2 Laminar flow cabinet, using aseptic techniques. CHO-T cells were maintained in Ham's F-12 medium with L-glutamine with 10% (v/v) fetal bovine serum (FBS) and 450 µg/ml G-418 in 9 cm cell culture dishes. Unless otherwise stated, this medium composition was used throughout.

Cells were passaged at 90% confluency. Spent medium was removed. Dead cells were washed off by rinsing the cells with PBS (OXOID) (half volume of the culture medium). The cell monolayer was detached by trypsinising with Trypsin EDTA. Cells were examined under the microscope to make sure that all of the cells were detached. Detached cells were then transferred into 20 ml of fresh medium and spun at 1000 *g* for 2 min at 18°C. The cell pellet was resuspended in 2 ml fresh medium.

One tenth of the cell suspension was then seeded into a new labelled dish with the addition of fresh medium. The cells in new dish were incubated at 37°C/5% CO_2. Cells were observed under microscope to detect any changes in the cells or contamination everyday. Medium was changed every 48 h.

2.2.5. Transfection of CHO-T cells

CHO-T cells were passaged into 3.5 cm cell culture dishes one day before transfection to make sure that they could reach 60~70% confluency on the next day. Lipofectamins (Invitrogen) was used as transfection reagent. The ratio of transfection reagent to DNA was 8:1. On the day of transfection, solution A and solution B were prepared as follows:

- Solution A : 1 µg DNA + 100 µl serum free Ham's F-12 medium

- Solution B: 8 µl lipofectamins + 92 µl serum free Ham's F-12 medium

The two solutions were thoroughly mixed and incubated at RT for 35 min. During the period, medium for CHO-T cells was replaced by serum free Ham's F-12 medium for several times (approx. once/10 min). A and B solution mixtures were then mixed with 800 µl serum free Ham's F-12 medium and added onto the cells. Cells covered with DNA and lipofectamins mixture were then incubated at 37°C/5% CO_2 for approx. 5 h. Afterwards, the transfection mixture was replaced by fresh Ham's F-12 medium with L-glutamine with 10% (v/v) FBS and 450 µg/ml G-418. Cells were incubated at 37°C / 5% CO_2.

2.2.6. Immunochemistry and confocal microscopy

Cells seeded on cover slips one day prior to the experiment were washed with PBS and fixed with 4% paraformaldehyde (PFA) in PBS for 30 min at RT. Cells were washed with PBS three times. The fixed cells were incubated in blocking solution

(3% goat serum, 1% BSA in PBS, pH7.2) for 2 h at RT. The cells were then incubated in blocking solution in the presence of appropriately diluted primary antibody (Table 2.3) overnight at 4°C with shaking. On the next day, cells were washed 3 times (10 min each time) with wash solution (1% BSA in PBS). Cells were then incubated in blocking solution with the appropriately diluted secondary antibody (Table 2.3). Cells were then washed with wash solution and mounted in Vector shield (Vector Laboratories). Fluorescent signals were detected using confocal laser scanning microscope Zeiss LSM510META (Zeiss) at the appropriate wavelength. Pictures were taken using a 63× oil immersion lens.

2.2.7. Heterologous expression of the putative glucose transporters of the *C. elegans* in *Xenopus* oocytes

1) Preparation of *Xenopus* oocytes

Adult *Xenopus laevis* females (European *Xenopus* Resource Centre, Portsmouth) was anesthetized by immersion in 0.2% benzocaine in tap water for 15 min. Lobes of the ovary were surgically removed and rinsed with Ca^{2+} free OR-2 buffer (82.5 mM NaCl, 2.5 mM KCl, 1 mM $NaHPO_4$, 1 mM $MgCl_2$, 5 mM HEPES, pH 7.5). The ovary lobes were then placed in sterile petri-dish and teased into small pieces (~ 0.5 cm in diameter). Teased ovary lobe pieces were washed 3 times with Ca^{2+} free OR-2 buffer. 5 ml of the lobe pieces were transferred in a new sterile 50 ml conical tube. The oocytes were separated by adding 10 ml of collagenase type II (Sigma) (1.5 mg/ml, in Ca^{2+} free OR-2) to approximately equal volume of teased ovary pieces and incubating for 1.5 h with gentle agitation at 18°C. Oocytes were then washed 3 times with Ca^{2+} free OR-2 and once with complete ND96 buffer (96 mM NaCl, 2 mM KCl, 1 mM $MgCl_2$, 1.8 mM $CaCl_2$, 5 mM HEPES pH 7.5, 2.5 pyruvic acid, 1% FBS). Healthy stage V and VI oocytes were selected and maintained in complete ND96 with gentle agitation at 4°C for subsequent procedures.

2) Preparation of linearized DNA template

Test digests were performed prior to the experiment to determine the complete digest time for each DNA template by agarose gel electrophoresis. The following work was carried out in an RNAase free environment. 10 µg of template DNA were linearized by the appropriate restriction enzyme in a 100 µl system at 37°C for the appropriate amount of time. The digest mixture was then purified using the Wizard® SV Gel and PCR Clean-Up System (Promega). The concentration of purified DNA solution was adjusted to 200 ng/µl by freeze-drying.

3) In vitro cRNA transcription and purification of cRNA

The linearized plasmids were transcribed using T7 RNA polymerase in the presence of cap analog (mMESSAGE mMACHINE; Ambion, Austin, TX) following the instructions in the manual. The transcribed RNA was purified by phenol:chloroform extraction and isopropanol precipitation. Briefly, the transcription reaction was stopped by adding 115 µl nuclease-free water and 15 µl Ammonium Acetate Stop Solution (provided by the kit). The complementary RNA (cRNA) was extracted with same volume of phenol/chloroform (5:1 [v:v], for molecular biology, Sigma). The aqueous phase was recovered to new nuclease-free tube and cRNA was then extracted with same volume of chloroform (for molecular biology, Sigma). The extracted cRNA in the aqueous phase was then precipitated with the same volume of isopropanol. The mixture was stored at -20°C overnight. On the next day, cRNA was pelleted by centrifuging at 14000 *g*, 4°C for 15 min. Supernatant was then removed carefully. The cRNA was resuspended in nuclease-free water. The amount of purified cRNA was determined using an eppendorf photometer and the concentration of the solution was adjusted to 1 µg/µl by adding the appropriate amount of nuclease-free water. The cRNA solution was stored frozen at -80°C for subsequent procedure. All the above work was carried out in an RNAase free environment.

4) Microinjection of *Xenopus* oocytes

Capillary glass (Anachem) was pulled to micropipette on a P-30 vertical micropipette puller (Sutter instrument), using conditions of a high heat 990, pull force 580. The capillary was then filled with mineral oil (for molecular biology, Sigma) using a 1 ml syringe with 100 µl flat tip HPLC needle and attached to the injector. Excessive mineral oil was emptied. 2 µl of sample cRNA solution (1 µg/µl) or 2 µl of nuclease-free water was pipetted into the capillary for subsequent microinjection.

Healthy stage V and VI *Xenopus* oocytes were selected for the microinjection procedure. 50 ng of cRNA or the same volume (50 nl) of diethyl pyrocarbonate (DEPC)-treated water (as blank control) was injected into the oocytes under dissection microscope using the Nanoject Auto-Nanoliter injector (Drummond scientific company). Oocytes were maintained at 18°C in complete ND96 with the medium changed every day. 72 h after injection, healthy oocytes were selected for subsequent experiments.

2.2.8. Transport assays in the *Xenopus* oocytes

1) Glucose transport assay

Healthy *Xenopus* oocytes injected with appropriate cRNA or H_2O were washed 3 times with incomplete ND96 buffer (96 mM NaCl, 2 mM KCl, 1 mM $MgCl_2$, 1.8 mM $CaCl_2$, 5 mM HEPES, pH 7.5) and incubated in incomplete ND96 for 1h at 18°C. Oocytes were then transferred in groups of 5 to each well of a 12-well plate (Nunc) in triplicate. Glucose transport activity of the oocytes was determined by incubating groups of 5 oocytes in incomplete ND96 with or without the appropriate amount of D-glucose for 30 sec before the addition of U-[^{14}C]-glucose (Amersham, GE Healthcare) (0.3 µCi per assay). The reaction was stopped after 60 min by rapidly washing the oocytes 3 times with ice-cold incomplete ND96 containing 300 µM phloretin. Each group of oocytes was solubilized in 500 µl solubilization buffer (1%

SDS [w/v]) for 3~4 h at RT. 450 µl of the lysate of each group was transferred into individual scintillation vial and used for determination of radioactivity in addition of scintillation liquid on a scintillation counter.

2) Trehalose transport assay

✧ **Trehalose uptake**

Healthy *Xenopus* oocytes injected with appropriate cRNA or H_2O were washed 3 times with incomplete ND96 buffer (96 mM NaCl, 2 mM KCl, 1 mM $MgCl_2$, 1.8 mM $CaCl_2$, 5 mM HEPES, pH 7.5) and incubated in incomplete ND96 buffer for 1h at 18°C. Oocytes were then transferred in groups of 60 oocytes to each well of 12-well plate. The trehalose uptake was then carried out by incubating the oocytes in incomplete ND96 buffer with or without 100 mM trehalose at RT for 3 h. After the incubation, each group of oocytes was transfer to 4 ml polypropylene tube and washed 3 times with ice cold ddH_2O. The oocytes were then homogenized with 5 strokes in a 2 ml homogenized (Thomas Scientific) and resuspended in 1 ml ddH_2O. The suspension was centrifuged twice at 14,000 *g* for 10 min at 4°C. 800 µl of the supernatant was kept and stored at 4°C for subsequent procedure.

✧ **Trehalase treatment**

Citric acid stock buffer (1.35 M, pH 5.7 at 37°C) and Tris-HCl buffer (5 M, pH 7.5 at 37°C) were prepared in advance and store at RT. Trehalase enzyme solution was prepared on ice just before use by diluting the appropriate amount of trehalase (Sigma) in ice cold 135 mM citric acid buffer. A positive control solution was prepared by adding 100 mM trehalose stock solution to 135 mM citric acid buffer to the final concentration of 4 mM. A pre-experiment was carried out to determine the maximum time for 0.01 unit of trehalase completely digesting the amount of trehalose in 400 µl positive control solution. 400 µl supernatant from trahalose uptake experiment was mixed with 50 µl citric acid stock buffer and incubated in 37°C water bath. The digest

was initiated by adding the trehalase enzyme solution (0.01 unit per assay) to the sample solution, whereas in the negative control samples the trehalase enzyme solution was replaced by the same volume of 135 mM citric acid solution (pH 5.7 at 37°C). The mixture was incubated at 37°C for the time tested in the pre-experiment. The reaction was stopped by adding 25 µl of the Tris-HCl buffer (5 M, pH7.5 at 37°C). The mixture was then removed from the 37°C water bath and cooled to RT for subsequent glucose concentration analysis.

✧ **Glucse concentration analysis**

A Glucose (GO) Assay kit (Sigma) was used to determine the amount of glucose in the sample solution after the trehalase treatment (section 2.2.8 – 2). The instructions in the manual were followed. In brief, a standard curve of glucose using a 1 mg/ml glucose stock solution was prepared by adding 20 µl of 1 – 10 µg glucose solution (in 135 mM citric acid) to the Microtitre plate (Sterilin) in duplicate. The assay reagent was prepared by dissolving the contents of the Glucose Oxidase/Peroxidase Reagent capsule in 39.2 ml ddH_2O and then mixing with 800 µl o-Dianisidine Reagent. The assay reagent was stored in 2-8°C for one month. 150 µl of the sample solution was added to the Microtitre plate in triplicate. 200 µl of the assay reagent was mixed with sample solution and the mixture was then incubated at 37°C for 30 min. The absorbance of the reaction solution was measured at 540 nm on a microplate spectrophotometer (Tecan).

2.2.9. HA-antibody surface binding assay

1) HA-antibody surface binding assay in *Xenopus* oocytes

Healthy *Xenopus* oocytes injected with ddH_2O or sample cRNA were selected 72 h after injection. The oocytes were washed with incomplete ND96 buffer (96 mM NaCl, 2 mM KCl, 1 mM $MgCl_2$, 1.8 mM $CaCl_2$, 5 mM HEPES, pH 7.5). Anti-HA mouse

monoclonal antibody was diluted in 1:1000 (1 µg/ml) in incomplete ND96 buffer with 1% BSA. Groups of 6 oocytes were incubated in 100 µl primary antibody solution for 2 h at RT with inverting. The oocytes were then washed with incomplete ND96 buffer with 1% BSA 3 times (10 min each time). The secondary antibody solution was prepared by diluting anti-mouse IgG β-Galactosidase conjugate (SouthernBoitech) at 1:1000 (1 µg/ml) in incomplete ND96 buffer with 1% BSA. The oocytes were then incubated in secondary antibody solution for 1 h at RT. The oocytes were washed once with incomplete ND96 buffer with 1% BSA and 3 times with incomplete ND96 buffer. Groups of two oocytes were transferred to each well of the 96 well black plates (Greiner) containing 100 µl of incomplete ND96 buffer. A working solution was prepared just before use by adding the 40 mM Fluorescein di-β-D- galactopyranoside (FDG) stock solution in dimethylsulfoxide (DMSO) to incomplete ND96 to the final concentration of 0.2 mM. The surface binding was initiated by adding 100 µl of the working solution to each well. The fluorescence (emission 512 nm/excitation 488 nm) was measured in bottom reading mode using a flouresecent microtiter plate reader (FLUOstar Galaxy; BMG labtechnologies).

2) HA-antibody surface binding assay in primary rat adipocytes

✧ **Preparation of rat adipocytes**

Isolated rat adipocytes were prepared from the whole epididymal pads of male Wistar rats (180 – 200 g) as described (Taylor and Holman 1981; Simpson, Yver et al. 1983; Quon, Zarnowski et al. 1993). The rats were stunned and the necks were dislocated. The epididymal fat tissue was quickly removed and kept in 37°C pre-warmed Krebs-Ringer HEPES (KRH) buffer (140 mM NaCl, 4.7 mM KCl, 2.5 mM $CaCl_2$, 1.25 mM $MgSO_4$, 0.2 mM NaH_2PO_4, 10 mM HEPES, 200 nM adenosine, pH 7.4) with 1% (w/v) BSA added. The rinsed fat tissue was transferred in adipocyte digestion buffer (3.5% [w/v] BSA in KRH supplemented with 5 mM glucose and 500 µg/ml Collagenase type 1 from *Clostridium histolyticum*) in a 23 ml polystyrene

flat-bottomed tube (Sarstedt), and minced finely with scissors. The minced tissue suspension was shaken rapidly in a shaking water bath at 37°C for approx. 20 – 25 min until most of the tissue lumps were digested. The cell suspension was then filtered through a nylon mesh (250 µm mesh size, Lockertex), into a fresh 23 ml polystyrene flat-bottomed tube. The filtered cells were washed with KRH with 1% (w/v) BSA, and returned to 37°C water bath allowing the cells to float. The infranatant buffer was removed using a needle (2mm diameter X 100 mm) attached to a 20 ml plastic syringe. 15 – 20 ml KRH with 1% (w/v) BSA was added and the cells were gently resuspended and allowed to float. The above wash procedure was repeated twice. The cells were then washed twice with 37°C Dulbecco's modified Eagle's medium (DMEM) containing 25 mM glucose, 25 mM HEPES, 4 mM L-glutamine, 200 nM adenosine, and 75 µg/ml gentamycin. The cell suspension was adjusted to a cytocrit of 40% (≈ 5-6 x 10^6 cells/ml) by using a capillary tube which was centrifuged at 1000 *g* for 1 min and expressed as the ratio of the length of the packed cell fraction in the tube to the total length of the suspension in the tube. The cells were then incubated at 37°C and ready for further use.

✧ Transfection of the rat primary adipocytes by electroporation

The electroporation procedure was performed as described previously (Quon, Zarnowski et al. 1993; Al-Hasani, Hinck et al. 1998). 200 µl of DMEM medium containing 200 nM adenosine was mixed with 100 µg of carrier DNA (sheared herring sperm DNA, Invitrogen) and the appropriate amount of expression plasmids as indicated. The total concentration of plasmid DNA in each cuvette was adjusted to 5 µg/cuvette with empty pCIS2 vector. The mixture was added to a 0.4-cm gap-width cuvettes (Bio-rad). The isolated adipose cells incubated at 37°C were gently resuspended and 200 µl of the cells was added to the cuvette and gently mixed with the DNA mixture. The cuvette was quickly placed in the cuvette holder of the Gene Pluser Electroporator (Bio-rad) and slid into place such that the cuvette was in contact with the electrodes. The electroporation was carried out by applying one

pulse (12 ms, 400V) to the cells. 4 cuvettes of cells were pooled into a 15 ml conical tube. The cuvettes were washed once with 37°C DMEM medium containing 200 nM adenosine and the washed solution was also collected into the same conical tube. The cells were washed once with 37°C DMEM medium containing 200 nM adenosine and allowed to float. The infranatant was removed and the adipose cells were resuspended in 3 ml DMEM containing 3.5% BSA, 200 nM adenosine, and 75 µg/ml gentamycin. The cells were then transferred to 3 cm petri dish and incubated at 37°C, 5% CO2 for 5 h.

✧ **Cell surface antibody binding assay**

The dishes containing transfected adipose cells were removed from the incubator. Half of the medium was removed by 17 *g* blunt needle attached to 5 ml syringe. The cells were gently swirled to mix and transferred to 4 ml tubes which were marked with 1 ml and 2 ml on the side. The cells were washed twice with KRH buffer containing 200 nM adenosine by filling the buffer to at least 2 ml, allowing cells to float up and removing the infranatant each time. The cell suspension was then filled to 1 ml with KRH buffer containing 200 nM adenosine and 20 µl of the suspension was saved for protein gel analysis. The remaining cells were washed twice by repeating the same washing procedure as described above. The cell suspension was then filled to 2 ml with KRH buffer containing 200 nM adenosine and 1% BSA. The cells were stimulated by 60 nM (1 X 10^4 microunits/ml) insulin for 20 min at 37°C. After the stimulation, the subcellular trafficking was stopped by the addition of 2 mM KCN (freshly made just before use) and incubation at 37°C for 3 min. The cells were allowed to float up and infranatant was removed. The cells were then washed twice with KRH buffer containing 200 nM adenosine, 5% BSA and 2 mM KCN and resuspended in 1 ml of the same buffer. The primary antibody binding was carried out by the addition of 1 µg/ml of primary antibody and incubation at RT for 1 h. The cells were mixed gently every 10 – 15 min during the binding. After the primary binding, the cells were allowed to float up and infranatant was removed. The cells

were then washed twice with KRH buffer containing 200 nM adenosine, 5% BSA and filled to 1 ml. The secondary antibody was added to the cell suspension to the final concentration of 1 µg/ml. The suspension was incubated at RT for 1 h. The cells were mixed gently every 10 – 15 min during the binding. The cells were then washed once with KRH buffer containing 200 nM adenosine, 5% BSA and 2 mM KCN and 3 times with KRH buffer containing 200 nM adenosine and 2 mM KCN. The volume of the cell suspension was adjusted to 1 ml and 15 µl of the cells were saved for protein concentration assay.

A working solution was prepared just before use by adding the 40 mM Fluorescein di-β-D- galactopyranoside (FDG) stock solution in dimethylsulfoxide (DMSO) to KRH buffer containing 2 mM KCN to the final concentration of 0.2 mM. 90 µl of KRH buffer was added to wells of the 96 well black plates (Greiner). 10 µl of the cell suspension was added to each well of the plate by ends cut tips. Each sample was analyzed in triplicate. The surface binding was initiated by adding 100 µl of the working solution to each well. The fluorescence (emission 512 nm/excitation 488 nm) was measured in bottom reading mode using a flouresecent microtiter plate reader (FLUOstar Galaxy; BMG labtechnologies).

2.2.10. RNA-interference (RNAi) in *C. elegans*

RNAi in the *C. elegans* was performed by feeding the worms with RNAi bacteria on agar plates following the methods described in Wormbook (Ahringer (ed.) 2006). NGM agar plates containing 50 µg/ml ampicillin and 1 mM isopropyl β-D-1-thiogalacto-pyranoside (IPTG) were prepared 4-7 days before seeding. RNAi bacterial stains were streaked on the LB plates containing 50 µg/ml ampicillin and 10 µg/ml tetracycline and allowed to grow at 37°C overnight. Single colonies were inoculated into LB medium containing 50 µg/ml ampicillin. The culture was allowed to grow at 37°C, 250 *g* shaking for 8 h. The NGM plates were then seeded with the bacterial culture, allowed to dry and the expression of double stranded RNA (dsRNA)

was induced overnight at RT.

Desired worm strains were grown on standard NGM plates seeded with OP50 bacteria untill most of the hermaphrodites became gravid and the bacteria were just consumed. The standard bleaching/washing protocol to obtain embryo were carried out as described (Stiernagle 2006). Worms from 2 9 cm NGM plates were washed off the plates with sterile dH_2O. The liquid was collected into a sterile 15 ml conical centrifuge tube. The tube was centrifuged 30 sec at 1000 *g* to pellet the gravid hermaphrodites, and the volume of the liquid was adjusted to 7 ml. The worms were bleached by the addition of 500 mM NaOH and 1% household bleach (5% solution of sodium hypochlorite). The worms were incubated in the bleaching solution for 10 min with vortexing every 2 min. The released eggs were pelleted by centrifugation in a table top centrifuge (Beckman) for 30 sec at 1300 *g*. The supernatant was removed to the volume of 0.3 ml. The pelleted eggs were washed twice with sterile dH_2O and once with M9 buffer (22 mM KH_2HPO_4, 22 mM Na_2HPO_4, 85 mM NaCl, 1 mM $MgSO_4$, 1 mM $CaCl_2$) by adding the washing solution to the volume of 6 ml, vortexing for a few sec and spinning for 30 sec at 1300 *g*. The embryos were incubated in M9 buffer to hatch overnight at RT with shaking at 250 *g*.

The synchronized starved L1 larvae were pelleted by centrifuging at 800 *g* for 45 sec. Supernatant was removed to the appropriate volume allowing 100 µl of the L1 larvae suspension being transferred to the NGM plates seeded with RNAi bacteria. The worms were grown to the desired stage on the RNAi plates and transferred to new NGM plates seeded with RNAi bacteria before the RNAi food source was consumed.

2.2.11. Quantitative realtime PCR (QPCR)

Synchronized or asynchronous worms growing on the RNAi plates were washed off the plates with ice cold sterile M9 buffer and pelleted by centrifuging at 1000 *g* for 1 min. The worm pellet was then washed once with ice cold sterile M9 buffer and twice

with ice cold DEPC treated ddH_2O to completely remove the bacteria food source. Total RNA isolation was carried out as described in section 2.2.2-1). RNA quantification was assessed by UV-spectrophotometer (Eppendorf). cDNAs were synthesized with random hexamers using SuperScript™ III First-Strand Synthesis for RT-PCR system (Invitrogen) according to the manufacturer's protocol. The concentration of the cDNA was adjusted to 1 ng/µl with nuclease-free H_2O. Real-time PCR was performed using iTaq™ SYBR® Green Supermix with ROX kit in 96-well unskirted PCR white plates (Bio-rad). Each sample was analyzed in triplicates.

The QPCR primers are listed in Table 2.13A. The PCR mixture for each reaction was set up following the composition listed in Table 2.13B. The reaction was carried out in a real-time thermal cycler (Mx3000P QPCR system, Stratagene) using the cycling conditions listed in Table 2.13C. The data was analyzed using MxPro™ QPCR Software supplied with the Mx3000P QPCR system.

Table 2.13 Primers, reaction system and cycling conditions for the QPCR

A. Primers

Primer Name	Sequence
H17qPCR1left	GGCCAGCTACTCAGCCATC
H17qPCR1right	ATTTCGGAGACGAAGAACCA
H17qPCR2left	TGCTCCTTTTCGTCATCTCC
H17qPCR2right	TGGAGTTCGCGTTTCCAC

B. Reaction system

Component	Amount per reaction (total 15 µl)
cDNA	5 ng (5 µl)
Forward Primer (15 pM stock)	0.5 µl
Reverse Primer (15 pM stock)	0.5 µl
2X SYBR® Green Supermix	7.5 µl
nuclease-free H_2O	1.5µl

C. Cycling conditions

Segment	Number of cycles	Temperature	Duration
1	1	95°C	1 minutes 30 seconds
2	20	95°C	15 seconds
		55°C	30 seconds
		95°C	30 seconds

2.2.12. Lifespan assay

Lifespan assays were performed at 20°C. Young adult worms were allowed to lay eggs overnight on NGM plates seeded with either *E. coli* OP50 or RNAi bacteria. The progeny were allowed to grow on the corresponding plates until the L4 larvae stage at 18°C. The L4 larvae were then transferred onto NGM plates containing 50 µM 5-fluoro-2′- deoxyuridine (FUDR) seeded with appropriated bacteria to prevent the growth of progeny and maintained at 20°C until all the worms on the plate died. For worms growing on the RNAi NGM plates, they were transferred to new plates before the bacteria food source was consumed. The adult population was scored every day or every other day. Animals that crawled off the plates or exploded were censored. Animals that failed to respond to a gentle prodding with a platinum wire were scored

as dead. Day 0 of lifespan was the day that the eggs were laid. Statistical analysis was performed with Kaplan-Meier method. The assays were repeated two times and similar results were observed in both experiments.

2.2.13. Glucose uptake assay in *C. elegans*

Synchronized worms were grown on NGM plates seeded with appropriate bacteria until L4 larvae. The worms were washed off the plates with M9 buffer and collected in a 15 ml centrifuge tube. The worms were pelleted by centrifugation at 800 *g* for 1 min and washed three times with M9 buffer to completely remove the bacteria. The worms were resuspended in 300 µl M9 buffer and transferred to new agarose plates containing 50 µg/ml ampicillin, 50 µM FUDR and without bacteria seeded. The worms were starved on the plate for 18 h at 18°C. The starved worms were then washed off the plates and pelleted by centrifuging. The worm pellets were resuspended in 350 µl of M9 buffer. 100 µl of the worm suspension was added to a 5 ml bijou tube with 350 µl M9 buffer added. Each sample was analyzed in triplicates. The glucose uptake was initiated by the addition of D-glucose stock solution containing U-[^{14}C]-D-glucose to the final concentration of 50 µM and 1 µCi per assay. The worms were incubated at 18°C for 1 h. The uptake was stopped by flash freezing the worm suspension in liquid nitrogen. The frozen worms were then thawed and 250 µl of M9 buffer was added to the worm suspension. The mixture was sonicated on ice with a tip sonicator. The mixture was sonicated at amplitude of 27 microns for 5 times 15 sec with intervals of 60 sec on ice. The suspension was then centrifuged at 14,000 *g* at 4°C for 15 min. 450 µl of the supernatant was transferred to a 1.5 ml tube. 50 µl of the supernatant was saved for protein assay. The fat content was extracted by the addition of 500 µl of heptane to the tube and votexing. The organic phase and aqueous phase were allowed to separate. 450 µl of the organic phase was then transferred to scintillation vials and mixed with 5 ml scintillation liquid (Fisher). The radioactivity was determined using a scintillation counter.

2.2.14. Glucose oxidation in *C. elegans*

Uniformly labeled [^{14}C]-D-glucose oxidation was determined as described (Schulz, Zarse et al. 2007) with some modification. Each sample was analyzed in triplicate. Synchronized starved worms were prepared as described in section 2.2.13. 100 µl of worm suspension was added to the bottom of a bijou tube containing 350 µl M9 buffer. A lid-removed 1.5 ml tube containing 1 ml 0.1 M KOH was placed in the bijou tube to trap the produced CO_2 as shown in Figure 2.2. The reaction was initiated by the addition of 50 µM D-glucose with 0.6 µCi/100 µl U-[^{14}C]-D-glucose per assay. The lid of the bijou tube was then sealed with parafilm. The reaction was stopped by removing the 1.5 ml tube from the bijou tube. The worm suspension was transferred to new 1.5 ml tube and flash frozen in liquid nitrogen. The suspension was then thawed and sonicated as described in section 2.2.13. 50 µl of the supernatant after centrifugation was saved for protein assay. 950 µl of the KOH solution was transferred to scintillation vials and mixed with 5 ml scintillation liquid. The radioactivity was determined using a scintillation counter.

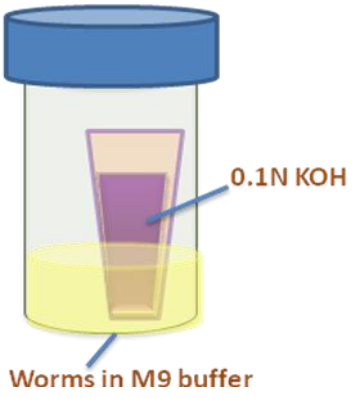

Figure 2.2 Schematic diagram of the CO_2 trapping system.

2.2.15. Data analysis

Densitometric analysis of western blots was performed using Labwork version 4 (UVP). Graphical analysis was performed using GraphPad PRISM version 5.0 (Graphpad Software, Inc) and Microsoft office Excel (Microsoft). Statistical analysis was carried out using the PRISM programme with unpaired and paired two-tailed t tests as indicated in the figure legend.

Chapter 3 A search for putative glucose transporters in *C. elegans* and their subsequent cloning

3.1 Introduction

3.1.1 Structure of the GLUT family

Although the substrate specificity and the affinity to the substrate differ in the GLUT family members (see section 1.3.2), analysis of the predicted amino acid sequences of the mammalian glucose transporters (GLUTs) shows that these members are highly homologous with one another and share similar protein structures. Orthologs found in other species including cyanobacteria (Zhang, Durand et al. 1989), *E. coli* (Maiden, Jones-Mortimer et al. 1988), *Zymomonas mobilis* (Barnell, Yi et al. 1990), yeast (Celenza, Marshall-Carlson et al. 1988; Szkutnicka, Tschopp et al. 1989), algae (Sauer and Tanner 1989), protozoa (Cairns, Collard et al. 1989; Bringaud and Baltz 1992) and plants (Sauer, Friedlander et al. 1990) were also found to possess high levels of sequence similarity with the mammalian GLUTs.

Among the mammalian GLUTs that have been cloned, the structure of GLUT1 has been best characterized. Hydropathy analysis of the predicted amino acid sequence of GLUT1 indicated a protein containing 12 membrane-spanning α-helical domains with both the amino and carboxyl termini oriented intracellularly (Mueckler, Caruso et al. 1985). The 12 transmembrane helices combine to form a central aqueous pore or channel through which the substrate crosses the lipid bilayer (Hruz and Mueckler 2001; Manolescu, Witkowska et al. 2007). This model was supported by a comprehensive series of studies using cysteine scanning mutagenesis with up to 8 of the 12 helices contributing to parts of the surface lining of the pore (Mueckler and Makepeace 2006) (Figure 3.1). The model was further supported by recent X-ray crystal structure analysis of two related bacterial proteins, the proton coupled lactose transporter LacY and the glycerol-3-phosphate transporter GlpT. The analysis

indicated a barrel structure in which two clusters of six transmembrane helices surrounded the aqueous pore in the centre (Abramson, Smirnova et al. 2003; Huang, Lemieux et al. 2003). Computer analysis of the structure of GLUT1, using the coordinates for GlpT, generated a very similar model (Salas-Burgos, Iserovich et al. 2004). Large loops between helices 1 and 2 and between helices 6 and 7 were also predicted (Hruz and Mueckler 2001). The large loop between helices 6 and 7 divides the structure into two halves, the N-terminal domain and the C-terminal domain (Gould and Holman 1993). The cytoplasmic orientation of the carboxyl terminus and large sequence connecting transmembrane segments 6 and 7 has been confirmed by proteolytic cleavage and immunological epitope mapping experiments (Hruz and Mueckler 2001). In addition, a single extracellular N-linked glycosylation site was also predicted to be located between transmembrane helices 1 and 2. Sequence alignment and analysis of other GLUT isoforms showed a similar size of these proteins (~500 amino acid), and characterized by a topology identical to that proposed for GLUT1, including the conservation of the N-linked glycosylation site (Baldwin 1993; Gould and Holman 1993; Olson and Pessin 1996).

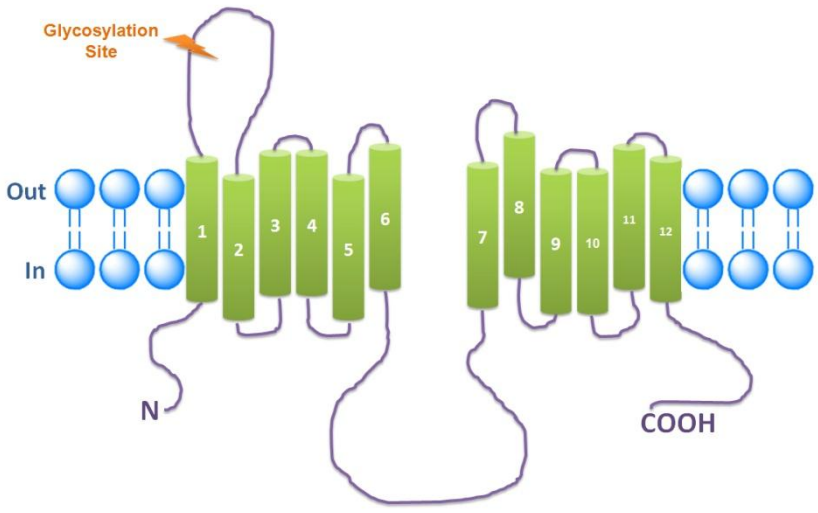

Figure 3.1 The characteristic structure of the GLUTs family. The structure of the GLUTs family is characterized by twelve transmembrane regions, cytoplasmic N- and C- terminus and large loop between helices 6 and 7, and N-linked glycosylation site on the first large exofacial loop (Gould and Holman 1993).

Despite the overall similarity in the structural organization, there is a considerable divergence in the specific amino acid sequences through out the GLUTs family. For example, only 38% of all the amino acids are conserved between the GLUT1-4 isoforms (Olson and Pessin 1996). However, the greatest degree of amino acid sequence identity was found in the transmembrane domains whereas the most divergence was found in the large cytoplasmic loop between helices 6 and 7 and in the N- and C- terminus of these proteins (Baldwin 1993; Olson and Pessin 1996). According to the sequence alignment, several motifs were found to be conserved in the glucose transporters including GRR/K between helices 2 and 3 in the N-terminal half and correspondingly between helices 7 and 8 in the C-terminal half, and EXXXXXXR between helices 4 and 5 in the N-terminal half and correspondingly between helices 10 and 11 in the C-terminal half (Baldwin 1993; Gould and Holman 1993). Other characteristic glucose transporter motifs include PMY in helix 4, PESPRY/FLL in loop 6, GPGPIP/TW in helix 10, and VPETKG in the C-terminal tail (Zhao and Keating 2007). Moreover, the motif QQXSG- NXXXYY in helix 7 is also found to be present in all the mammalian transporters and is highly conserved in all members of the wider glucose transporter superfamily (Figure 3.2) (Baldwin 1993; Gould and Holman 1993; Manolescu, Witkowska et al. 2007). Molecular modelling and mutational experiments suggest that the highly conserved residues in helical regions line on the faces of the helices that are directed to the centre of the protein and away from the membrane lipid and may be involved in the ligand recognition (Gould and Holman 1993; Manolescu, Witkowska et al. 2007).

Figure 3.2 The conserved motifs of the GLUTs family. The conserved motifs of the GLUTs superfamily include GRR/K between helices 2 and 3 in the N-terminal half and correspondingly between helices 7 and 8 in the C-terminal half, EXXXXXXR between helices 4 and 5 in the N-terminal half and correspondingly between helices 10 and 11 in the C-terminal half, PMY in helix 4, PESPRY/FLL in loop 6, QQXSG-NXXYY in helix 7, GPGPIP/TW in helices 10, and VPETKG in the C-terminal tail (Gould and Holman 1993; Zhao and Keating 2007).


TM1
TM2
TM3
TM4
TM5
TM6
TM7
TM8
TM9
TM10
TM11
TM12
GRR(K)
PMY
PESPRY/FLL
QQXSG N YY

3.1.2 Research objectives and experimental approach

The fully sequenced *C. elegans* genome and highly conserved motifs and structures in the glucose transporter superfamily provide the possibility of analyzing the sequence of the putative *C. elegans* glucose transporters and further cloning and functional study of proteins of interest. Therefore, the aims of this chapter are: 1) to analyze the sequence of the predicted worm sugar transporters listed in Wormbase (http://www.wormbase.org/) to determine the possible worm glucose transporter proteins; 2) to clone the putative worm glucose transporters into pT7Blue vector allowing subsequent gene manipulation; 3) to introduce the human influenza hemagglutinin (HA) epitope tag sequence into the predicted first exofacial loop by site-directed mutagenesis for antibody detection of the target proteins; 4) to clone the target proteins into pT7-TS vector for heterologous expression of the proteins in *Xenopus* oocytes (Figure 3.3).

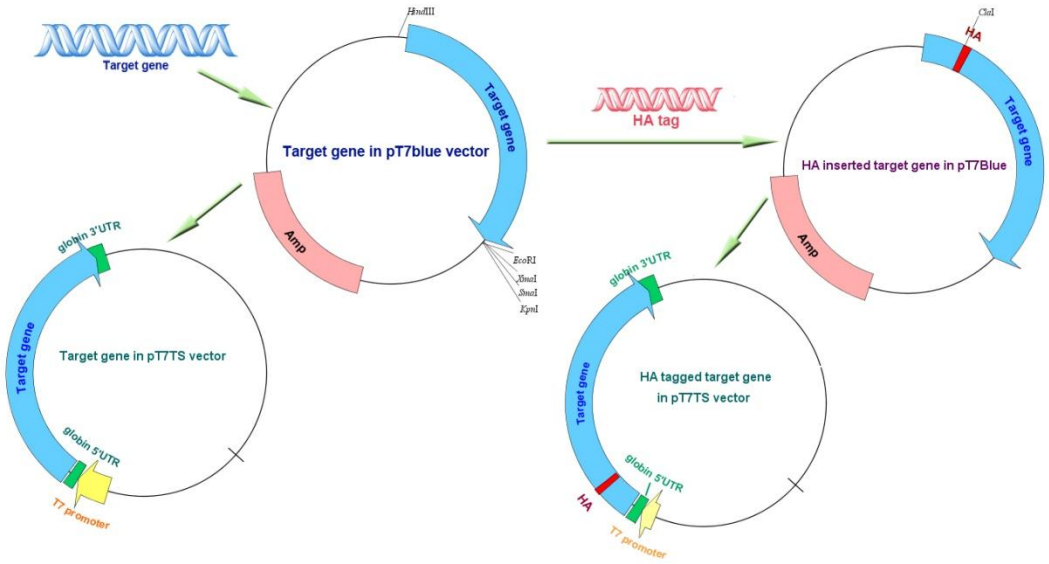

Figure 3.3 The schematic diagram of the cloning procedure for the genes of interest. After amplification from the cDNA library the target gene would be ligated into pT7Blue vector for subsequent gene manipulation. HA-tag would be inserted into the first exofacial loop of the putative proteins. Both the tagged and non-tagged version of protein would be cloned into pT7TS vector for heterologous expression of the proteins in *Xenopus* oocytes.

3.2 Results

3.2.1 Searching for candidate glucose transporters in *C. elegans*

Putative glucose transporters were first searched in NCBI protein database (http://www.ncbi.nlm.nih.gov/sites/entrez?db=pubmed) with 156 results (protein sequences were predicted from cDNA sequences). These putative proteins were then cross-compared with the motif report list of the major facilitator superfamily (PFAM:PF07690) (189 proteins) and the motif report list of the sugar transporter (PFAM:PF00083) (65 proteins). The “best BLAST hits from selected species” listed in the protein description in Wormbase for each protein was considered. The RNAi phenotype in the function section of the gene summary in Wormbase for each protein was also taken into consideration. The putative proteins which had mammalian GLUTs orthologs and/or had the metabolic- and/or lifespan-related RNAi phenotypes were then subjected to the alignment with mammalian GLUT1 and GLUT4. T-coffee (http://tcoffee.vital-it.ch/cgi-bin/Tcoffee/tcoffeecgi/index.cgi?stage1=1&daction=TCOFFEE::Advanced) was used for the alignment of protein sequences (Notredame, Higgins et al. 2000; Moretti, Armougom et al. 2007).

In mammals, GLUT4 is the major insulin responsive glucose transporter. It can increase glucose uptake in mammals by translocating from intracellular storage vesicles to the plasma membrane via the PI3-kinase and PKB pathway (Holman and Sandoval 2001). The insulin signaling pathway is also well conserved in the worm (see section 1.1.1). It was considered interesting to determine whether there was similar insulin responsive glucose transporter translocation system in worms. Worm gene K09C4.1 (K09) encodes a putative 521-amino-acid protein which is predicted to be the ortholog of human GLUT4 (BLAST E value: 4e-21). The gene was cloned from worm total cDNA library into pT7Blue vector by a previous MRes student Anastasia Tsakmaki and Dr. Scott Lawrence, and this construct was used for subsequent cloning.

Worm gene H17B01.1 (H17) has two transcripts, H17B01.1a (H17a, 492 aa) and H17B01.1b (H17b, 510 aa). There are about 21-amino-acid difference in the N-terminus between the two transcripts (Figure 3.4A). Both of the two putative proteins were predicted to be orthologs of human GLUT3 (Blast e-value: 1e-97, 43% identity). Worm gene R09B5.11 (R09) encodes a putative membrane protein which is predicted to be the ortholog of human GLUT1 (Blast e-value: 5.3e-90, 36% identity). Although there is no obvious metabolic or life-span related RNAi phenotype for H17 and R09, the protein sequence alignments with human GLUT1 and GLUT4 of the two proteins showed very high similarity and the characteristic glucose transporter motifs were all found to be present in the two putative proteins (Figure 3.4B).

Figure 3.4 A. Difference between the two transcripts of H17B01.1 in protein sequence. There are 18 amino acids more in the N-terminus of H17b than in H17a. **B. Sequence alignment of H17B01.1 and R09b5.11 with human GLUT1 and GLUT4.** The characteristic motifs described in section 3.1.1 were highly conserved in the two worm putative proteins.

Both of the worm genes F14E5.1 (F14) and K09C4.5 (K4.5) were found to have the RNAi phenotype of fat content increased. F14 encodes a 472 aa protein and K4.5 encodes a 515 aa protein, both of which are predicted to be orthologs of human GLUT14. The proteins encoded by worm genes C35A11.4 (C35), Y39E4B.5 (Y39), and F48E5.2 (F48) are predicted to be the orthologs of human GLUT3, GLUT9 and

GLUT1 respectively. The ortholog of yeast glucose transporter encoded by worm gene T08B1.1 (T08) was also selected because of the slow growth RNAi phenotype.

The membrane topology of the selected proteins was predicted using three different protein topology prediction tools, including SOSUI (Hirokawa, Boon-Chieng et al. 1998), Predictprotein (Rost, Yachdav et al. 2004), and HMMTOP (Tusnady and Simon 1998) (Figure 3.5). All the putative proteins were predicted to have similar membrane topology with the GLUTs family which was characterized by the 10 ~ 12 transmembrane regions with cytoplasmic N- and C- terminus, large exofacial loop between helices 1 and 2 and large cytoplasmic loop between helices 6 and 7 (Gould and Holman 1993; Olson and Pessin 1996).

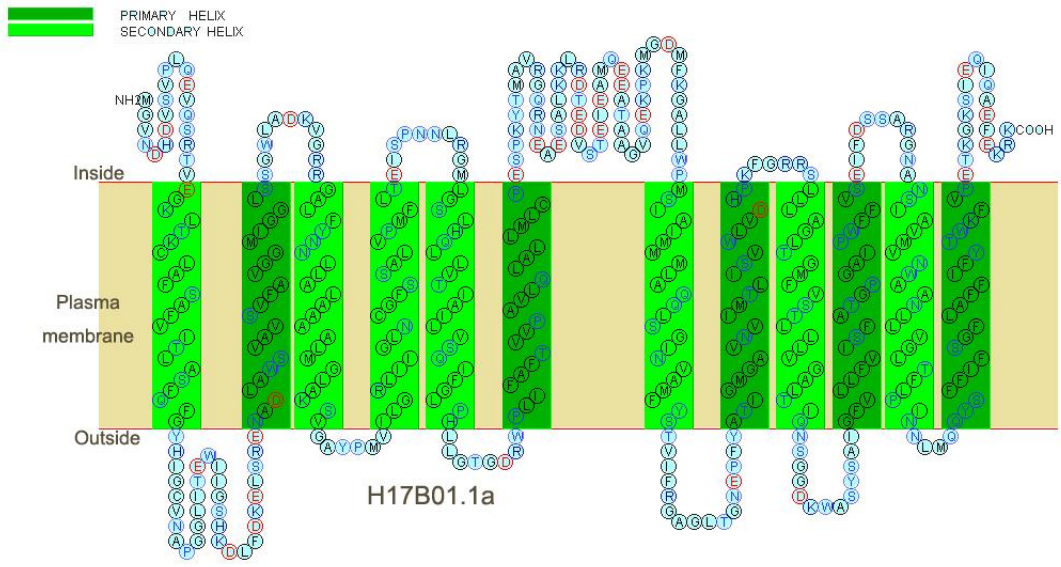

Figure 3.5 Predicted membrane topology of H17B01.1a as determined using SOSUI. Despite of minor difference in the positions of the helices, the selected putative glucose transporters were all predicted to have the characteristic 10 ~ 12 transmembrane regions by the protein

To sum up, nine worm genes were selected for subsequent cloning according to the sequence alignment and/or metabolic- or life-span- related RNAi phenotyes (Table 3.1) (See appendix 2) for the complete sequence alignments with human GLUT1 and GLUT4). The membrane topology prediction of each protein provided the possibility of inserting HA epitope tag into the first exofacial loop of the target proteins for antibody detection of the proteins.

Table 3.1 Selected putative glucose transporters

Putative GT* (Gene Name)	Amino acids	Human ortholog	Identity to ortholog	RNAi Phenotype
H17B01.1	A: 492 aa B: 510 aa	GLUT3	43%	
R09B5.11	516 aa	GLUT1	36%	
C35A11.4	515 aa	GLUT3	29%	Larval lethal, embryonic lethal
F14E5.1	472 aa	GLUT14	27%	Fat content increase
Y39E4B.5	505 aa	GLUT9	24%	Larval rest
F48E5.2	488 aa	GLUT1	23%	Embryonic lethal
K09C4.5	524 aa	GLUT14	22%	Fat content increase
K09C4.1	521 aa	GLUT4	20%	
T08B1.1	591 aa	Yeast glucose transporter	23%	Larval arrest, embryonic lethal, reduced brood size

*GT: glucose transporter

3.2.2 Cloning of the putative glucose transporters from *C. elegans* total cDNA library

A *C. elegans* cDNA library was first synthesized using total RNA extraction from worms of all stages. The sequence information of the target genes was obtained from WormBase. The target genes were amplified from the cDNA library using primers which were designed according to the predicted spliced form of the gene sequences (Figure 3.6). The primers were designed to bind several bases upstream of the start codon and downstream of the stop codon. A full list of primers used in the cloning of interest genes from the cDNA library is specified in Table 3.2.

Table 3.2 List of Primers used for cloning the putative glucose transporter genes from cDNA library

Gene Name	Gene Size	Primer Name	Primer Sequence
H17B01.1	a: 1479 bp	H17aFOR	AAATGGGTGTCAACGACC
		H17aREV	GCATTACTTCCTCTTCTCG
	b: 1533 bp	H17bFOR	ATGTCGGAAAAATCAAGAAGTG
		H17bREV	TTACTTCCTCTTCTCGAATTCG
		H17int	GGCCACTGATCTTTGCC
R09B5.11	1551 bp	R09FOR	ATGAACGCC GTTGTTGCC
		R09REV	CCGACTATGAACATATCCG
		R09intFOR	GGTGCCAA TGTTTCTTACCG
		R09intREV	CGGTAAGAAACATTGGCACC
C35A11.4	1548 bp	C35FOR	ATGGTGGAAGCACCCAGTTTTCGG
		C35REV	CTAGAGTCGATAAGATAAGG
		C35intFOR	CTGTGAGATTGATGAAGCC
		C35intREV	GGCTTCATCAATCTCACAG
F14E5.1	1419 bp	F14FOR	ATGTCAAATAGATTGTGGCC
		F14REV	TCATTTTTTTTTAAGTTCATTC
		F14intFOR	GGAGATGGTACAGATGC
		F14intREV	GCATCTGTACCATCTCC
Y39E4B.5	1518 bp	Y39FOR	ATGCGGTGGCAAACGATTCG
		Y39REV	TTAGTAAATTCGAAGATGTCC
		Y39intFOR	CATGAGCGAATATCAAGCC
		Y39intREV	GGCTTGATATTCGCTCATG
F48E5.2	1467 bp	F48FOR	CCAGTGACAACATGCAAAAACTCAATTGG
		F48REV	GGCTGTCATTATAATTTATTCATTCC
		F48intFOR	CGTCGTGGGTTTTTGTTGGG
		F48intREV	CCCAACAAAAACCCACGACG
K09C4.5	1575 bp	K4.5FOR	CCATTAGCAATCATGTTATTCAATGCGCC
		K4.5REV	GGCAATGAAGCAAGCAAACATCGCAGG
		K4.5intFOR	GGAGAAGAATTTGACACAGG
		K4.5intREV	CCTGTGTCAAATTCTTCTCC
T08B1.1	1776 bp	T08FOR	ATGTCAGAATTTGAAGAAG
		T08REV	CAGTCTTCCTTCACATTTGG
		T08intFOR	CGTCCTGACCTACGCTATGG
		T08intREV	CCATAGCGTAGGTCAGGACG

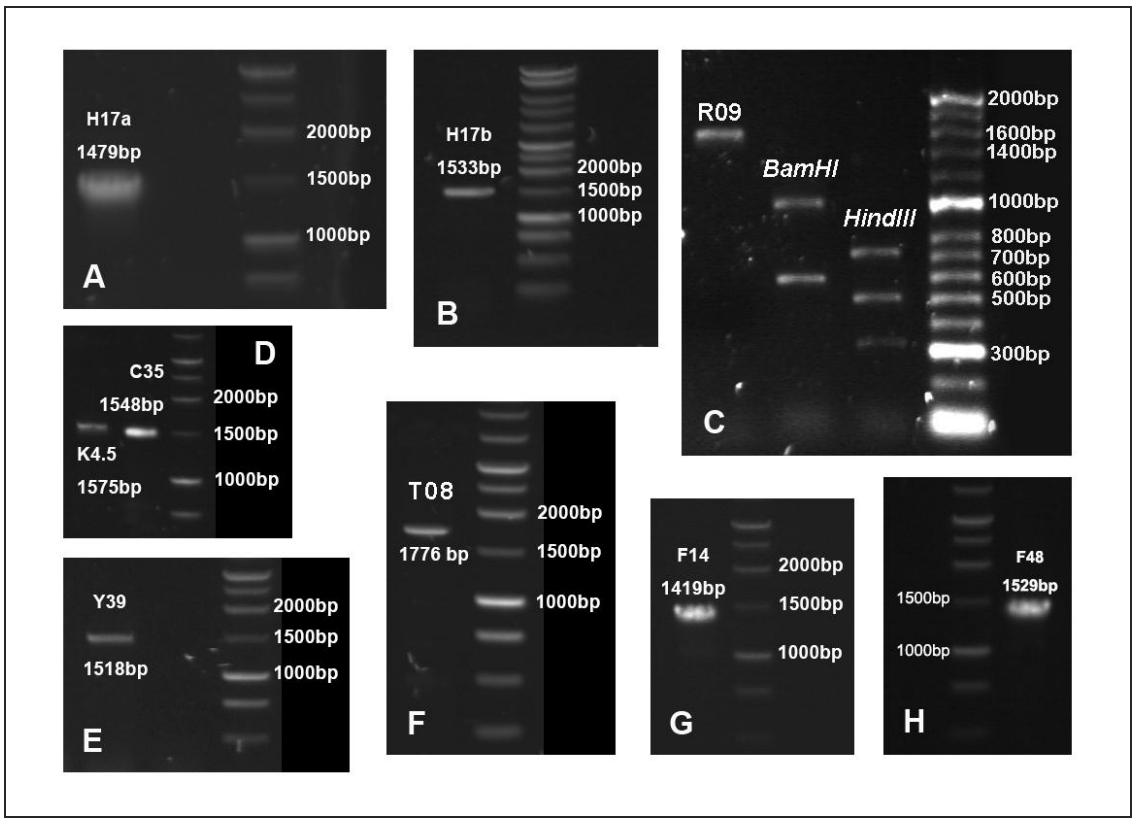

Figure 3.6 Amplification of the putative glucose transporter genes from worm total cDNA library. The genes of interest were amplified from the total cDNA library of worms at all stages with the primers listed in table 3.2 and analyzed on 1% (w/v) agarose gel with 1 kb DNA ladder (Promega) (**A-B, D-H**). **C: Test digestion of R09 after the amplification.** (1.2% Agarose gel, 2 Kb DNA ladder) R09 gene is about ~1.6 kb and can be digested into 2 fragments by BamHI (fragment size: 977bp, and 574bp) or digested into 4 fragments by HindIII (fragment size: 715bp, 491bp, 306bp and 39bp, the smallest fragment cannot be seen on the gel).

The amplified DNA fragments were then ligated into pT7Blue vector for subsequent manipulation using Perfectly Blunt® Cloning Kits (Novagen, UK) respectively. The multiple cloning site of pT7Blue vector (Figure 3.7) is located in middle of the lacZ gene allowing blue-white screening for the positive colonies. Transformed competent cells were inoculated on to the LB agar plates containing 0.1 mM of IPTG and 40 µg/ml X-gal. At least 15 white colonies were picked for colony PCR using the corresponding primers listed in table 3.2 (gel pictures not shown). Two of the colony PCR positive colonies were selected for DNA miniprep. 30 µg of the sample plasmid DNA was sequenced by MWG. The sequencing results were aligned with the target gene sequences in wormbase using multiple sequence alignment software by Florence Corpet (http://bioinfo.genopole-toulouse.prd.fr/multalin/multalin.html). Sequencing results were consistent with the sequences of the eight target genes recorded in the Wormbase.

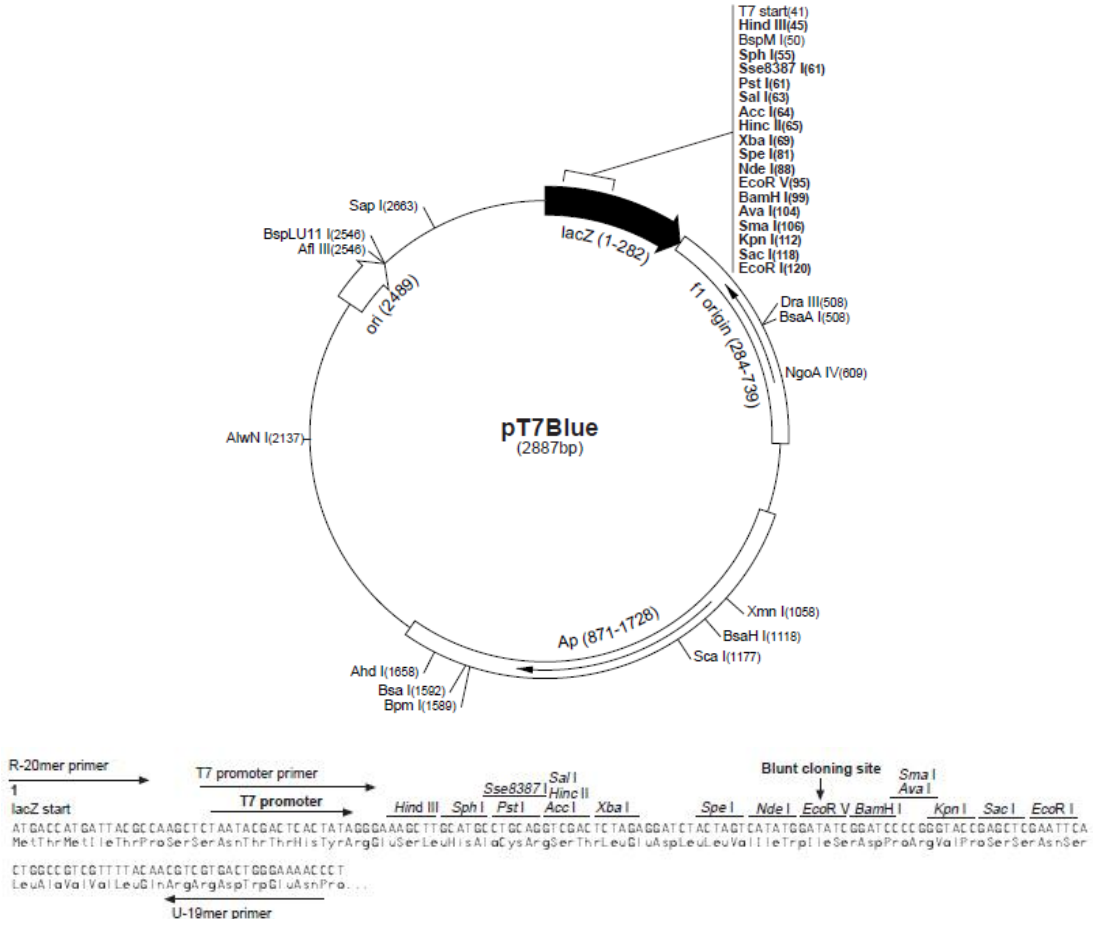

Figure 3.7 The map of pT7Blue vector and the cloning/expression region of the vector. The target genes were ligated into the EcoR V blunt cloning site.

3.2.3 HA insertion to the first exofacial loop

In order to allow further functional study of the putative proteins, it is necessary to make the target proteins to be detectable by the antibody techniques. However, there were no specific antibodies available for the putative proteins; therefore, inserting a universal epitope tag into the appropriate position of the protein would provide the possibility of further functional study of the proteins of interest. The influenza hemagglutinin epitope (HA) was chosen to insert into the first exofacial loop of the target proteins as previously described (Quon, Guerre-Millo et al. 1994).

The membrane topology prediction for each target protein was used to determine the insertion site of the HA-tag (Table 3.3). The Bsu36I restriction site (recognition site: CCTNAGG) was introduced into the pT7Blue constructs using Quickchange® site-directed mutagenesis kit (Stratagene, UK). The mutation site was confirmed by sequencing and alignment with the original sequence. The mutated plasmid was then digested with Bsu36I and dephosphorylated by TSAP enzyme to prevent the linearized DNA from re-ligation.

Table 3.3 Insertion site of the HA-tag in the putative glucose transporter proteins

Gene Name		Position of the HA insertion	Mutated Amino Acid
H17B01.1	a	T57 – E58	--
	b	P70 – G71	--
R09B5.11		P71 – G72	--
C35A11.4		M42 – N43	M42 → P, N43 → D
F14E5.1		T55 – E56	
Y39E4B.5		L45 – R46	R46 →A, Q47 → E, P48 → A
F48E5.2		N42 – E43	--
K09C4.5		P51 – T52	T52 → A
K09C4.1		T54 – E55	T54 → E
T08B1.1		D76 – W77	D76 → E, W77 → G

The double-stranded DNA oligonucleotide coding for the HA tag was annealed from two single-stranded oligonucleotides. The annealed double-stranded DNA oligo was phosphorylated as described in section 2.2.2-11). The phosphorylated oligo was ligated with the dephosphorylated linearized vector. The sense oligonucleotide was 5'-TGA GAT CGA TTA TCC TTA TGA TGT TCC TGA TTA TGC-3'. The antisense oligonucleotide was 5'-TCA GCA TAA TCA GGA ACA TCA TAA GGA TAA TCG ATC-3'. This encoded for a peptide, IDYPYDVPDYAE, which was inserted into the position listed in table 3.3 in each gene sequence. There is a unique ClaI site (recognition site: ATCGAT) in the HA sequence allowing the test digestion after the ligation. The ClaI site was first screened in the sequence of the amplification region in the target gene so that the size of the fragments (after test digestion) could be estimated. The insertion was verified first by ClaI digestion after the colony PCR (Table 3.4, Figure 3.8), and then by direct sequencing of the regions including the oligonucleotide insert.

Table 3.4 The size of the fragments after ClaI digestion for verifying the presence of HA insertion into the putative glucose transporter genes.

Gene Name		The size of the fragments after ClaI digestion	
		+ HA	- HA
H17B01.1	**a**	1301bp, 181bp, 44bp	1482bp, 44bp
	b	1316bp, 215bp, 41bp	1531bp,41bp
R09B5.11		1327bp, 218bp	1560bp
C35A11.4		1456bp, 131bp	1551bp
F14E5.1		1288bp, 173bp	1425bp
Y39E4B.5		865bp, 546bp, 143bp	1008bp, 546bp
F48E5.2		1375bp, 134bp	1503bp
K09C4.5		1423bp, 164 bp	1551bp
K09C4.1		1438bp, 164bp	1602bp
T08B1.1		906bp, 676bp, 230bp	1100bp, 676bp

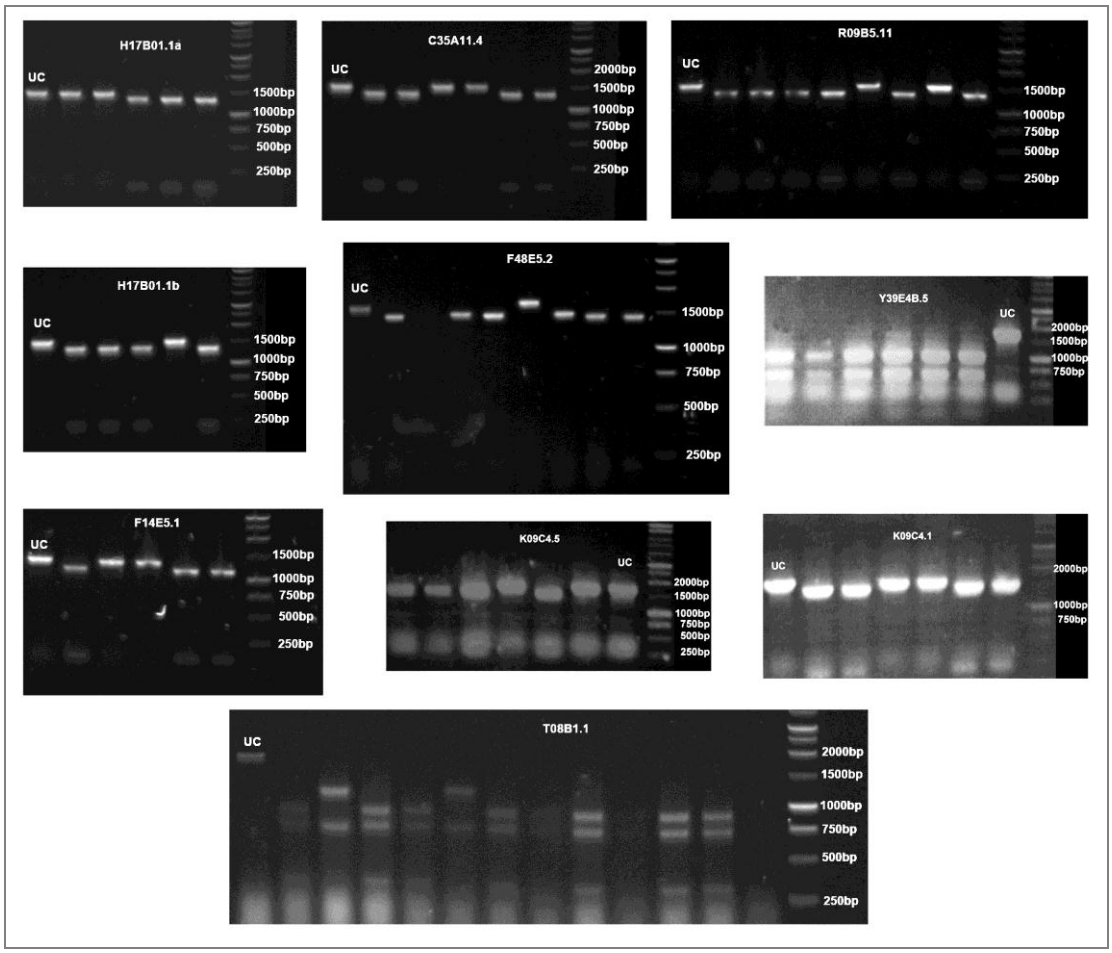

Figure 3.8 ClaI test digest for the verification of HA-tag insertion into the putative glucose transporter genes. UC: uncut, PCR product with no ClaI added to the digestion mixture. The genes of interest were amplified using primers listed in table 3.2 in colony PCR. The PCR products were then digested with ClaI for 1 hour at 37°C. The digestion mixtures were analyzed on 1.5% (w/v) agarose gel with 1 kb DNA ladder (Promega). Positive colony were then determined according to the size of the fragments comparing with the prediction in table 3.4.

3.2.4 Cloning of the putative glucose transporters into a heterologous expression vector

The oocytes of South-African clawed frog *Xenopus laevis* have been widely used for the expression of mammalian channels and transporters, as well as for the *in vitro* study of channels function and regulation of *C. elegans* (Nishimura, Pallardo et al. 1993; Bianchi and Driscoll 2006; Mueckler and Makepeace 2006). The most common approach for expression of exogenous proteins in *Xenopus* oocytes is to inject in vitro transcribed cRNA into the oocyte cytoplasm (Bianchi and Driscoll 2006). In order to ensure the stability of the transcribed sequence and efficient translation into *Xenopus* oocytes, the cloned cDNA of the putative glucose transproters was inserted into the pT7TS vector. The pT7TS plasmid contains the 5' and 3' untranslated regions (UTRs) of *Xenopus* β-globin mRNA (Figure 3.9), which was isolated from a modified version of the translation vector pSP64T (Krieg and Melton 1984) and then was cloned into pGEM4Z (Promega). Sense strand transcription is driven by T7 promoter.

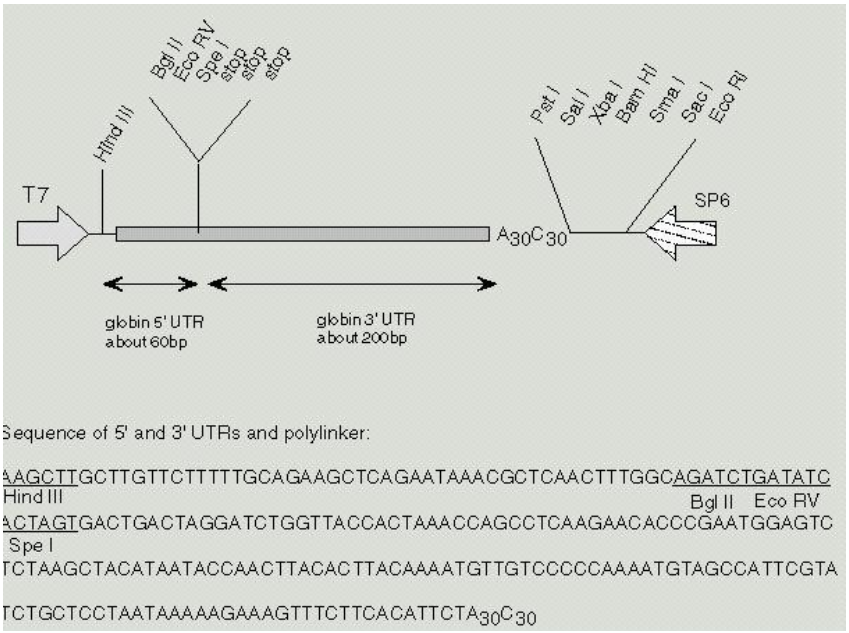

Figure 3.9 The *Xenopus* β-globin UTRs flanked multiple cloning region of pT7TS vector. The 5' and 3' UTRs of *Xenopus* β-globin mRNA was inserted into pGEM4Z vector. The sense strand transcription was driven by T7 promoter and the antisense strand transcription was driven by SP6 promoter. The vector has stop codons in all 3 reading frames downstream of the multiple cloning site.

The cloned cDNA of the target genes was inserted between the BglII and SpeI sites so that the transcription was driven by T7 promoter. The sequences of the target genes were first screened to remove the two restriction sites (BglII and SpeI) with silent mutation. Both of the cDNA fragments with or without HA-tag were then amplified with primers containing BglII and SpeI sites and binding with pT7blue sequence upstream and downstream of the target genes respectively. Both the vector plasmid and the amplified fragments were then digested with BglII and SpeI (Figure 3.10). The digested fragments were ligated with T4 DNA ligase and transformed into XL-1 Blue competent cells. The presence of the target genes in the pT7TS vector was first verified with colony PCR with the primers listed in table 3.2, then verified by sequencing.

In order to set up a positive control in the transport activity study, a pT7TS-GLUT1 was constructed. The rabbit GLUT1 gene fragment was amplified from pUC19-GLUT1 construct (constructed by Dr. Edwards Lee, a previous PhD student in this laboratory) with primers containing BglII and SpeI sites respectively. The fragment was then ligated into the pT7TS vector after the double digestion. The successful ligation was verified first by colony PCR with primers binding with the beginning and the end of the GLUT1 sequence, and then by sequencing. A HA-tagged version of pT7TS-GLUT1 was also constructed. The HA tag was inserted into the first exofacial loop of GLUT1 between I40 and E41 (Figure 3.11)

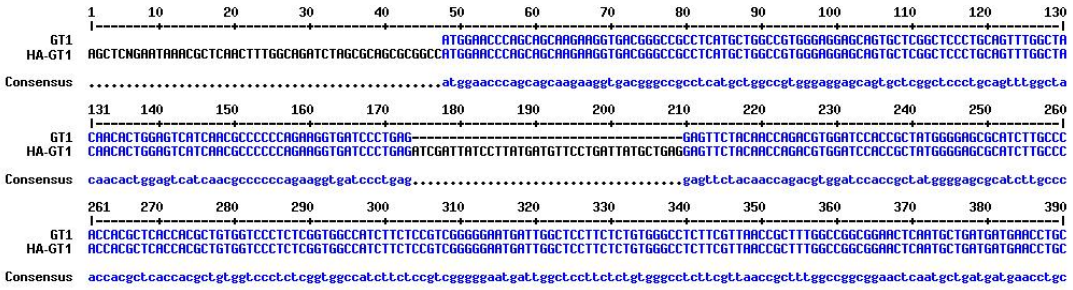

Figure 3.11 The sequence alignment of GLUT1 and HA-GLUT1. The *Bsu36*I site inserted GLUT1 sequence was aligned with the sequencing result of pT7TS-HA-GLUT1. The HA tag was inserted between I40 and E41.

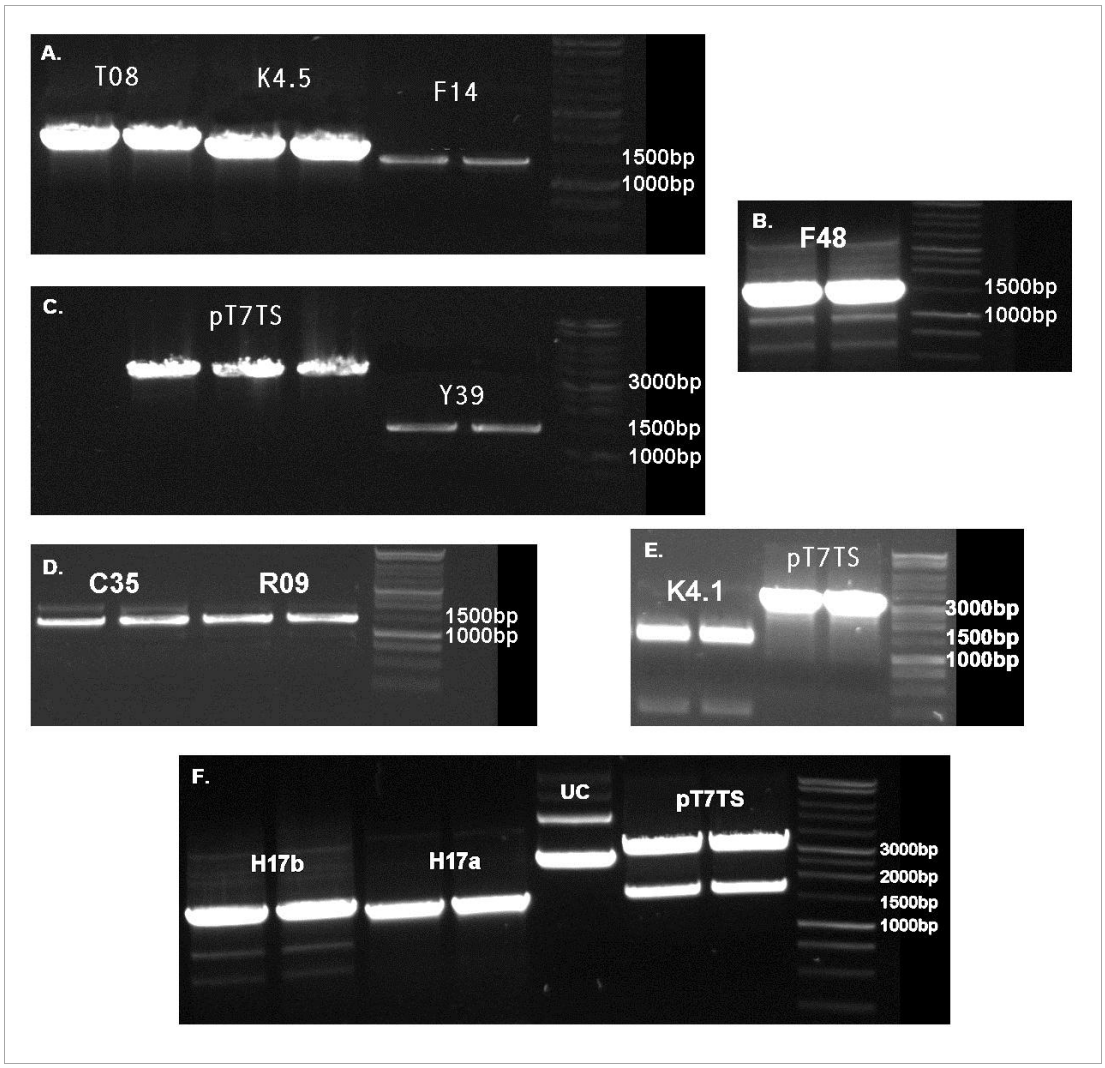

Figure 3.10 Bgl II and Spe I double digest of the cloned cDNAs of the 10 putative glucose transporters and the pT7TS vector. The cDNAs of the cloned putative proteins in pT7-Blue vector were first amplified with primers containing BglII and SpeI restriction sites at 5'and 3' ends respectively. The PCR products were then digested with BglII and SpeI enzymes in Promega restriction enzyme buffer D at 37°C for 4-5 hours. The pT7TS was also digested with the two enzymes to produce a ~3100 bp linearized fragment. Digested fragments were analyzed on 1% agarose gel and then cleaned for subsequent ligation procedure. In figure F. pT7TS-R09, instead of the pT7TS plasmid, was digested to produce the ~3100 bp vector and ~ 1500bp R09 fragment so that the vector backbone was able to be separated more easily.

3.3 Discussion and conclusion

In this chapter, nine putative worm glucose transporter genes (H17B01.1, R09B5.11, C35A11.4, F14E5.1, Y39E4B.5, F48E5.2, K09C4.5, K09C4.1, and T08B1.1) were selected and cloned according to the sequence alignment and/or metabolic- or life-span- related RNAi phenotypes (Table 3.1). Membrane topology prediction for these putative proteins showed the characterized 10-12 transmembrane regions with cytoplasimc N- and C- terminus as well as large cytoplasmic loop between helices 6 and 7. Except for the yeast glucose transporter ortholog T08B1.1, all the rest of the putative glucose transporters showed high alignment score with human GLUT1 and GLUT4 in the T-coffee protein alignment program indicating high sequence similarity between the putative proteins and the mammalian glucose transporters. However, only H17B01.1 and R09B5.11 have almost all the characteristic motifs of the glucose transporters. The metabolic and growth related RNAi phenotypes of the other putative proteins make them interesting target to study the role of the glucose transporter in the life-span regulation. However, the first step would be to confirm the glucose transport activity of these proteins. The insertion of HA-tag into the first exofacial loop of the putative proteins would allow antibody detection of the expression of the putative proteins; thus, allow the visualization of the subcellular localization of the putative proteins, as well as the comparison of the expression levels of different putative proteins in the study of the transport activity.

The *Xenopus* oocytes contain accumulated stores of enzymes, organelles and proteins that are normally used after fertilization which can be recruited for the expression of heterologous proteins after the injection of the corresponding mRNA (Bianchi and Driscoll 2006). Moreover, the frog oocytes are built to survive for long periods of time outside the body; therefore, the low exogenous nutrient uptake makes the oocytes particularly suitable for the study of the sugar uptake activity of the sugar transporters. Thus, the *Xenopus* oocytes expression system was chosen for the expression of the putative worm glucose transporters. The HA-tagged and

non-tagged cDNA of the ten putative proteins were inserted into the *Xenopus* translation plasmid pT7TS respectively. Successful cloning of the cDNAs into the translation plasmid pT7TS allows the subsequent *in vitro* study of the glucose transport activity of the cloned putative glucose transporters.

Chapter 4 An *in vitro* functional study of the putative *C. elegans* glucose transporters

4.1 Introduction

The carbohydrate energy sources in *C. elegans* are primarily stored as cellular glycogen, however, significant amounts of trehalose and glucose are also present (Braeckman, Houthoofd et al. 2009). Trehalose has been shown to have important physiological functions in nematodes, including *C. elegans* (Pellerone, Archer et al. 2003). Moreover, trehalose is assumed to be the major transported sugar during the dauer stage of the worms (McElwee, Schuster et al. 2004). Hence, the identification of glucose and trehalose transporters may provide important information for the understanding of the carbohydrate metabolism in the worms. *C. elegans* orthologs of the GLUT superfamily, as well as most of the enzymes involved in the main pathways of intermediary metabolism, have been predicted according to the worm cDNA(s) in Wormbase. However, this can only provide the information that the sugar transport system and standard metabolic pathways are conserved in the worms. The activities of these predicted proteins can only be determined by gene expression and functional studies. Therefore, the current studies (described below) of the mammalian GLUTs, and trehalose transporters in other species, will provide helpful references in the investigation of glucose and trehalose transporters in the *C. elegans.*

4.1.1 The characteristics of two representative mammalian GLUT proteins

The proteins of mammalian GLUT superfamily are the products of distinct genes and are expressed in a highly controlled tissue-specific fashion (Gould and Holman 1993). These transporters are also different in their functional characteristics, such as the substrate specificity, the K_m values, and their binding-affinities to the inhibitory

ligands cytochalasin B and forskolin (Scheepers, Joost et al. 2004) (detailed in section 1.3.2). Despite little being known for the glucose transporters in *C. elegans*, the structural similarity of the transporters suggests that many features of the mammalian GLUTs family could turn out to be shared by the homologues.

Among the mammalian GLUTs superfamily proteins, GLUT1 and GLUT4 are the most extensively studied (also discussed in section 1.3.2). GLUT1 is widely distributed in tissues with the highest expression levels in erythrocytes and endothelial cells of the brain. It is responsible for the basic supply of cells with glucose. The glucose transporter GLUT4 is the major insulin-responsive transporter that is predominantly restricted to striated muscle and adipose tissue. In the basal state, the majority of GLUT4 locates in intracellular compartments, GLUT4 vesicles, while only a very small amount of the transport cycles to and from the cell surface. When the insulin signalling cascade is stimulated upon the binding of insulin to insulin receptor, the exocytic rate of GLUT4 is significantly increased while the endocytosis of GLUT4 is reduced (Figure.4.1) (Bryant, Govers et al. 2002; Watson, Kanzaki et al. 2004; Dugani and Klip 2005). Thus the glucose uptake is increased. Once the blood glucose concentration is brought down, circulating insulin returns to basal level. GLUT4 molecules on the cell surface are internalized through clathrin-coated pits and are recycled back to intracellular compartments (Bryant, Govers et al. 2002; Watson, Kanzaki et al. 2004; Dugani and Klip 2005). During its cycling to and from the cell surface, GLUT4 traffics through several intracellular compartments, including endosomes and the trans-Golgi network (Holman and Sandoval 2001).

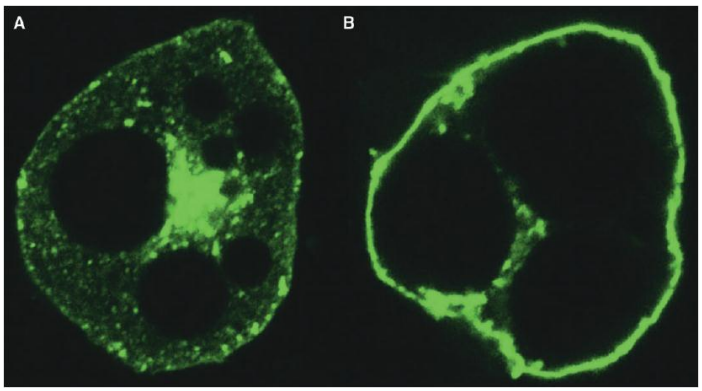

Figure 4.1 Insulin stimulation results in the translocation of GLUT4 from intracellular storage sites to the plasma membrane (Watson, Kanzaki et al. 2004). Glut4 labelled with enhanced green fluorescent protein (EGFP) fusion construct was transfected into differentiated 3T3L1 adipocytes. The cells were incubated with (A) or without (B) of insulin for 30 min. The cells were then fixed and pictures were taken using confocal fluorescent microscopy.

4.1.2 The role of trehalose in *C. elegans* physiology

Trehalose is a soluble, non-reducing disaccharide of glucose which is naturally present in a wide range of organisms, including bacteria, yeasts, fungi, insects, invertebrates, and plants (Elbein, Pan et al. 2003). In the model nematode *C. elegans*, trehalose is also present in its all life cycle stages in significant quantities (up to 2.3% dry weight), with the highest concentrations found in eggs and dauer larvae (Pellerone, Archer et al. 2003), the two stages that are highly resistant to environmental stresses. Only *α,α*-trehalose (1-*O*-(*α*-D-glucopyranosyl)-*α*-D-glucopyranoside, structure in Figure 4.2) is found in biological material among the three isomers: *α,α*-trehalose, *α,β*-trehalose and *β,β*-trehalose (Elbein 1974). The disaccharide is synthesized in cells from metabolites of glucose and is readily hydrolysed to glucose. Therefore, it can function in cells as a less chemically reactive store of the reactive form glucose (Behm 1997). Trehalose is a multifunctional compound with a variety of functions in the worms' physiology (Behm 1997), including: 1) serving as an energy and carbon reserve; 2) acting as a stabilizer and protectant of proteins and membranes; 3) providing protection from stress such as heat, damage of oxygen radicals, and cold (Behm 1997; Elbein, Pan et al. 2003).

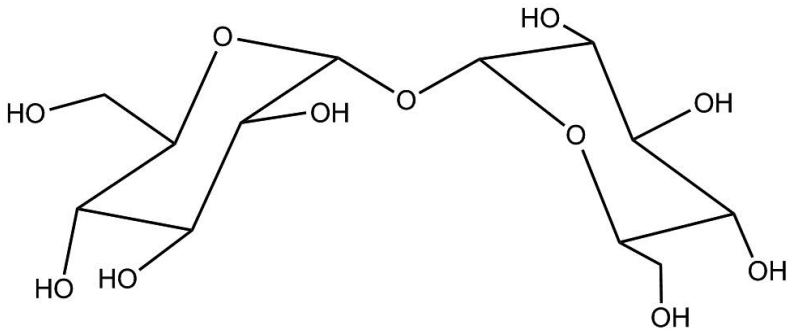

Figure 4.2 The chemical structure of the naturally occurring isomer of trehalose, *α,α*-trehalose. (Adapted from (Behm 1997))

While playing an important role in the worms' physiology, trehalose is an uncharged and osmotically active small molecule that cannot pass freely across biological membranes (Elbein, Pan et al. 2003). Hence, the trehalose transport system will be essential for trehalose to transport in and out of the cells to achieve its physiological function. However, there is hardly any report about the trehalose transport system in *C. elegans*. Certain transporters have been found to promote the permeation of trehalose across the plasma membrane in archaea and bacteria (*MalEFGK*$_2$) (Boos and Shuman 1998) and yeast (*MAL11/AGT1*) (Han, Cotty et al. 1995; Stambuk, De Araujo et al. 1996; Stambuk, da Silva et al. 1999). However, the substrate selectivity of the two transporters also includes α-glucopyranoside, sucrose, and maltose (Boos and Shuman 1998; Stambuk, da Silva et al. 1999). Moreover the direction of trehalose transport of these transporters is only inward (Stambuk, De Araujo et al. 1996; Boos and Shuman 1998). Okuda *et al.* reported the first trehalose-specific transporter, trehalose transporter 1 (TRET1), in the larvae of the sleeping chironomid, *Polyedilun vanderplanki* (Kikawada, Saito et al. 2007). TRET1 was reported to be a trehalose-specific facilitated transporter. The direction of the transportation was suggested to be reversible depending on the concentration gradient of trehalose. Protein sequence analysis showed that TRET1 also has a domain for sugar transport, of which the family contains the GLUT/SLC2A family and belongs to the major facilitator superfamily (MFS). The membrane topology prediction of TRET1 shows a

12-transmembrane structure, which is the characteristic structure for the MFS (Kikawada, Saito et al. 2007). Therefore, while studying the glucose transport activities of the putative glucose transporters, it is also worth to test the trehalose transport activities of these proteins.

4.1.3 Research objectives and experimental approach

The cloning of nine putative *C. elegans* glucose transporters allowed the possibility of studying the characteristics of these proteins including the substrate specificity, cellular localization and so on. The aims of this chapter include: 1) to examine the glucose and trehalose affinity of the putative transporters using the *Xenopus* oocytes expression system; 2) to examine the cellular localization of the target protein upon identifying the glucose transporter within the nine candidates; 3) to test the possible insulin response of the identified glucose transporter protein in the insulin sensitive system.

4.2 Results

4.2.1 Expression of the candidate proteins in *Xenopus* oocytes

The nine putative glucose transporter proteins with or without HA insertion were cloned into pT7TS vector (described in section 3.2.4). These constructs were then linearized by restriction enzyme (listed in table 4.1) at the downstream of the putative proteins' coding region. The linearization of the plasmids was checked by agarose gel electrophoresis. The linearized plasmids were purified and then transcribed using the T7 RNA polymerase in the presence of cap analog (described in section 2.2.7). The transcribed RNA was purified by phenol/chloroform method and was adjusted to the concentration of 1 µg/µl for the injection into *Xenopus* oocytes.

Table 4.1 The restriction enzymes used in the linearization of the pT7TS constructs

Construct	Restriction Enzyme	Construct	Restriction Enzyme
pT7TS-(HA)–C35	PstI	pT7TS-(HA)–H17a	SalI
pT7TS-(HA)–F14	PstI	pT7TS-(HA)–H17b	PstI
pT7TS-(HA)–F48	SalI	pT7TS-(HA)–T08	SalI
pT7TS-(HA)–K09	PstI	pT7TS-(HA)–Y39	PstI
pT7TS-(HA)–K4.5	PstI	pT7TS-(HA)–GLUT1	SalI
pT7TS-(HA)–R09	XbaI		

Both of the constructs with (HA) or without HA insertion was linearized by the listed restriction enzyme at 37°C for 5 hours and then purified and the concentration of the linearized plasmid was adusted to 200 ng/μl.

Xenopus oocytes were prepared as described in section 2.2.7. After an overnight incubation period, healthy oocytes were selected for injection with 50 ng of capped RNA of the putative proteins or GLUT1. A group of negative control was prepared by injecting the oocyte with the same volume (50 nl) of DEPC-treated water. Injected oocytes were maintained at 18°C in complete ND96 with the medium changed every day. In the intact cells, antibody can bind to the HA –tagged putative transporters only when the transporters are located in the plasma membrane since the HA tag was inserted to the first exofacial loop of these proteins. Two days after the injection, the surface expression of the HA-tagged putative proteins was determined by HA-antibody surface binding assay (described in section 2.2.9, Figure 4.3). All of the putative proteins were expressed on the cell surface. The two transcripts of H17, H17a and H17b, exhibited the highest expression level on the cell surface, while K09 showed the lowest expression level on the cell surface.

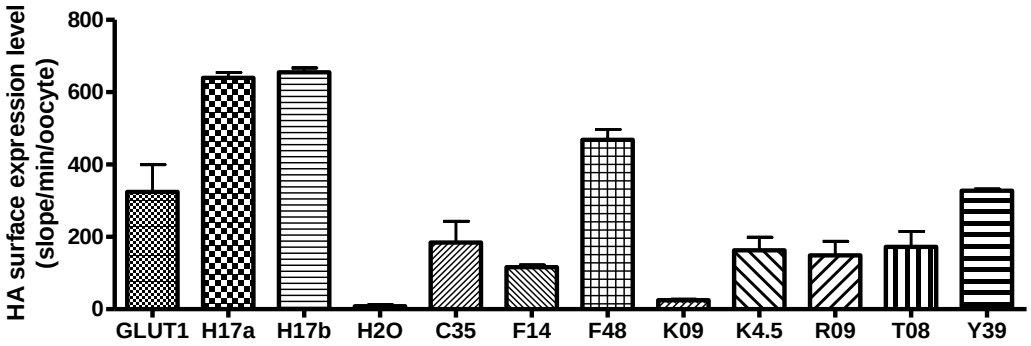

Figure 4.3 The expression levels of the HA-tagged putative proteins and GLUT1 in *Xenopus* oocytes. 50 ng of the cRNA of the HA-tagged putative transporters or HA-GLUT1 was injected into healthy *Xenopus* oocytes. Two days after the injection, healthy oocytes were selected for HA-antiody surface binding assay. All the putative glucose transporters were expressed on the cell surface at different level. The two transcript of H17 showed the highest expression level on the cell surface. The experiment was repeated three times. Each value is the mean ± SEM.

4.2.2 Glucose transport activities of the putative glucose transporters in *Xenopus* oocytes

Healthy *Xenopus* oocytes injected with cRNA of non-HA-tagged putative glucose transporters and GLUT1 were selected for the glucose transport assay. The oocytes were first starved in non-nutrient buffer for 1 h. A group of 5 oocytes for each sample was incubated in the incomplete-ND96 buffer with 50 μM D-glucose for 30 sec. The assay was initiated by the addition of 0.3 μCi of the U-[^{14}C]-glucose to each assay. After 1 h of incubation, each group of oocytes was homogenized and the radioactivity of each sample was determined by the scintillation counter in addition of scintillation liquid. The same procedure was also carried out on the oocytes injected with DPEC-treated water as the negative control. Among all the tested putative glucose transporters, only H17a and H17b showed significant glucose transport activity comparing with the negative control (Figure 4.4A). The rest of the putative transporters all showed no significant difference in the transport levels comparing with the negative control (Figure 4.4B), suggesting that glucose was not the favourable substrate of these putative transporters. Thus, H17a and H17b were identified as the glucose transporter in *C. elegans*. However, whether K09 has the

glucose affinity or not is not clear due to the low expression of the protein on the plasma membrane (Figure 4.3).

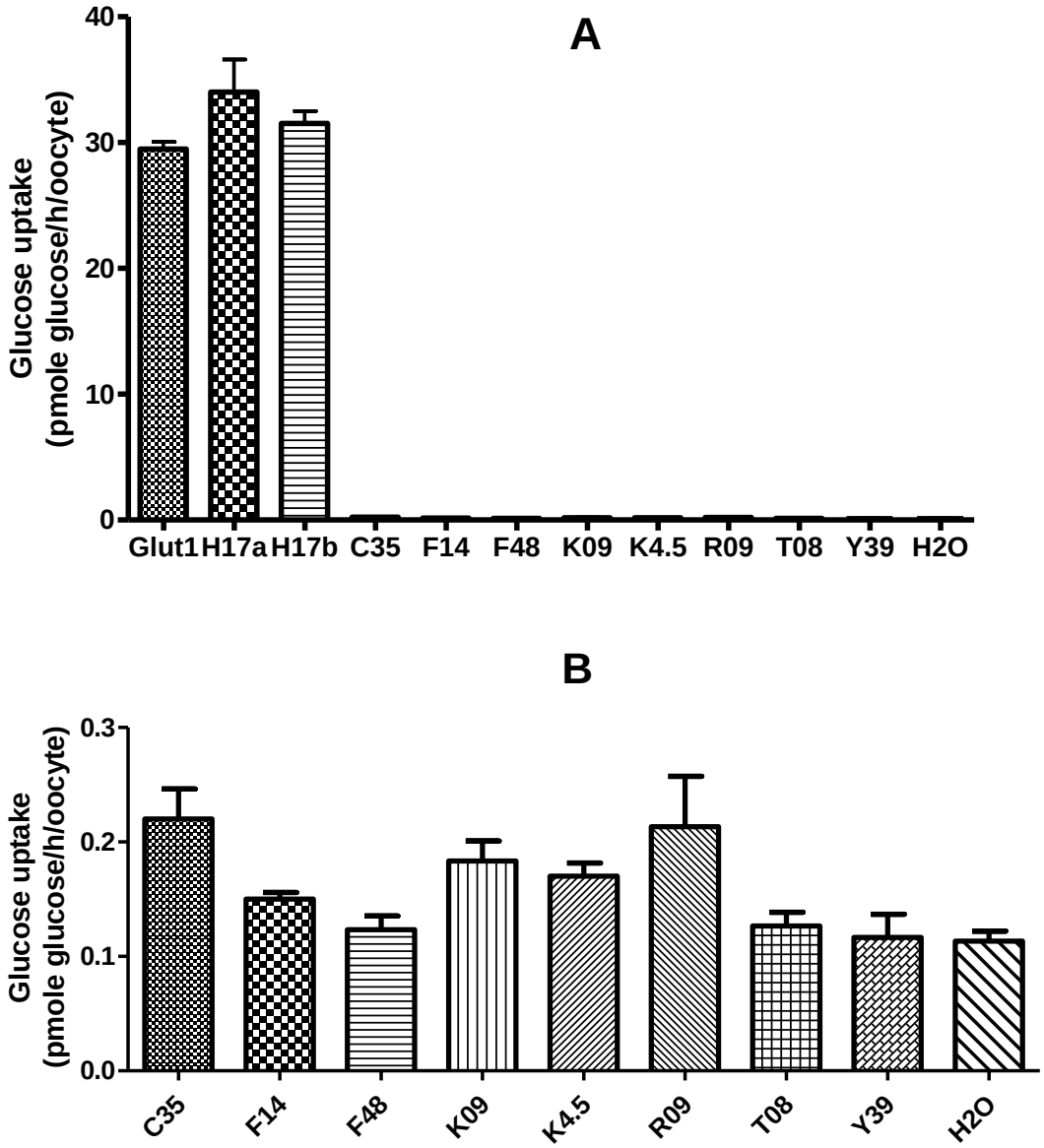

Figure 4.4 The glucose transport activity of the putative transporters in *Xenopus* oocytes. 50 ng of the cRNA of the putative transporter or GLUT1 was injected into healthy *Xenopus* oocytes. Oocytes were also injected with 50 nl of the DEPC-treated water as the negative control in the following assay. Two days after the injection, healthy oocytes were selected for glucose transport assay. **A.** Among the ten cloned putative transporters, only the protein of H17a and H17b exhibited significant glucose transport activity comparing with the negative control and similar transport activity to the rabbit GLUT1 in *Xenopus* oocytes. **B.** The rest of the eight putative transporter showed no glucose affinity (the transport levels were not significantly higher than the level of water injected oocytes) comparing with the glucose affinity of the positive control, rabbit GLUT1. The experiment was repeated three times. Each value is the mean ± SEM.

In order to normalize the transport activities of H17a and H17b to their expression levels on the cell surface, the glucose transport activities of HA-tagged H17a and b and HA-GLUT1 (as the positive control) were also examined using the same conditions as used for the non-tagged proteins (1h starvation, incomplete-ND96 with 50 μM D-glucose, 0.3 μCi U-[^{14}C]-Glucose for each assay). HA-antibody surface binding assays were also conducted on each group of the oocytes. Although expressed on the cell surface (Figure 4.5B), all the three transporters showed low level of transport activity (the amount of transported glucose of the three transporter were not significantly different from that of the water control, $P > 0.05$) (Figure 4.5A). Both of the HA-tagged and non-HA-tagged version of the three proteins were then tested in the same experiment. The result showed that the glucose transport activities of the three transporters were almost completely disrupted by the insertion of HA tag in the first exofacial loop (Figure 4.5C)

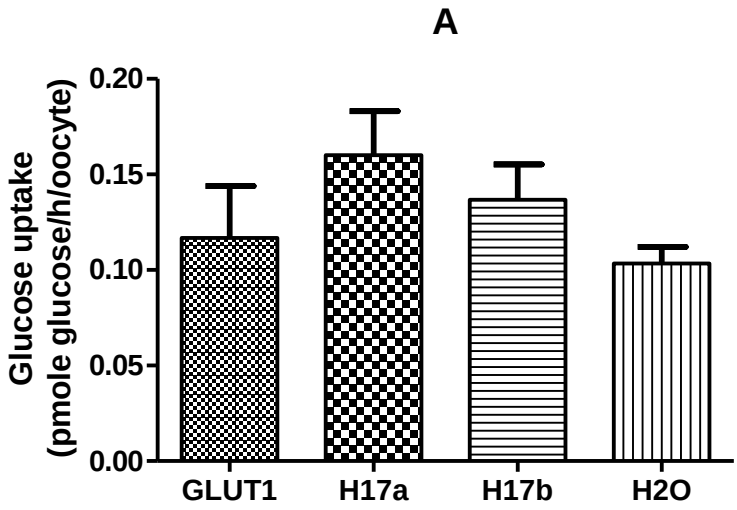

Figure 4.5 The glucose transport activity was disrupted by the insertion of HA tag into the first exofacial loop of the three transporters, H17a, H17b, and GLUT1. Oocytes were injected with cRNA of either HA-tagged or non-HA-tagged H17a, H17b and GLUT1 respectively. The injected oocytes were then subjected to glucose transport assay (1 h uptake, 50 μM glucose, 0.3 μCi of U-[^{14}C]-Glucose). The experiment was repeated three times. Each value is the mean ± SEM. **A.** All of the three HA-tagged transporters showed low glucose transport activity ($P_{H17a\ vs\ H_2O} = 0.08$, $P_{H17b\ vs\ H_2O} = 0.18$, $P_{GLUT1\ vs\ H_2O} = 0.67$).

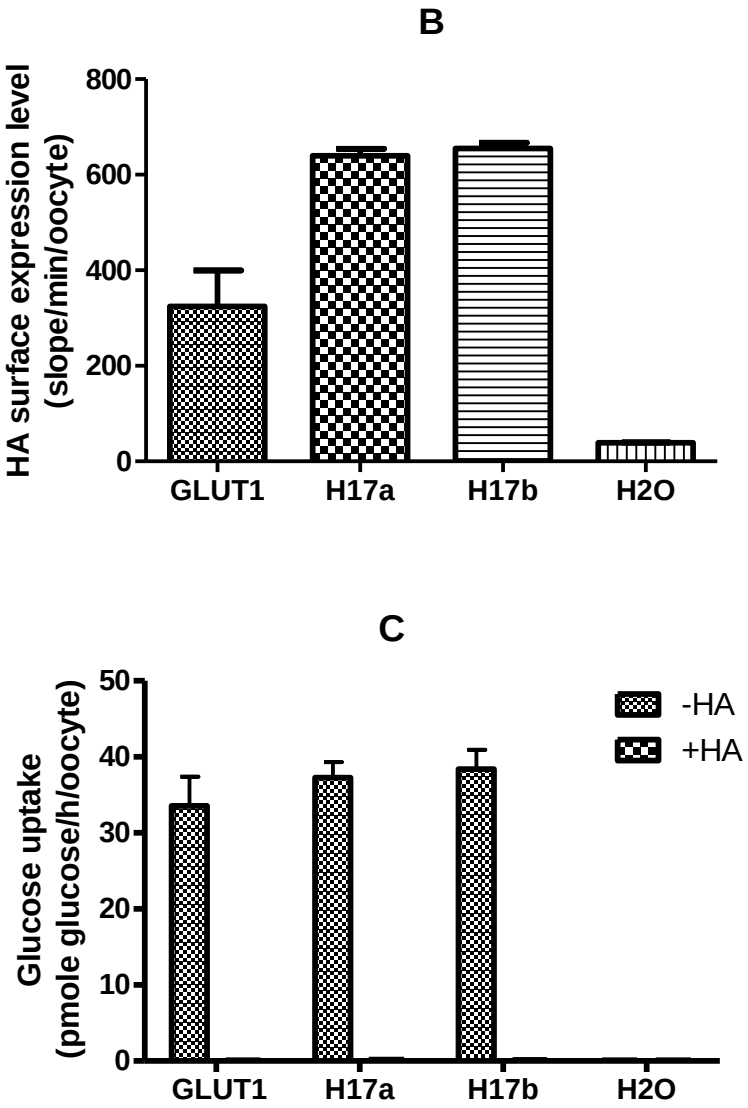

Figure 4.5 The glucose transport activity was disrupted by the insertion of HA tag into the first exofacial loop of the three transporters, H17a, H17b, and GLUT1. Oocytes were injected with cRNA of either HA-tagged or non-HA-tagged H17a, H17b and GLUT1 respectively. The injected oocytes were then subjected to glucose transport assay (1 h uptake, 50 μM glucose, 0.3 μCi of U-[^{14}C]-Glucose). The experiment was repeated three times. Each value is the mean ± SEM. **B.** The expression levels of H17a, H17b and GLUT1 on the cell surface. **C.** Comparing with the amount of glucose uptake of the non-HA-tagged proteins, the glucose transport activities of the three HA-tagged proteins were almost complete disrupted.

4.2.3 Trehalose transport activities of the putative glucose transporters

The trehalose transporter in insect, TRET1, was suggested to have the domain for sugar transport and belong to the MSF (Kikawada, Saito et al. 2007), moreover, trehalose plays an important role in the physiology of *C. elegans* (described in section 4.1.2) (Pellerone, Archer et al. 2003). Sequence alignment showed that TRET1 had high similarity to the ten selected putative glucose transporters (Table 4.2). Therefore, we decided to test the trehalose transport activities for the putative transporters.

Table 4.2 TCoffee scores for the alignment of the putative transporters with TRET1

Protein	TCoffee score	Construct	Enzyme
C35	76	R09	71
F14	77	H17a	81
F48	67	T08	57
K09	58	Y39	65
K4.5	62		

The value of TCoffee score > 50 suggests a good similarity between the two aligned sequences. The higher the score is, the higher similarity is shared between the two sequences (Notredame, Higgins et al. 2000). All of the TCoffee values of the putative transporters aligned with TRET1 were higher than 50, suggesting that these proteins shared high similarity to TRET1.

Trehalose can be hydrolyzed to glucose by trehalase (Dahlqvist 1968). Glucose is oxidized to gluconic acid and hydrogen peroxide by glucose oxidase. Hydrogen peroxide reacts with o-dianisidine in the presence of peroxidase to form a colored product. Oxidized o-dianisidine reacts with sulphuric acid to form a more stable pink colored product. The intensity of the pink color measured at 540 nm is proportional to the original glucose concentration (Bergmeyer 1974) (Figure 4.6). The amount of the trehalose uptake by the oocytes can, thus, be determined. Based on the above principle, the following experiment was designed: *Xenopus* oocytes expressing the non-HA-tagged putative transporters were prepared as described in section 2.2.7. The oocytes were starved for 1 h before the uptake. A group of 60 oocytes for each sample were then incubated in incomplete-ND96 buffer (nutrient free) containing

100mM trehalose for 3 h at 18°C. The uptake reaction was stopped by washing the oocytes quickly for 3 times in large amount of ice cold ddH_2O. The oocytes were then homogenized and the yolk protein was collected by centrifuging and discarded. The supernatant of each sample was then treated with trehalase. The concentration of glucose was analyzed using the Glucose (GO) assay kit (described in section 2.2.8). The amount of the trehalose uptake by the oocytes was then calculated according to the glucose concentration.

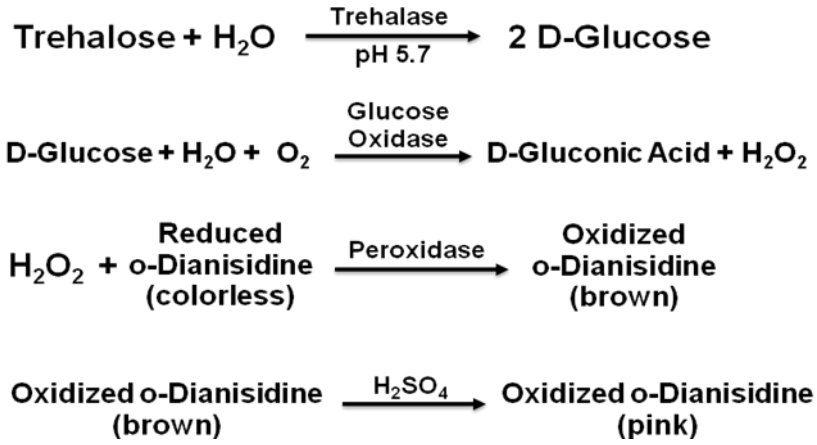

Figure 4.6 The principle of trehalose assay. Trehalose can be hydrolyzed into two D-glucose by trehalase in acidic environment. Glucose is oxidized to gluconic acid and hydrogen peroxide by glucose oxidase. Hydrogen peroxide reacts with o-dianisidine in the presence of peroxidise to form a coloured product. Oxidized o-dianisidine reacts with sulphuric acid to form a more stable pink coloured product. The intensity of the pink colour measured at 540 nm is proportional to the original glucose concentration.

All of the ten putative transporters were tested for trehalose transport activity (Figure 4.7). Except from H17a and H17b, the rest of the eight proteins showed no trehalose transport activity (the P values of there trehalose uptake of these proteins vs. water control were all larger than 0.05). The transport levels of H17a and H17b were significantly different from that of the water injected negative control (P_{H17a} = 0.0017, P_{H17b} = 0.0272). The amount of trehalose uptake in H17a samples was about 3 fold higher than in the negative control, while the uptake amount in H17b was about 2 fold higher than in the negative control. This result suggests that the two proteins, H17a and H17b, are also capable of transporting trehalose.

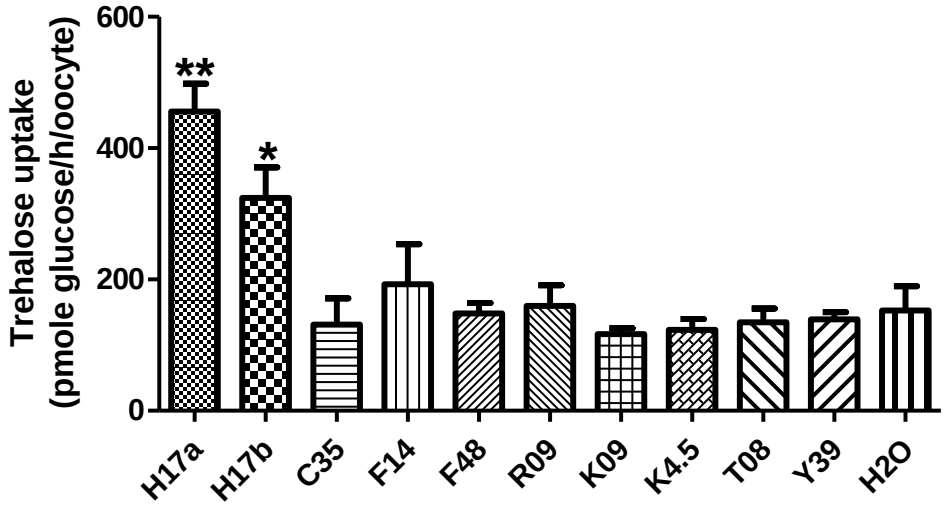

Figure 4.7 The trehalose uptake in the ten putative *C. elegans* transporters. Healthy ooctyes injected with the cRNAs of the putative transporter were incubated in incomplete-ND96 buffer with 100 mM trehalose for 3 h. The cell lysates were diluted and treated with trehalase first and then subjected to Glucose Oxidase (GO) assay to determine the concentration of the hydrolyzed glucose. The amount of trehalose uptake was then calculated according to the glucose concentration in the cell lysates. Except from H17a and H17b, the rest of the eight proteins showed no trehalose transport activity (the results of the transport level were not significant to that of the negative control, $P > 0.05$). The transport levels of H17a and H17b were significantly different from that of the water injected negative control ($^{**}P_{H17a} = 0.0017$, $^{*}P_{H17b} = 0.0272$). The experiment was repeated three times. Each value is the mean ± SEM.

4.2.4 Kinetics of the glucose transport for H17a and H17b

Among the ten cloned putative glucose transporters in *C. elegans*, only the two transcripts of H17 exhibited both glucose and trehalose transport activity, therefore, we decided to mainly focus on the study of the two proteins, H17a (492 aa) and H17b, (510 aa). There are about 21-amino-acid difference in the N-terminus between the two transcripts (Figure 3.4A). Both of the two putative proteins were predicted to be orthologs of human GLUT3 (Blast e-value: 1e-97, 43% identity), which belongs to the class I facilitative transporters. The glucose transport of the facilitative transporters exhibits simple, hyperbolic Michaelis-Menten kinetics (Baldwin 1993). Kinetic analysis was conducted on both H17a and H17b.

Xenopus oocytes injected with cRNA of H17a and H17b were used in the kinetic analysis. A group of five oocytes was incubated 1 h in incomplete-ND96 buffers containing D-glucose with a concentration gradient (2 mM, 5 mM, 12.5 mM, 20 mM, and 25 mM respectively). The reaction was initiated by the addition of 0.3 μCi of U-[^{14}C]-Glucose to each assay. The glucose uptake was measured by the radioactivity in the cells lysates after the reaction. The procedure was repeated three times. The results were then analyzed by GraphPad to fit the equation: $[S]/V = (K_m/V_{max}) + ([S] / V_{max})$ ([S]: substrate concentration, V: initial reaction rate). The results showed that the K_m and V_{max} values of H17a activity for glucose were 6.52±1.85 mM and 2.93±0.25 pmole/min/oocyte (Figure 4.8A); while the K_m and V_{max} values of H17b activity for glucose were 9.57±2.55 mM and 3.47±0.37 pmole/min/oocyte (Figure 4.8B). The K_m value of H17a is lower than that of H17b suggesting that H17a has a higher affinity to glucose than H17b in the glucose transport.

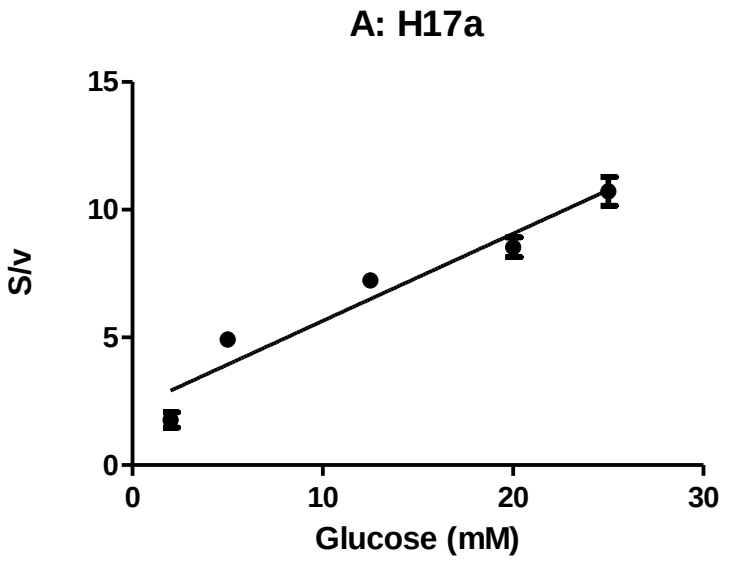

$K_m = 6.52 \pm 1.85$ mM

$V_{max} = 2.93 \pm 0.25$ pmole/min/oocyte

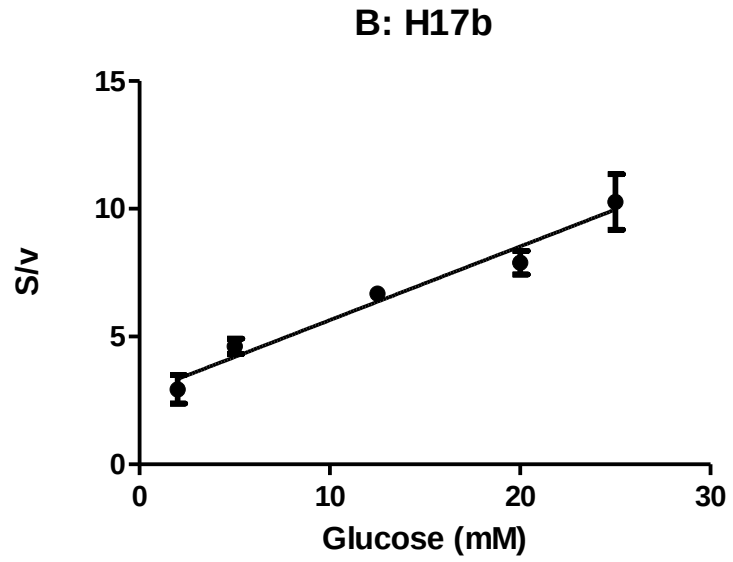

$K_m = 9.57 \pm 2.55$ mM

$V_{max} = 3.47 \pm 0.37$ pmole/min/oocyte

Figure 4.8 Kinetics analysis of glucose transport activities of H17a (A) and H17B (B). *Xenopus* oocytes expressing H17a and H17b were incubated in the indicated concentrations of glucose for 1 h. Uptake data were fitted to the Michealis-Menten equations. K_m and V_{max} were calculated by nonlinear regression analysis. The experiment was repeated three times. Each value is the mean ± SEM.

4.2.5 Cellular localization of H17a and H17b

The expression pattern for H17 stated in the Wormbase demonstrates that the gene is very broadly expressed in all life stages of *C. elegans*. Green fluorescent protein (GFP) fused reporter gene assay showed that the expression of H17 was observed in neurons, pharynx, hypodermis, and muscles (WormBase 2009) (Figure 4.9).

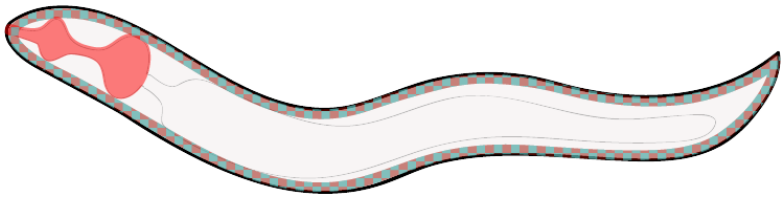

Figure 4.9 The schematic diagram of the expression pattern of H17 in *C. elegans*. GFP reporter gene data (Wormbase Expr1684 [http://www.wormbase.org/db/gene/expression?name=Expr1684;class=Expr_pattern]) showed that the expression of H17 was observed in neurons, pharynx, hypodermis, and muscles (the pink area in the picture). The picture was adapted from (WormBase 2009)

In order to visualize the cellular localization of H17, H17a and H17b were expressed in the CHO-T cells. Firstly, the HA-tagged H17a and H17b genes were fused with enhanced green fluorescent protein (EGFP) at the C-terminus and then cloned into mammalian expression vector pcDNA3.1(+) (Figure 4.10A). The stop codon of H17a and H17b was removed by silent mutation using site-directed mutagenesis, an AgeI restriction site was added at the downstream of the two H17 genes so that the EGFP fragment cut from pEGFP-N1 vector could be ligated in frame. The primers used for deleting the stop codon of the two genes are as follows (the mutated base and Age I recognition site are in red):

H17astopdelFor: CGAGAAGAGGAAGTCACCGTTCCATATGACTAGTAGATCC

H17astopdelRev: GGATCTACTAGTCATATGGAACGGTGACTTCCTCTTCTCG

H17bstopdelFor: CGAGAAGAGGAAGTCACCGGTTATGACTAGTAGATCC

H17bstopdelRev: GGATCTACTAGTCATAACCGGTGACTTCCTCTTCTCG

After the mutagenesis, the mutated HA-H17a and -b (~1500bp) were cut out from pT7Blue vector by Acc65I and AgeI. The EGFP fragment (~720bp) was cut put from pEGFP-N1 vector by AgeI and NotI. The vector pcDNA3.1 was digested with Acc65I

and NotI (Figure 4.10B). The three fragments were then ligated to form the new construct: pcDNA-HA-H17a/b- EGFP. The sequence of the two constructs were sequenced and aligned with the original sequence for any sequence alterations occurred during the cloning procedure. The clones which did not have any alterations were selected and used in the following expression in CHO-T cells. When expressed in cells, the HA tag in the first exofacial loop would allow the detection of the target proteins on the cell surface, while the EGFP fused at the C-terminus of the two proteins was able to indicate the localization of the proteins inside the cells.

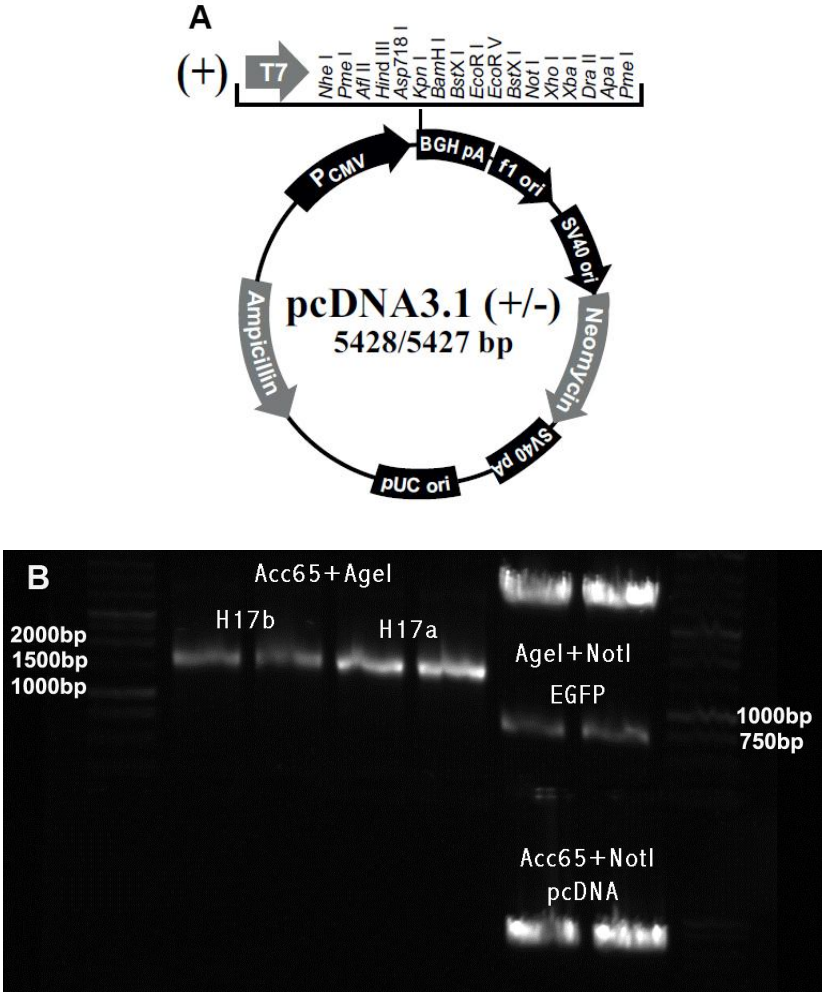

Figure 4.10 The construction of pcDNA-HA-H17a/b-EGFP. A. The map of pcDNA3.1(+). **B.** The agarose gel picture of the three fragments constructing pcDNA-HA-H17a/b-EGFP. The stop codon of HA-H17a/b was removed by silent mutation while an AgeI site was added to the downstream of the two genes. The EGFP fragment was cut out by AgeI and NotI so that the fragment could be ligated in frame with the HA-H17a/b fragment.

The pcDNA-HA-H17a/b-EGFP construct was then transfected into CHO-T cells using the transfection reagent, Lipofectamins (described in section 2.2.5) and allowed to express for 24 h. The cells were then fixed with PFA and blocked with the blocking reagent. The cells were then first incubated with the primary mouse HA-antibody at the dilution of 1:1000 and second incubated with goat anti mouse Alexa-633 conjugated antibody at the dilution of 1:1000. Finally the cells were mounted on slides and examined using the confocal laser scanning microscope. The cellular expression of H17a/b showed similar patterns. Both of the proteins were expressed on the plasma membrane while grainy expression around the perinulear region in the cytosol was also observed (Figure 4.11Basal panels).

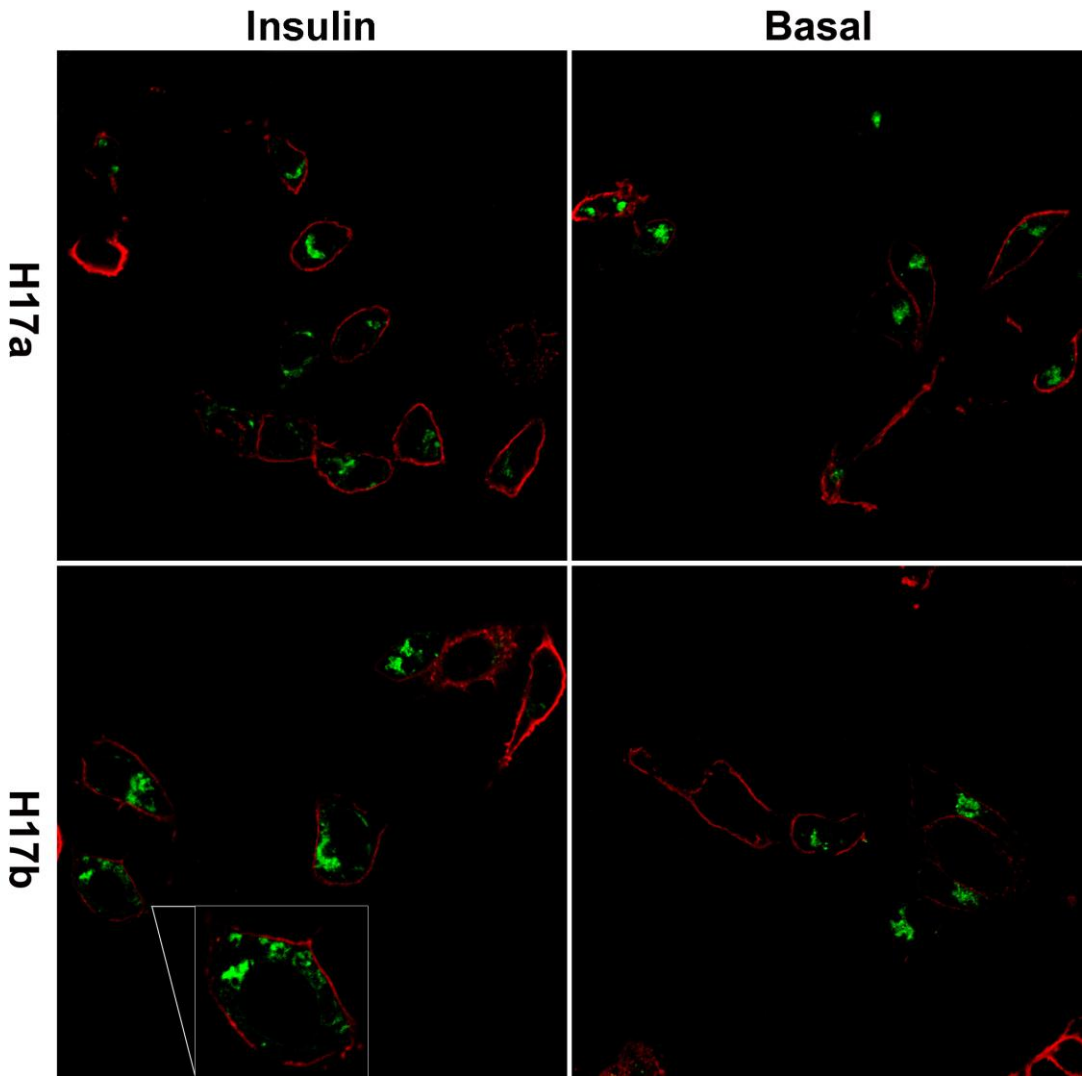

Figure 4.11 The cellular localization of H17a/b. The pcDNA-HA-H17a/b-EGFP was transfected into CHO-T cells respectively using the transfection reagent and allowed to express for 24 h. The cells were than incubated with HA antibody and stained with Alexa-633 conjugated antibody. The pictures were taken by confocal laser microscope at the wavelength of 488 nm (for EGFP) and 633 nm (for Alexa 633). **Insulin panels:** The cells were first stimulated with 100 nM insulin for 30 min at 37°C and then preceded to the same fixation and immunostaining procedure as the basal cells. The experiment was repeated three times and similar expression pattern were observed.

4.2.6 Insulin response of H17a and H17b

One of the most important signalling pathways related to glucose transport is the insulin signalling pathway. There is about 21-amino-acid difference in the N-terminus between the two transcripts of H17 (Figure 3.4A). Eleven serines are presented in the N- terminus of H17b, which is indicating that the protein may be phosphorylated and, thus, may be involved in the signal transduction pathways. Because of such considerations, we decided to test the insulin response on H17a and H17b localisation.

- ***The intracellular translocation and glucose transport activity of H17 in response to insulin stimulation in CHO-T cells***

The CHO-T cells are a cell line that stably expresses the insulin receptor. These cells provided platform in which the insulin response (e.g. the intracellular translocation or glucose transport activity in response to insulin stimulation) of a target protein can be tested. The HA tag in the first exofacial loop of H17a/b allows the detection of the protein on the cell surface without permeabilizing the cells. If any of the two proteins was responsive to insulin stimulation, we would expect to have certain levels of translocation from the intracellular compartment to the cell surface, which would be reflected on the increase of HA:EGFP signal ratio. Therefore, the insulin responsiveness of H17a/b can be determined by comparing the strength of the HA signals on the cell surface and the EGFP signals inside the cells between the basal and insulin stimulated status.

The pcDNA-HA-H17a/b-EGFP construct was transfected into CHO-T cells, respectively, and allowed to express for 24 h. A group of the transfected cells was then stimulated with 100 nM insulin for 30 min at 37°C. The HA and EGFP signals were then examined using a confocal laser microscope after the immunostaining procedure. There were no significant signal difference in HA signals nor in EGFP signals between the insulin and basal state of the cells. Cells with strong HA signals (indicating that large amount of H17a/b proteins were on the cell surface) were found

in both basal and insulin state with similar number of cells. The cells with strong EGFP signal but weak HA signal (indicating that most of the proteins were in the intracellular compartment) were also observed with a similar cell numbers in both state (Figure 4.11). Thus, examining the insulin response by comparing the HA:EGFP signal ratio was not successful.

A possible insulin signalling response leading to transporter activation was then examined in glucose transport assays in CHO-T cells. Because the variation in the radioactivity signals is much more sensitive than the fluorescent signals. The expression construct of pcDNA-H17a/b was constructed by inserting either H17a or H17b gene between the Acc65 I and Xba I sites in the pcDNA3.1 vector. CHO-T cells transfected with pcDNA-H17a/b were incubated at 37°C for 24 h to allow the expression of H17a/b. The cells were starved in Ham's F-12 medium with L-glutamine without FBS for 1 h. The cells were treated with or without insulin (100 nM) for 30 min at 37°C. The cells were then subjected to glucose transport assays (described in section 2.2.8) (50 µM glucose in Ham's F-12 medium with L-glutamine, 0.2 µCi of U- [^{14}C]-glucose for each assay).

The endogenous glucose uptake level of CHO-T cells is rather high (Figure 4.12A). When stimulated by insulin, the level of glucose uptake in H17a expressing cells was 1.3 fold higher than the level of the cell transfected with empty vector, while that of the H17b expressing cells was 1.2 fold higher. In the basal state, the levels of glucose uptake in H17a and H17b expressing cells were 1.2 and 1.5 fold higher than the levels of basal cells transfected with empty vector respectively (Figure 4.12A). For comparisons of the glucose uptake levels between the cells expressing H17a/b in insulin and basal state, the endogenous uptake was substracted. However, the glucose uptake levels of H17a and –b between insulin and basal state were not significantly different (P_{H17a} = 0.3591 > 0.05, P_{H17b} = 0.2016 > 0.05) (Figure 4.12 B). Thus, the glucose transport activity of neither of H17a nor –b was responsive to insulin stimulation when expressed in CHO-T cells.

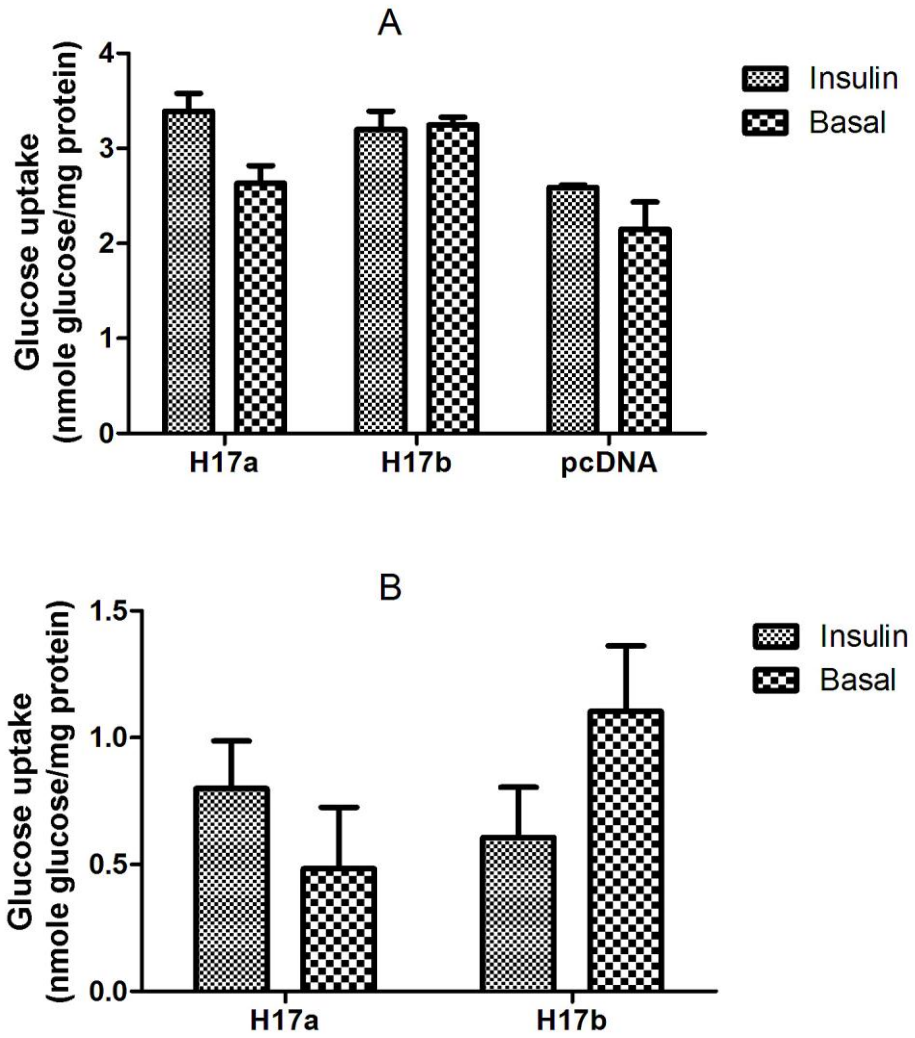

Figure 4.12 The glucose transport of H17a/b in CHO-T cells. Either pcDNA -H17a/b or the empty pcDNA3.1 vector was transfected into CHO-T cells respectively using the transfection reagent and allowed to express for 24 h. The cells were treated with or without insulin (100 nM) at 37°C for 30 min before being subjected to glucose transport assay. The transport assays were carried out under the condition of 50 μM glucose in Ham' F12 medium in addition of 0.2 μCi U-[^{14}C]-glucose per assay. **A.** The glucose transport levels at insulin and basal state including the negative control transfected with empty vector. **B.** The glucose transport levels of H17a/b at insulin and basal state with background value substracted. The experiment was repeated three times. Each value is the mean ± SEM.

- ***Intracellular translocation of H17 in response to insulin stimulation in primary rat adipocytes***

In the typical insulin responsive system such as primary rat adipocytes, stimulation by insulin leads to HA-GLUT4 translocation to the plasma membrane, where the HA tag in the first exofacial loop can be detected by anti-HA primary antibody. The primary antibody then binds with the IgG β-galactosidase conjugate secondary antibody. β-galactosidase catalyzes the hydrolysis of its fluorogenic substrate FDG. The process is first to fluorescein monogalactoside (FMG) and then to highly fluorescent fluorescein (Okada and Rechsteiner 1982; Lin, Yang et al. 1994). The fluorescence (emission 512 nm/excitation 488 nm) can then be measured with a fluorescent microtiter plate reader. Thus the amount of HA-GLUT4 translocated to the plasma membrane is able to be described (Quon, Zarnowski et al. 1993; Quon, Guerre-Millo et al. 1994). The responses of H17a and –b to insulin were also tested using this assay.

Both H17a and –b were expressed on the cell plasma membrane in basal state. Therefore, it was very important that the two transporters were not over expressed in the adipocytes. Because over expression might lead to accumulation of the proteins on the plasma membrane. This would compromise the accuracy of the fluorescent signal detection. Therefore, the high copy number expression vector pcDNA was not suitable for the expression in primary rat adipocytes. Under such consideration, HA-H17a and –b fragments were ligated into a low copy number expression vector pCIS2 between the BglII and ApaI sites to form the expression constructs: pCIS-HA-H17a and pCIS-HA-H17b. The two constructs and pCIS-HA-GLUT4 (as positive control) were transfected into primary rat adipocytes by electroporation. The basal level of cell surface HA-GLUT4 was proportional to the amount of DNA transfected. As the amount of transfected DNA was increased, the basal levels of cell surface HA-GLUT4 also increased accompanied by a decrease in the fold stimulation by insulin (Quon, Guerre-Millo et al. 1994). The transfection condition for HA-GLUT4 was already optimized to 100 ng DNA per cuvette by Dr. Francoise

Koumanov. This gave the best insulin stimulation effect under the experimental conditions used in the lab as an optimum level of expressed GLUT4 was achieved. The transfection condition of HA-H17a and –b was optimized to 1.5 μg and 1 μg DNA per cuvette respectively, so that the total HA-H17a and -b expression level was similar to that of the HA-GLUT4 (Figure 4.13B).

The cells were incubated at 37°C for 5 h to allow expression before being subjected to the cell surface HA-antibody binding assay (described in section 2.2.9). The cells were treated with or without insulin (60 nm) in KRH buffer at 20°C for 20 min. The anit-GLUT4 antibody and anti-HA antibody were used in the western blot respectively to indicate the total protein and total HA-H17a and –b or total HA-GLUT4 levels in each sample (Figure 4.13A and B). The density of each band of the western blots was analyzed using Labworks software (version 4, UVP). The data of the cell surface fluorescent increase for each sample were then normalized to the total protein level as well as the total H17a and –b level expressed in the adipocytes. The data were also corrected for nonspecific binding. As shown in Figure 4.13C, an 8.6-fold increase in the cell surface HA-GLUT4 was observed with insulin stimulation. Whereas, the HA-H17a level on cell surface in the insulin state versus in the basal state was not significantly different ($P > 0.05$), while the HA-H17b level on cell surface in the basal state was even higher than in the basal state. Thus, no increase in the cell surface HA-H17a or –b was observed with insulin stimulation. This result suggests that H17a and –b are not insulin responsive when expressed in the primary rat adipocytes, either.

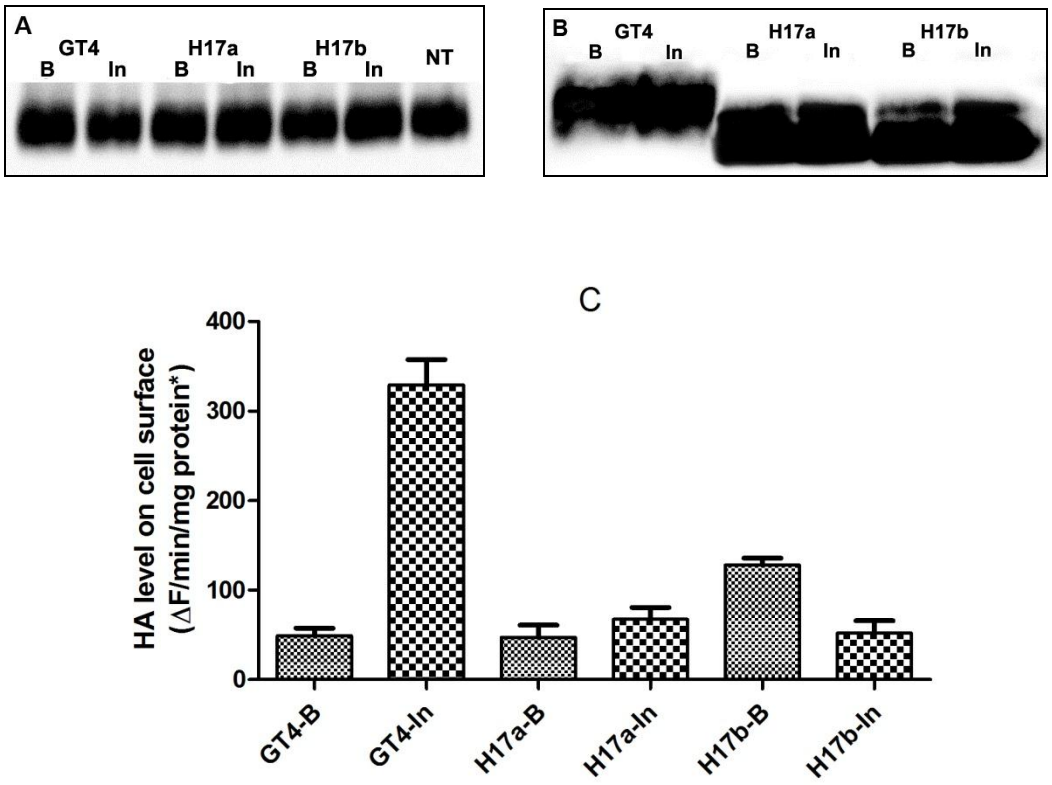

Figure 4.13 The insulin response of H17a and –b in the primary rat adipocytes. The primary rat adipocytes were transfected with HA-GLUT4 (100 ng/cuvette), HA-H17a (1.5 μg/cuvette), and HA-H17b (1 μg/cuvette) by electroporation. After incubated in DMEM containing 3.5% BSA, 200 nM adenosine, and 75 μg/ml gentamycin, at 37°C for 5 h, the cells were subjected to HA-antibody surface binding assay. **A.** GLUT4 immunoblot of the transfected cells. Cell lysates from 5 μl of the resuspended cells were loaded on each lane. **B.** HA immunoblot of the transfected cells. Cell lysates from 15μl of the resuspended cells were loaded on each lane. **C.** Cell surface HA binding assay for HA-GLUT4, HA-H17a and –b. Cells expressing the above three proteins were treated with or without insulin (60 nM) at 20°C for 20 min, followed by KCN (4mM) treatment for 3 min to stop the translocation. Cells were then incubated for 1 h with anti-HA mouse antibody. After washing, cells were incubated with a secondary anti-mouse IgG β-galactosidase conjugate antibody for 1 h. The fluorescent signal was measured using a fluorescent microtiter plate reader (emission 512 nm/excitation 488 nm).*Results from each experiment were normalized for total protein level and total HA level. ΔF: the increase of the fluorescent signals, B: basal, In: insulin. The experiment was repeated three times. Each value is the mean ± SEM.

4.3 Discussion and conclusion

This chapter is mainly focused on the description of *in vitro* functional studies of the ten putative glucose transporters in *C. elegans* whose cloning was reported in Chapter 3. Both the glucose transport activity and trehalose transport activity were examined for the ten proteins when being expressed in *Xenopus* oocytes. Among all the cloned putative glucose transporters, only the two transcripts of the gene H17B01.1, H17a (worm protein ID: CE27184, 492 aa) and H17b (worm protein ID: CE27184, 510 aa), showed both glucose and trehalose transport activities. This is, for the first time, a glucose transporter identified in the worm *C. elegans*.

The two proteins, H17a and –b, have both been reported as the orthologs of human GLUT3 (Blast e-value: 1e-97, 43% identity), which is a high affinity glucose transporter in the class I facilitative transporter family. Protein sequence analysis suggests that all the key motifs of the GLUT superfamily are found in H17 protein sequence (Figure 3.4B). Protein membrane topology prediction suggests that both of the proteins have the typical GLUT family membrane topology which is characterized by the 12 transmembrane-region structure with cytoplasmic N- and C- terminus, large exofacial loop between helices 1 and 2 and large cytoplasmic loop between helices 6 and 7 (Gould and Holman 1993; Olson and Pessin 1996) (detailed in section 3.1.1). Class I and II mammalian glucose transporter proteins bear an N-linked glycosylation site in loop 1 (Baldwin 1993; Gould and Holman 1993; Olson and Pessin 1996). This N-glycosylation site is proved to be essential in the targeting and stability of GLUT1, as well as maintaining the high-affinity transport of glucose for these proteins (Asano, Katagiri et al. 1991; Asano, Takata et al. 1993). When HA-H17a and –b are expressed in the *Xenopus* oocytes, the glucose transport activities of the two proteins are almost completely disrupted by the insertion of HA tag in the first exofacial loop (Figure 4.14). This suggests that the first exofacial loop plays an essential role in the binding of glucose. Moreover, an N-glycosylation site may also exist in the first exofacial loop of H17. The insertion of HA tag may alter the

conformational structure of loop1 which would result in the un-availability of the glycosylation site and, therefore, cause the protein to fail to transport glucose across the cell membrane.

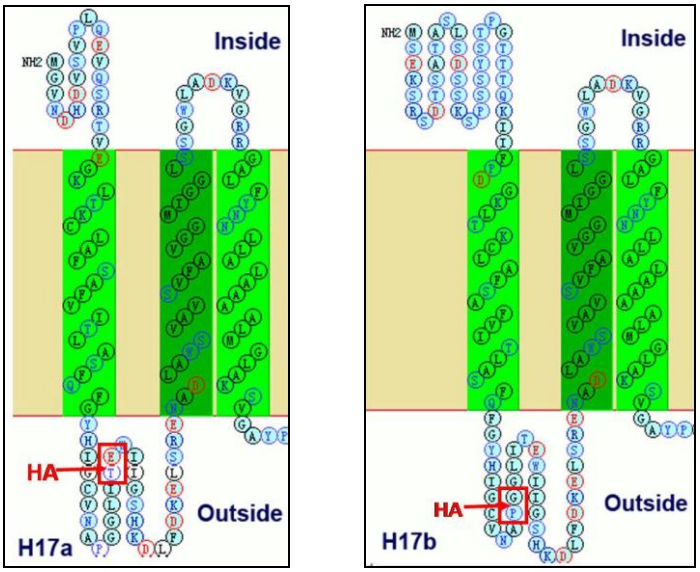

Figure 4.14 The position of HA insertion in the two H17 proteins. The HA tag was inserted between T57 and E58 for H17a and between P70 and G71 for H17b.

Mammalian GLUT1 is ubiquitously expressed and GLUT3 is mainly expressed in neurons (Manolescu, Witkowska et al. 2007; Zhao and Keating 2007). However, the expression of H17 is observed through-out all the life stages to be very broadly expressed in tissues including neurons, pharynx, hypodermis, muscle which all are the sites with high glucose demands. The K_m of H17a and –b for glucose uptake is ~6.5 mM and ~ 9.6 mM respectively when expressed in the *Xenopus* oocytes. These K_m values are comparable with those of GLUT1, 5 mM, GLUT4, 5 mM, and GLUT3, 1 mM, indicating that H17 is a high-affinity glucose transporter in *C. elegans*. All of the above findings suggest that H17 may act as a major glucose transporter in *C. elegans.* Moreover, H17 also shows trehalose transport activity when expressed in *Xenopus* oocytes. The disaccharide trehalose plays important role in the *C. elegans* physiology (discussed in section 4.1.2). Recently, trehalose is also found to be able to extend the lifespan of the worm (Honda, Tanaka et al. 2010). However, trehalose cannot pass freely across biological membranes (Elbein, Pan et al. 2003). Therefore,

H17 may also play a role in the mechanism of trehalose extending the longevity in *C. elegans*.

H17a and –b were also expressed in CHO-T cells and primary rat adipocyte to test the possibility of insulin response. The presence of multiple serines in the N-terminus of H17b suggests that the protein can be phosphorylated and involved in signal transduction. However, the two proteins are not responsive for insulin stimulation in either of the mammalian expression systems studied. The insulin responsive test in rat primary adipocytes is based on the increased number of the transporter on the plasma membrane in response to insulin stimulation. The FQQI or LL motif at the C-terminus of mammalian GLUT4 is required for the translocation of GLUT4 from intracellular compartment to the plasma membrane in response to insulin stimulation (Melvin, Marsh et al. 1999). Sequence alignment shows that H17 is lacking a similar motif at the C-terminus. Furthermore, the expression of HA-H17-EGFP shows that the cellular localization of H17 is mainly on plasma membrane (Figure 4.11) which is similar to the expression pattern of GLUT1 (Shanmugam, McBrayer et al. 2009). Therefore H17 translocation between cell membrane and intracellular compartments may not be responsive to the insulin (or insulin-like ligands in *C. elegans*) stimulation. However, whether H17 is involved as a downstream target of the insulin signalling pathway or any other signal transduction in *C. elegans* remains to be unveiled.

Although the rest of the eight putative transporters (C35, F14, F48, K09, K4.5, R09, T08, and Y39) are all predicted to be the orthologs of the human GLUT superfamily (Table 3.1) and all the corresponding human orthologs of the GLUT superfamily are capable of transporting glucose with high affinity, none of these putative transporters show either glucose or trehalose transport activity when expressed in *Xenopus* oocytes. For the mammalian GLUT superfamily, several studies on GLUT1-5 suggest that, within helix *7*, there are a number of residues that are very important for functional activity of the transporters. The motif “QLS” in this region is a site involved in substrate recognition. GLUT1, 3, and 4, which transport glucose but not fructose,

have the QLS sequence in helix 7, whereas GLUT2 and 5, that both transport fructose have HVA or MGG, respectively in the corresponding position (Manolescu, Witkowska et al. 2007). Sequence alignments of the nine putative transporters with human GLUT1 and GLUT4 show that only H17 has the “QLS” motif in helix 7 among these proteins. This finding is consistent with the above conclusion and indicates that the key motifs of glucose transport are also conserved in the worms. In *C. elegans*, glucose and glycogen, followed by trehalose, fructose and sucrose can be utilized as energy sources (Lu 1993). Moreover, long-chain fatty acids, ethanol, n-propanol and acetate can also be utilized as energy sources (Lu, Hugenberg et al. 1978). In the wormbase gene profile, all of the eight putative transporters are reported to have the protein domains of general substrate transporter (INTERPRO:IPR005828). The general substrate transporter protein domain is composed of the protein domain of sugar/inositol transporter, citrate-proton symport, phosphate permease, and organic cation transport protein (INTERPRO 2009). Therefore glucose may not be the favourable substrate for these putative transporters and the substrate specificity of these proteins are yet to be discovered.

To sum up, a high-affinity glucose transporter, H17B01.1, for the worm *C. elegans* is identified in this chapter. There are two transcripts of H17B01.1, H17a (492 aa) and H17b (510 aa), both of which are capable of transporting glucose with high affinity, as well as trehalose, when expressed in *Xenopus* oocytes. The cellular localization of H17 is mainly on the plasma membrane while expression around the perinuclear region is also observed. Both of the two transcripts are not insulin responsive when expressed in the CHO-T cells and rat primary adipocytes. The rest of eight putative transporters cloned in Chapter 3 do not transport either glucose or trehalose when expressed in *Xenopus* oocytes.

Chapter 5 An *in vivo* functional study of H17a/b in *C. elegans*

5.1 Introduction

5.1.1 The role of glucose in the regulation of lifespan

Calorie restriction (CR) and insulin/IGF-I-like signalling (IIS) are two pathways affecting lifespan in a variety of species. Genetic studies in *C. elegans* suggest that CR and IIS regulate the worm lifespan through distinct cellular signalling pathways (detailed in section 1.1). For example, the FOXO transcription factor, DAF-16, is essential for longevity in IIS mutants, but is dispensable for the lifespan extension through CR. Moreover, CR is able to further lengthen lifespan of long-lived worms lacking IIS due to a mutation in the kinase domain of the DAF-2 (Lakowski and Hekimi 1998; Houthoofd, Braeckman et al. 2003; Hansen, Hsu et al. 2005). However, there is also evidence suggesting that CR and IIS converge on downstream targets that act to promote longevity. In *C. elegans*, certain superoxide dismutase (*sod*) genes are specific targets of either CR or IIS, while other *sod* genes are targets of both pathways (Panowski, Wolff et al. 2007). In *Drosophila*, CR sensitivity was altered in *chico* (insulin receptor substrate in *Drosophila*) mutants, which have extended lifespan from disrupted IIS (Clancy, Gems et al. 2002). However, much work is still needed to fully understand the interactions between the two pathways.

Glucose is the major source of energy in eukaryotic organisms. In mammals, glucose homeostasis is maintained by processes regulated by the two hormones, insulin and glucagon (discussed in section 1.2). Therefore, glucose lack may not be only related to the CR mediated lifespan extension but also connected to the IIS mediated lifespan extension. However, the role of glucose metabolism in the multicellular eukaryote in regards to life expectancy is largely unknown. The worm, *C. elegans,* is

a suitable model organism for studying the role of glucose in the life span regulation because of its short life span, the relative ease in modifying its genome, and its simple insulin receptor system (the *daf-2* signalling pathway) (Schulz, Zarse et al. 2007; Lee, Murphy et al. 2009; Schlotterer, Kukudov et al. 2009).

Several recent studies indicate that glucose does play a role in the regulation of lifespan of *C. elegans*. Schulz et al. found that glycolysis in *C. elegans* could be impaired by treatment with 2-deoxy-D-glucose (DOG) (Schulz, Zarse et al. 2007). The lifespan of the worms was then extended by the reduced glucose metabolism. Schulz et al. demonstrated that glucose restriction promotes mitochondrial metabolism, causing increased reactive oxygen species (ROS) formation (Schulz, Zarse et al. 2007). However, this idea that glucose shortens life span by inhibiting respiration is challenged by the work of Lee et al. who demonstrate that glucose shortens the life span of *C. elegans* by down-regulating DAF-16/FOXO activity and aquaporin gene expression (Lee, Murphy et al. 2009). Based on the findings that the AMPK subunit AAK-2 was inactivated by glucose treatment, and that DOG did not lengthen the life span of *aak-2* null mutants, a model was proposed to suggest that glucose may shorten life span by inactivating the AMP-dependent kinase (AMPK) (Schulz, Zarse et al. 2007). This model predicted that glucose would not further decrease the life span of *aak-2* null mutants. However, Lee et al. reported that the short life span of the worms caused by loss of *aak-2* was further decreased by glucose feeding to the same extent as wild-type worms (Lee, Murphy et al. 2009). This finding, therefore, indicated that glucose does not shorten the life span of *C. elegans* by inactivating AMPK.

Taken together, glucose loading shortens the life span of *C. elegans,* while glucose restriction can extend the life span of the worms. However, the mechanism by which increased glucose availability regulates the life span of *C. elegans* (either by inhibiting the respiration or through the IIS pathway) remains controversial and much work still needs to be done to unveil the mechanisms involved in this process.

The first step of the glucose metabolism is the transportation of glucose across the plasma membrane by the glucose transporters. In mammals, the low-level of basal glucose uptake required to sustain respiration in all cells is maintained by the facilitative glucose transporter, GLUT1. In the meantime, the glucose homeostasis is mainly regulated by two hormones: insulin and glucagon. The first step by which insulin regulates the blood glucose level involves the regulated transport of glucose into the cell, mediated by GLUT4. Insulin increases glucose uptake mainly by enriching the concentration of GLUT4 proteins on the plasma membrane (Chang, Chiang et al. 2004). *C. elegans* has orthologs for most of the key enzymes involved in eukaryotic intermediate metabolism, suggesting that the major metabolic pathways are probably present in the species (Braeckman, Houthoofd et al. 2009). However, the glucose transporter family in *C. elegans* is very poorly described. Furthermore, whether the similar insulin responsive glucose transport system is present in the worm is yet to be discovered. Thus, by investigating the relationships between the glucose transporters and the life expectancy of *C. elegans*, or the link of the glucose transporters to the IIS pathway in the worms may also provide threads to the understanding of how glucose effects the life span of *C. elegans.*

5.1.2 Research objectives and experimental approach

The identification of the first glucose transporter, H17B01.1 (H17), in *C. elegans* allows the study of whether this glucose transporter is related to the life span regulation in *C. elegans*. The availability of complete genome sequences provides the rapid approach of studying the individual gene's function in *C. elegans* by RNA interference (RNAi). There are three ways of carrying out RNAi in *C. elegans*: injection (Fire, Xu et al. 1998), soaking (Tabara, Grishok et al. 1998), and feeding (Timmons and Fire 1998). RNAi by feeding is to feed the worms with bacteria producing the desired dsRNA and score the phenotype of the fed worms or their progeny. This method allows one to carry out RNAi on a large number of animals at once with least labour intensive and low cost. Thus, RNAi by feeding is used to study

the *in vivo* function of the gene H17 (Ahringer ed. 2006).

Upon the above consideration, the aims of this chapter are: 1). to construct the bacteria producing H17 dsRNA; 2). to investigate the effect of H17 knockdown on the lifespan of *C. elegans*; 3). to study the glucose metabolism in the H17 knockdown worms; 4). to study the relationship of H17 and the IIS pathway in *C. elegans.*

5.2 Results

5.2.1 The construction of H17 RNAi bacteria strain and RNAi of H17 in *C. elegans*

The first step of carrying out RNAi on *C. elegans* by feeding involves engineering bacteria to produce the dsRNA of the target gene (Timmons and Fire 1998). The cloning vector, L4440, containing two convergent T7 polymerase promoters in opposite orientation separated by a multiple cloning site (Timmons and Fire 1998) (Figure 5.1A) and bacteria strain, HT115 (Takiff, Chen et al. 1989; Dasgupta, Fernandez et al. 1998), was used for the engineering of H17 dsRNA producing bacteria (Timmons, Court et al. 2001). A ~ 400bp fragment (Figure 5.1B) was amplified with primers (Table 5.1) from pT7-H17a and pT7-H17b respectively. The amplified fragments were then ligated into the L4440 vector between the Acc65 I and Xba I restriction site (Figure 5.1C). The constructs of L4440-H17a and L4440-H17b were transformed into HT115 competent cells to form the desired H17 dsRNA producing bacteria. When induced with appropriate concentration of IPTG, the bacteria would be able to produce H17 dsRNA.

Table 5.1 The primers for amplifying the H17 a & b DNA template for RNAi constructs

Primer	Sequence	Fragment size
17aRNAifor	CGG GGC CCC GAT AAA TGG	417 bp
17aRNAirev	GCT CCA ATC TAG ACT TAG CC	
17bRNAifor	CGG GGC CCC GAT ATG TCG	395 bp
17bRNAirev	CCA CGT CTT CTA GAC CTT ATC G	

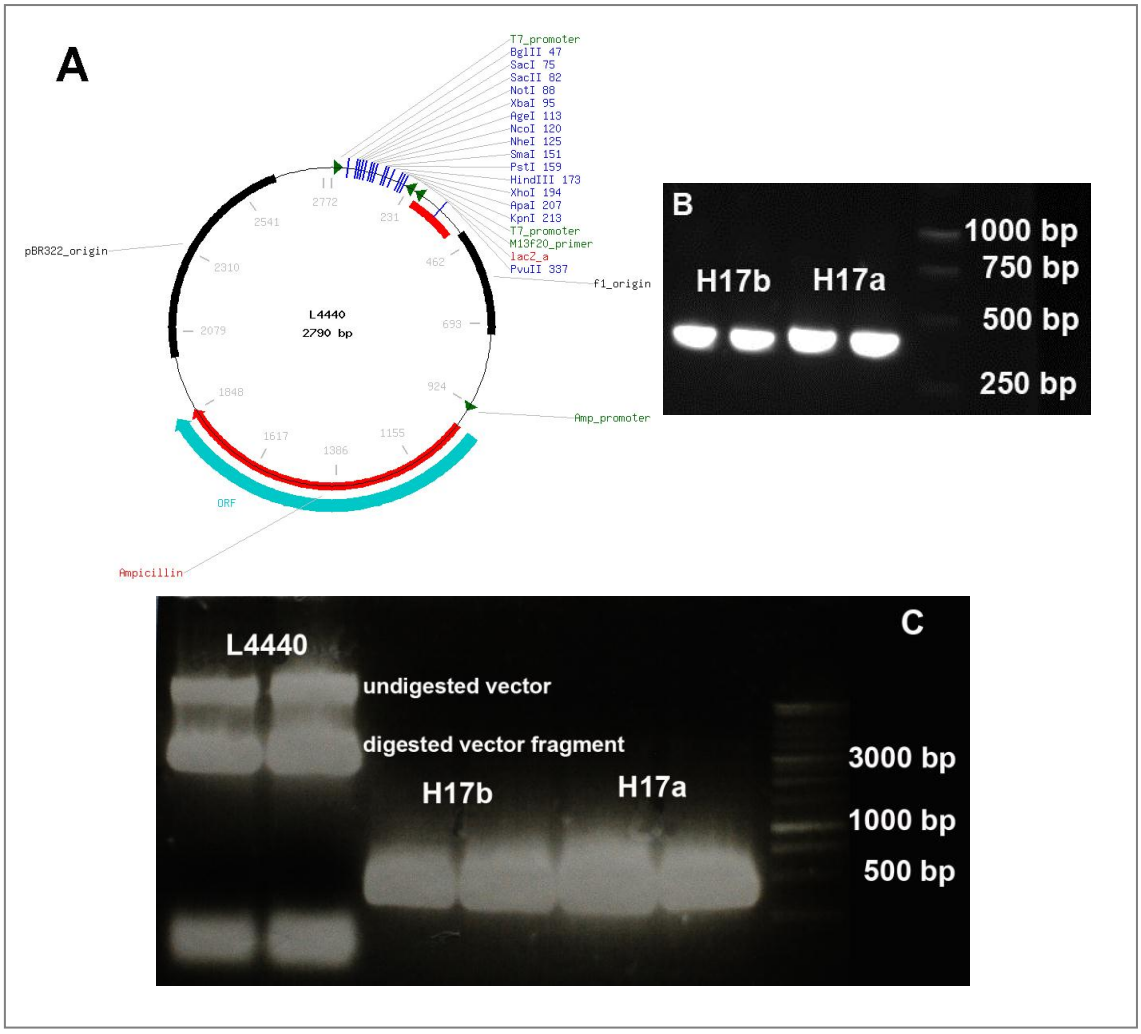

Figure 5.1 The construction of H17 RNAi bacteria strain. A. The map of L4440 (Adapted from Addgene [http://www.addgene.org/pgvec1?f=c&identifier=1654&atqx=L4440&cmd=findpl]). **B.** The Amplification of H17a and b fragments from pT7 H17 a/b. The PCR products were analyzed on a 1.5% agarose gel. **C.** Restriction enzyme digestion of the L4440 vector and H17 a /b fragments with Acc65 I and Xba I. The digestion products were analyzed on a 1% agarose gel.

In order to monitor the effectiveness of the RNAi of H17 in *C. elegans*, a positive control of *unc-22* RNAi, which gave a noticeable "twitching" phenotype when the *unc-22* RNAi worked (Timmons, Court et al. 2001), was used in parallel with each of the RNAi experiment. The "twitching" phenotype of *unc-22* would give a direct way of examine whether the RNAi had worked or not. When 80% of the worms were showing the "twitching" phenotype, the parallel RNAi experiments were assumed to have work as well. And the subsequent experiments would then be carried out.

NGM plates containing 50 μg/ml ampicillin and 1 mM IPTG were prepared and allowed to dry for 4-7 days before seeding the bacteria food source to give the best RNAi effect (Ahringer (ed.) 2006). LB liquid cultures of HT115 carrying L4440 (negative control), L4440-H17a, L4440-H17b, and L4440-*unc-22* (positive control) were prepared respectively by growing the single colony of each construct in LB medium containing 50 μg/ml ampicillin with shaking at 300 rpm, 37°C for 6~8 h. The cultures were then seeded on the NGM plates containing 50 μg/ml ampicillin and 1 mM IPTG and allowed to induce overnight at RT.

Synchronized and starved wild-type *C. elegans* L1 larvae were prepared (detailed in section 2.2.10) and seeded onto the NGM plates with RNAi bacteria food source. The worms were allowed to grow on the RNAi plates without exhausting the bacteria food until desired stage for subsequent experiments. The efficiency of the H17 knockdown was examined by QPCR (detailed in section 2.2.11). The gene *act-1* (forward primer: ccaggaattgctgatcgtatgcagaa and reverse primer: tggagagggaagcga-ggataga) was used as housekeeping gene to normalize the RNA level of H17 (Li, Tewari et al. 2007). As shown in Figure 5.2, the RNA levels of both H17a and H17b were significantly and reliably knocked down by ~80% (H17a: 80.8±4.8%, H17b: 79.7±6.0%) when treated with the engineered bacteria expressing H17 dsRNA. Therefore, the L4440-H17a and L4440-H17b constructs were used in the subsequent experiment.

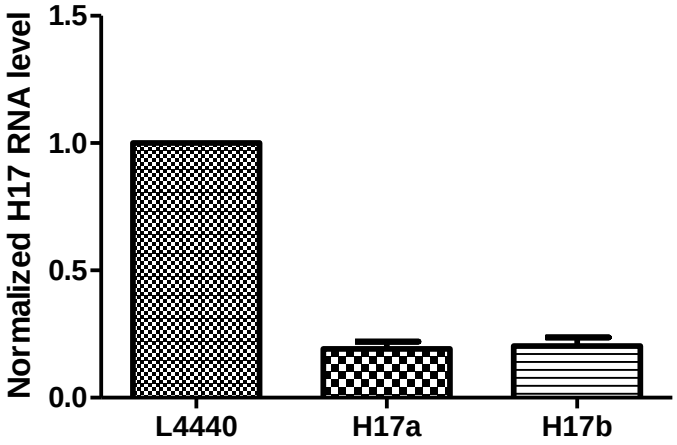

Figure 5.2 The RNAi of H17a and b in WT *C. elegans*. Total RNA was isolated from worms of all stages for each sample and quantified with UV-spectrophotometer. The cDNA from same amount of total RNA was then synthesized for each sample. The mRNA levels of H17a or b were then assessed respectively by Q-RCR using the primers listed in table 2.11. Each sample was analyzed in triplicates. The experiment was repeated three times. Each value is the mean ± SEM.

5.2.2 The effect of H17 knockdown on the lifespan of *C. elegans*

Glucose restriction is able to extend the life span of *C. elegans* (Schulz, Zarse et al. 2007). Since H17 is reported to have a ubiquitously expression in *C. elegans* (described in section 4.2.5), the glucose uptake maybe restricted by knocking down the expression of H17 and the lifespan of the worms may, thus, be extended. Therefore, the wild-type (WT) worms were subjected to H17 RNAi and the lifespan of these worms were analyzed by lifespan assay (detailed in section 2.2.12). As shown in Figure 5.3 and Table 5.3, the worms subjected with H17a RNAi, H17b RNAi or L4440 vector exhibited similar survival curve and the same median survival of 15~16 days. The results suggested that the life span of the WT worms was not significantly affected by the knock down of either H17a or H17b. In addition, unlike the food deprivation which can induce the dauer formation (Fielenbach and Antebi 2008), there was no noticeable increase of dauer phenotype in the H17 knocked-down WT worms. Moreover, the H17 knocked-down worms did not show any slow growth comparing with the control worms which were fed with bacteria carrying L4440 vector only.

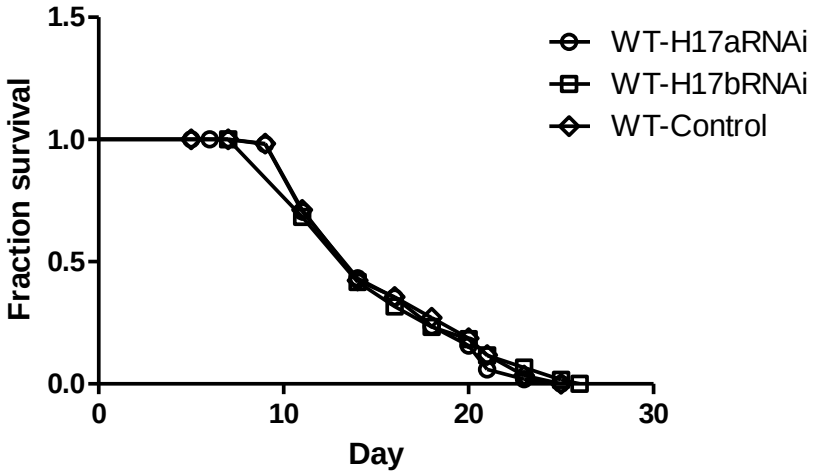

Figure 5.3 The lifespan assay in H17 RNAi WT *C. elegans*. WT young adult worms were allowed to lay eggs on the RNAi bacteria seeded NGM plates. The progeny were allowed to grow to L4 larvae stage at 20°C and then transferred to new RNAi bacteria seeded NGM plates containing 50 μM FUDR. The worms were allowed to grow till death without exhausting the RNAi bacteria food source. Day 0 of lifespan was the day that eggs were laid. Animals that failed to respond to a gentle prodding with a platinum wire were scored as dead. The data was analyzed with Kaplan-Meier method.

Meissner et al. reported that while the worm lifespan was not affected by the elimination of the worm intestinal peptide transporter, *pep-2*, the lifespan of the double mutant of *pep-2* and *daf-2* was extended by 60% compared to the *daf-2* single mutant (Meissner, Boll et al. 2004). The IIS pathway in worms is initiated by the activation of DAF-2 by the secreted insulin-like ligands, and is followed by the activation of AGE-1, production of second messenger PIP_3 and the activation of the AKT family kinases (Paradis and Ruvkun 1998; Hertweck, Gobel et al. 2004) (detailed in section 1.1.1). Therefore, we decided to check whether the knockdown of H17 would have any effect on the life span of the IIS pathway mutant worms. Three IIS pathway mutant strains were chosen for the subsequent experiments. They are: *daf-2* mutant (*e1370,* CB1370), *age-1* mutant (*hx546*, TJ1052), and *akt-1* mutant (*mg144*, GR1310) (Table 5.2). Among the three strains, *e1370* is a temperature sensitive strain with 100% dauer formation at 25°C and 15% dauer formation at 20°C (Gems, Sutton et al. 1998). Hence, the strain is maintained at 15°C before being seeded on to the RNAi NGM plates. All of the three strains were then subjected to lifespan assay at 20°C.

Table 5.2 Selected IIS pathway mutant worm strains for subsequent experiment

Strain name	Mutated gene	Mammalian ortholog	Phenotype
CB1370 (*e1370*)	*daf-2*	Insulin receptor	Temperature sensitive dauer constitutive. Maintain at 15°C. 100% dauer at 25°C. 15% dauer formation at 20°C.long lived, M-mating + low temperature only.
TJ1052 (*hx546*)	*age-1*	PI3K	Long live & stress resistance. Normal fertility.
GR1310 (*mg144*)	*akt-1*	AKT/PKB	No visible phenotype. Dominant suppressor of daf-c phenotype***** of *age-1*

* daf-c phenotype: dauer-constitutive phenotype. (worms inappropriately form dauer larvae under favorable conditions)

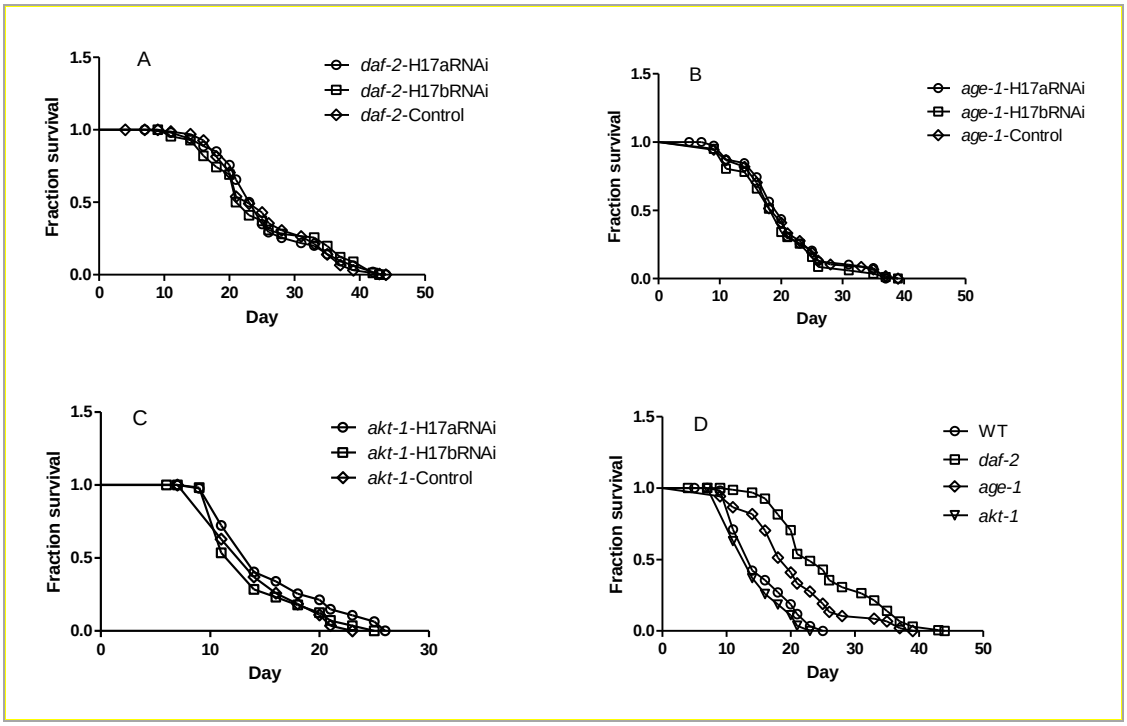

Figure 5.4 The lifespan assays in H17 RNAi IIS mutant worm strains. A. Lifespan assay for H17 RNAi *daf-2* (*e1370*) mutants. **B.** Lifespan assay for H17 RNAi *age-1* (*hx546*) mutants. **C.** Lifespan assay for H17 RNAi *akt-1* (*mg144*) mutants. **D.** Lifespan comparison of the controls (fed with bacteria carrying L4440) under different mutant gene background. Young adult worms were allowed to lay eggs on the RNAi bacteria seeded NGM plates. The progeny were allowed to grow to L4 larvae stage at 20°C and then transferred to new RNAi bacteria seeded NGM plates containing 50 μM FUDR. The worms were allowed to grow till death without exhausting the RNAi bacteria food source. Day 0 of lifespan was the day that eggs were laid. Animals that failed to respond to a gentle prodding with a platinum wire were scored as dead. The data was analyzed with Kaplan-Meier method.

As shown in Figure 5.4D, the median lifespan of the control mutant worms (worms fed with bacteria carrying L4440) was: 23.63 ± 1.56 days (*daf-2*, *e1370*), 20.16 ± 0.54 days (*age-1, hx546*), and 14.96 ± 0.38 days (*akt-1, mg144*). These results were consistent with the median lifespan of the above mutants reported in other published literatures (Kenyon, Chang et al. 1993; Dorman, Albinder et al. 1995; Gems, Sutton et al. 1998; Paradis and Ruvkun 1998). However, the median lifespan of H17 RNAi mutant worms was not significantly different from that of the control mutants (Figure 5.4A-C, Table 5.3). Hence, the lifespan of the IIS pathway mutants was not affected by the knockdown of H17.

Table 5.3 Lifespan assays in the WT and IIS mutants under H17 RNAi condition

Strain	RNAi	Mean lifespan days (±SD)	Max lifespan	N (censored)*
WT	Control	15.46 (0.33)	25	118 (2)
	H17a	15.48 (0.37)	25	102 (4)
	H17b	15.36 (0.35)	26	120 (3)
daf-2 (*e1370*)	Control	23.63 (1.56)	44	163 (4)
	H17a	24.00 (0.50)	44	160 (2)
	H17b	22.00 (0.88)	43	156 (2)
age-1 (*hx546*)	Control	20.16 (0.54)	39	105 (0)
	H17a	20.50 (0.44)	37	78 (2)
	H17b	20.12 (0.53)	39	82 (0)
akt-1 (*mg144*)	Control	14.96 (0.38)	23	108 (2)
	H17a	15.38 (0.33)	26	94 (3)
	H17b	14.22 (0.39)	25	112 (3)

XLSTAT-life statistical software (Addinsoft, New York, NY, USA) was used to plot survival data by the Kaplan–Meier method.

* Total death scored (number of censored values)

5.2.3 The effect of H17 knockdown on the glucose metabolism in *C. elegans*

In *C. elegans*, glucose is oxidized to CO_2 and water to provide ATP as the major energy source. Except from being stored as glycogen, excess glucose can be alternatively broken down to acetyl-CoA by glycolysis, and then converted to and

stored as fats (Ashrafi 2007). It was reported that loss of function of *daf-2* caused fat accumulation in adults (Ashrafi 2007). Moreover, the global shifts in metabolic pathways were also reported to be associated with dauer larvae and *daf-2* mutant adults (Holt and Riddle 2003; Burnell, Houthoofd et al. 2005; Ashrafi 2007). These shifts were found to be similar to the metabolic adjustments observed in nutrient deprived or fasting mammals. These adjustments favour energy conservation, fat storage, and utilization of stored reservoirs (Ashrafi 2007). Therefore, the influence of H17 knockdown on the glucose metabolism was also investigated by examining the CO_2 release rate and the amount of fat converted from glucose metabolism in the WT and the IIS mutant worms.

Both H17a and H17b were knocked down in the same worm so that the maximum effect could be observed in the experiments. Since the expression stage of H17a and H17b was unknown, in order to make sure that both H17a and H17b were knocked down in the same worm, equal volume of H17a and H17b cultures with similar OD_{600} reading were mixed before seeding. The young adult worms which had being grown on the RNAi bacteria mixture plates were then allowed to lay eggs on the RNAi NGM plates until the L4 stage. In order to eliminate any influence from the glucose produced from digested bacteria, the L4 larvae were starved 18h to exhaust the ingested bacteria before being subjected to the subsequent experiments. A parallel plate of worms for each RNAi condition was also set up and starved. The worms on these parallel plates were collected for QPCR to examine the mRNA level of H17 after the starvation. The mRNA level of H17 each of the mutants was knocked down to 32.63 ± 2.46% (WT), 42.26 ± 2.44% (*daf-2*, *e1370*), 41.30 ± 4.43% (*age-1*, *hx546*), and 28.37 ± 2.94% (*akt-1*, *mg144*) comparing with the controls for each group (Figure 5.5).

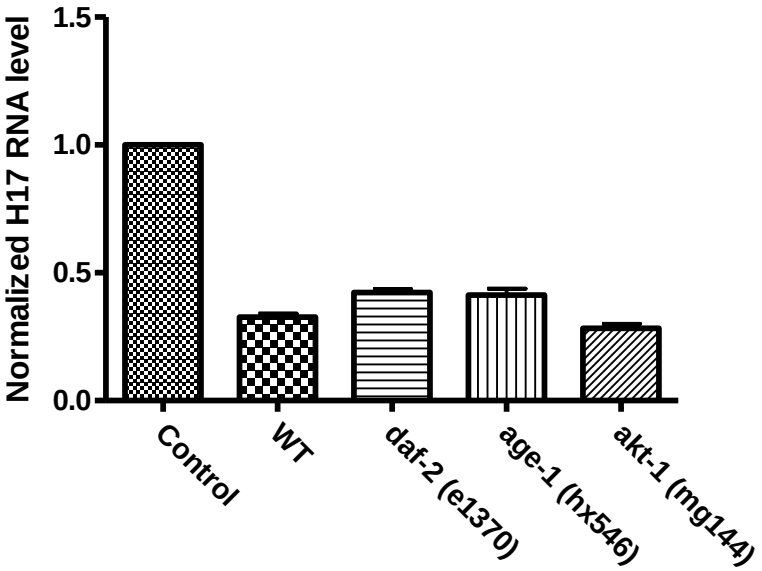

Figure 5.5 The H17 mRNA levels in H17 RNAi WT and IIS mutant worms after 18 h starvation. H17a and H17b RNAi bacteria were mixed at 1:1 ratio before seeded to the NGM plates. Young adult worms grown on RNAi plates from eggs were washed with M9 buffer and transferred to new agarose plates containing 50 μg/ml ampicillin, 50 μM FUDR and without bacteria seeded. Worms were starved for 18 h. Total RNA was then extracted from starved worms for QPCR analysis of the H17 mRNA levels using the primers listed in table 2.11. Each sample was analyzed in triplicates. The experiment was repeated three times. Each value is the mean ± SEM.

The glucose to fat conversion was examined by glucose uptake assays (detailed in 2.2.13). Fats were extracted from the worm lysates with the organic solvent, heptane. If the radio-active U-[^{14}C]-D-glucose taken up by the worms was converted to fat, the fat content would, therefore, be radio-active and the radioactivity could be detected by the scintillation counter. As shown in Figure 5.6, the rates of glucose converted to fat in the control worms (worms fed with bacteria carrying L4440) of each group (WT, *daf-2* (*e1370*), *age-1* (*hx546*), *akt-1* (*mg144*)) were not significantly different from each other. The knockdown of H17 caused a small increase of glucose to fat conversion in the WT worms (P=0.0565) whereas the glucose to fat conversion in the H17 RNAi *daf-2* mutant was significantly increased (P=0.0254) by ~64%. On the contrary, the knockdown of H17 in the *akt-1* mutant led to a small decrease of the glucose to fat conversion. However, the conversion rate in the H17 RNAi *age-1* mutant was not significantly altered.

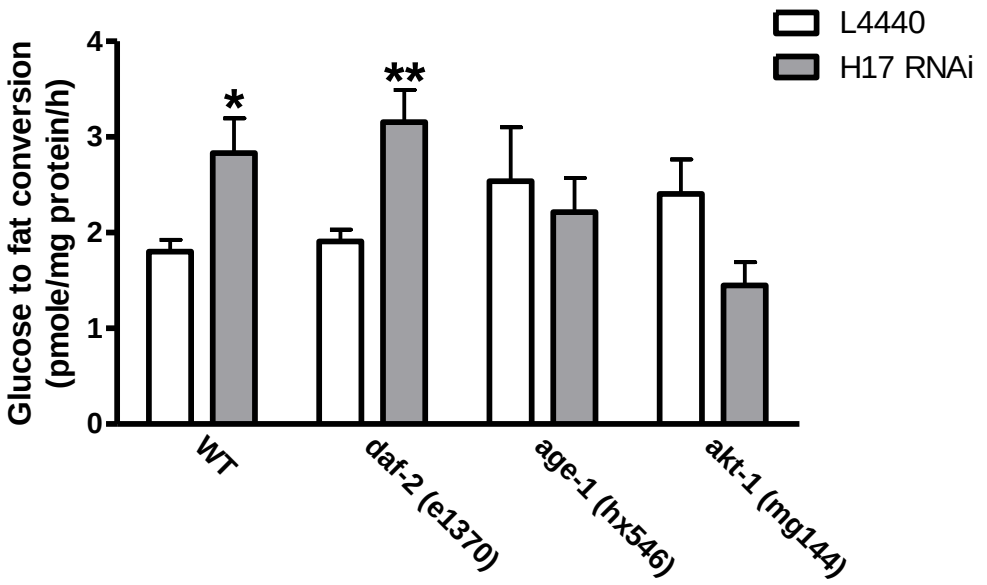

Figure 5.6 Glucose to fat conversion assays in H17 RNAi WT and IIS mutant worm strains. Synchronized starved adult worms were incubated 1 h at 20°C in M9 buffer containing 50 μM D-glucose with 1μCi U-[C^{14}]-D-glucose added for each assay. The fat content of each sample was extracted from worm lysates with heptane. The radio activity of the organic phase was counted using a scintillation counter. *A small increase of the glucose to fat conversion (P = 0.0565) in WT worms; ** a significant increase of glucose to fat conversion (P = 0.0254) in *daf-2* (*e1370*) mutants. Each sample was analyzed in triplicates. The experiment was repeated three times. Each value is the mean ± SEM.

The glucose oxidation rate was tested in both WT and IIS pathway mutants as described in section 2.2.14. In the control worms, the glucose oxidation rates were decreased in both *daf-2* and *age-1* mutants (P_{daf-2}=0.0147, P_{age-1}=0.0031) comparing to the rate of the WT worms. The H17 knockdown induced small decrease of the glucose oxidation rates in the WT, *age-1*, and *akt-1* mutants (P_{WT}=0.0471, P_{age-1}=0.0478, P_{akt-1}=0.0057) (Figure 5.7). Whereas, in the *daf-2* mutant, the glucose oxidation rate was greatly increased (P=0.0003) (about 2.7 fold increased than in the control mutant worms) by the knockdown of H17.

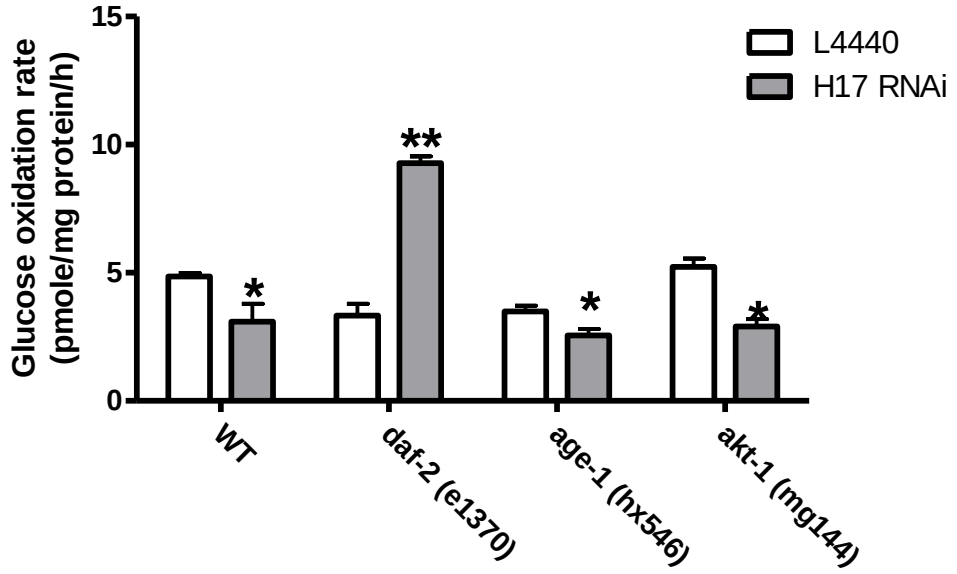

Figure 5.7 The glucose oxidation assays in H17 RNAi WT and IIS mutant worm strains. In an airtight sealed bijou tube (Figure 2.2), synchronized starved adult worms were incubated 1 h at 20°C in M9 buffer containing 50 μM D-glucose with 1μCi U-[^{14}C]-D-glucose added for each assay. Released CO_2 was absorbed by 0.1 M KOH. The radio activity of the KOH solution was counted using a scintillation counter. *Decreased glucose oxidation rates (P_{WT}=0.0471, $P_{age\text{-}1}$=0.0478, $P_{akt\text{-}1}$=0.0057). **Increased glucose oxidation rate (P=0.0003). Each sample was analyzed in triplicates. The experiment was repeated three times. Each value is the mean ± SEM.

5.3 Discussion and conclusion

In this chapter, the *in vivo* function of H17 was investigated under the condition of gene knockdown using RNAi. The studies described in this chapter were mainly focused on the effect of H17 knockdown on the lifespan and glucose metabolism in the WT and IIS pathway mutant worms.

Being identified as a glucose transporter with almost ubiquitous expression in *C. elegans* of all stages (detailed in Chapter 4), H17 had the potential of being the major glucose transporter in *C. elegans*. Previous studies demonstrate that glucose shortens the lifespan of *C. elegans* while glucose restriction is able to extend the lifespan of the worms (Schulz, Zarse et al. 2007; Lee, Murphy et al. 2009; Schlotterer, Kukudov et al. 2009). If H17 were the major glucose transporter in the worms, the knockdown of H17 expression would decrease the glucose uptake level in the worms

and establish the glucose restriction status in the worms. Thus, the lifespan of the worms would be extended when the expression of H17 was continuously suppressed during the lifespan assay.

However, the lifespan assay results showed that the knockdown of H17 expression was not able to extend the lifespan either in the WT worms or in the IIS mutant worms. When maintained on 2-deoxy-D-glucose (DOG) plates (discussed in section 5.1), the worms almost completely lost the ability to oxidize exogenous glucose (Schulz, Zarse et al. 2007). Both short term (treating the worms with DOG in the first 6 days of early adult life) and continuous impairment of glucose metabolism were able to extend the *C. elegans* lifespan (Schulz, Zarse et al. 2007). These findings suggest that an almost completely impairment of either glucose metabolism or glucose uptake might be necessary for the lifespan extension effect being observed. Whereas in our case, the expression of H17 was knocked down by 80%, hence the glucose uptake in the worms was not completely disrupted. Moreover, the results of glucose uptake assays and glucose oxidation assays in WT worms also suggested that the exogenous glucose metabolism was not impaired by the H17 knockdown. Furthermore, when cultured on the bacteria seeded NGM plates, worms directly absorb lipid species (triglycerides, phospholipids, sphingolipids, etc.) from the bacterial food source (Braeckman, Houthoofd et al. 2009). Hence it is possible that the worms are more dependent on the bacteria food as the calorie source. Therefore the knockdown of H17 expression was not able to affect the lifespan of the worms. Finally, due to the poorly understood glucose transport system in *C. elegans*, a lot of the questions are still unknown, such as, whether H17 is the major glucose transporter in *C. elegans*, or if there is any other glucose transporter in *C. elegans*. Thus, although H17 knockdown did not affect either the WT or the IIS mutant worms' lifespan this result is not sufficient to draw the conclusion that H17 could not affect the lifespan of *C. elegans*.

Although the H17 knockdown did not affect the lifespan of the worms, the glucose

metabolism in both the WT and the IIS mutant worms was affected. The decreased level of ^{14}C labelled CO_2 release (Figure 5.7) indicated that the glucose uptake level in the WT worms was brought down by the H17 knockdown. Schulz et al. reported that when the glycolysis was impaired by the DOG treatment in worms the levels of transcripts encoding proteins involved in lipid storage were significantly upregulated (Schulz, Zarse et al. 2007). This was coincident with our finding that the glucose to fat conversion level was increased in the H17 RNAi WT worms.

The long-lived *daf-2* mutants are thought to have an enhanced mitochondrial efficiency by exhibiting low oxygen consumption and higher ATP levels but relatively low calorimetric/respirometric ratio (Braeckman, Houthoofd et al. 2002). In contrast, low metabolic rates for the IIS mutants were also reported (Van Voorhies and Ward 1999). However, the analysis of transcriptional profiles of metabolism-related genes suggested that the citric acid cycle (TCA-cycle) and respiratory chain activities were not down-regulated in *daf-2* mutants (McElwee, Schuster et al. 2006). It has also been reported that the *daf-2* mutant worms have increased fat accumulation in intestinal and hypodermal cells (Kimura, Tissenbaum et al. 1997). Our results showed that the fat content derived from exogenous glucose (indicated as ^{14}C labelled fat in our experiments) was not increased in the *daf-2* mutant worms. Therefore, the increased fat storage in the *daf-2* mutant might be synthesized from other source other than exogenous glucose. Whereas in the H17 RNAi *daf-2* mutants, the level of ^{14}C labelled fat was significantly increased. Moreover, the glucose oxidation level was also significantly increased in the *daf-2* mutant worms. These increases observed in H17 RNAi *daf-2* mutant were not found in either *age-1* or *akt-1* mutants.

There are two possible explanations for the above results. Firstly, carbohydrates are primarily stored as glycogen as well as trehalose in *C. elegans* (Cooper and Van Gundy 1970; Hanover, Forsythe et al. 2005). The *daf-2* (*e1370*) animals were found to have an elevated fat storage (Kimura, Tissenbaum et al. 1997). Carissa et al.

reported that the *daf-2* (*e1370*) mutation resulted in the >2 fold higher proportion of synthesized fatty acids than in the WT worms (Perez and Van Gilst 2008). Hence, the glycogen may have been greatly broken down and converted to fat storage in the *daf-2* mutants. In the starving *daf-2* mutants, with possibly reduced glycogen level, part of the exogenous glucose may be converted to either glycogen or trehalose so that the balance between carbohydrate breakdown and fat synthesis can be kept. Therefore, this may account for the observation that the exogenous glucose derived fat content is not increased in the control *daf-2* mutants (*daf-2* mutants fed with bacteria carrying L4440 vector only). Whereas, the knockdown of H17 may lead to reduced glucose availability, hence the exogenous glucose may be extensively used to fat and CO_2 conversion rather than converted to glycogen. Thus the levels of exogenous glucose derived fat and CO_2 conversion may have both been increased in the H17 knockdown *daf-2* mutants.

Secondly, the starving *daf-2* mutant may enter an anaerobic metabolic status which is similar to the metabolic status of the dauer larvae since 15% of the worms enter dauer stage at 20°C for the *e1370* temperature sensitive strain. The reduction of glucose availability caused by the H17 knockdown may trigger a compensatory glucose uptake process in the worms and induce an effect which is partially similar to the “Pasteur effect” found in anaerobic yeast (increased glucose consumption, faster glucose metabolic rate (Krebs 1972)). When worms enter the anaerobic metabolic status, the transcription of enzymes involved in the pathways of fatty acids β-oxidation, glycolysis, glycongenesis is found to be enhanced, indicating that the stored fat content is converted into sugars, such as trehalose (Ashrafi 2007; Braeckman, Houthoofd et al. 2009), rather than glucose, is assumed to be the transported sugar under such conditions (McElwee, Schuster et al. 2004). The transporting trehalose is broken down to glucose and then enters the TCA-cycle. With increased glucose consumption, accelerated glucose metabolic rate and enhanced mitochondrial efficiency of the *daf-2* mutant background, the exogenous glucose to fat conversion and the production of CO_2 is, therefore, increased (Figure

5.8). In contrast, the *age-1* and *akt-1* mutants are not able to induce the worms enter the anaerobic metabolic status and hence, the increased CO_2 production is not observed in the H17 RNAi mutants. Further more, both the glucose to fat conversion and glucose oxidation are reduced in the *akt-1* mutant suggesting that the *akt-1* is also important in the glucose transport in *C. elegans*.

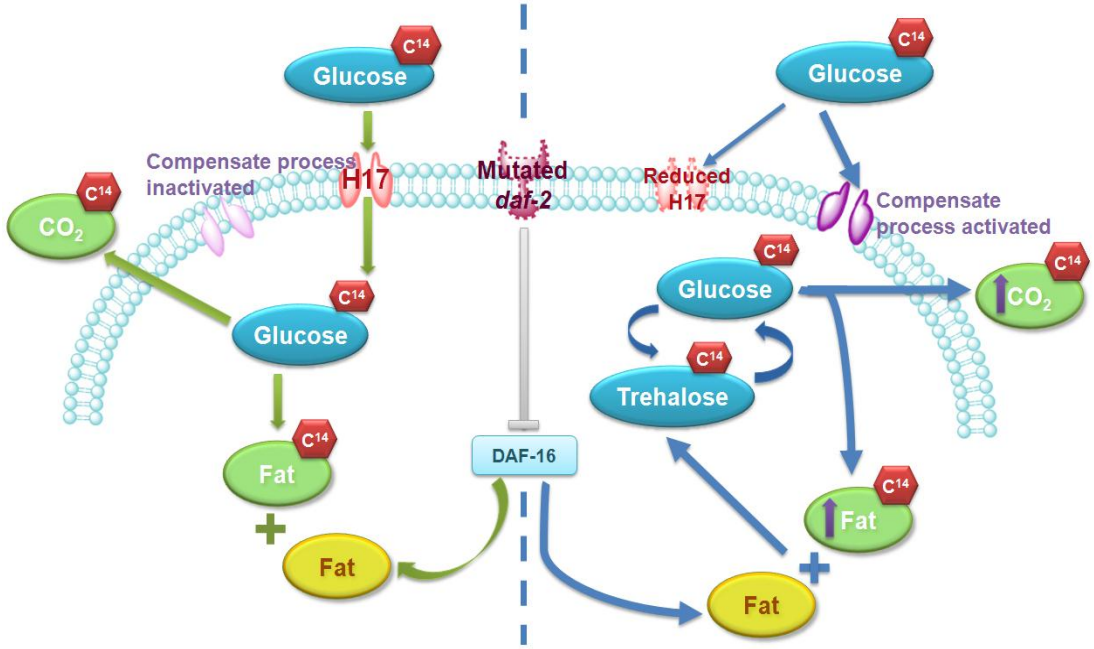

Figure 5.8 A hypothetic role of H17 in the glucose metabolism in *daf-2* mutant worms. In the starved *daf-2* (*e1370*) mutant worms, when H17 is expressed, the *daf-2* mutant exhibits typical glucose metabolic effect (green arrows) as reported in other literatures, such as enhanced mitochondrial efficiency, reduced CO2 production and increased lipid storage. When the H17 expression is knocked down, the glucose metabolism is shifted to the anaerobic status (blue arrows) where both the glucose consumption and glucose metabolism are increased. In the meantime, a compensate glucose uptake may also be induced to meet the need of the increased glucose consumption. Therefore, both the exogenous derived fat storage and CO_2 production may be increased in response to this compensatory process.

To sum up, the knockdown of H17 was not able to affect the life span of either WT or IIS mutant worms. H17 may play an important role in the glucose metabolism in both WT and IIS mutant worms. However, more work is needed to investigate the further details of the *in vivo* function of the worm glucose transporter, H17.

Chapter 6 Final conclusion and discussion

6.1 Final conclusion

This thesis focused on the identification of glucose transporter in *C. elegans* and the primary investigation of the *in vitro* and *in vivo* function of the identified glucose transporter.

In Chapter 3, nine putative worm glucose transporter genes (H17B01.1, R09B5.11, C35A11.4, F14E5.1, Y39E4B.5, F48E5.2, K09C4.5, K09C4.1, and T08B1.1) were selected for subsequent cloning based on the similarity of sequence motifs and membrane topology to the mammalian GLUT family, as well as the RNAi phenotype. Each of the putative glucose transporters was cloned into pT7-Blue vector to allow subsequent gene manipulation. The insertion of HA tag into the first exofacial loop of each protein allowed the *in vitro* detection of these putative transporters. The cloning of the putative transporters into the *Xenopus* translation vector, pT7TS, allowed the heterologous expression of the putative transporter in the *Xenopus* oocytes for the investigation of the glucose transport activity of these proteins.

Upon successful cloning of the nine putative transporters into the pT7TS vector, the glucose and trehalose transport activities of these proteins were investigated with *Xenopus* oocytes expression system in Chapter 4. *In vitro* characteristic studies of the putative transporters suggested that the two transcripts of H17, H17a and H17b, were the only two proteins that were transporting glucose with high affinity out of all the cloned proteins. Trehalose can also be transported by the H17a and H17b when expressed in *Xenopus* oocytes. The fact that the insertion of HA tag in the first exofacial loop completely disrupted the glucose transport ability of the protein indicated that the first exofacial loop was essential for the glucose transport activity for H17. When expressed in CHO-T cells, the cellular localization of H17 was observed on plasma membrane as well as perinuclear region. The two transcripts

shared similar expression pattern in the CHO-T cells. Neither H17a nor H17b were insulin responsive when expressed in CHO-T cells or primary rat adipocytes. These results indicate that whether H17 is a downstream target of the IIS pathway or of another signal transduction pathway remains to be unveiled.

The *in vivo* function of the H17 was investigated in Chapter 5. RNAi by feeding was used to knock down the expression of H17 in *C. elegans*. The effects of H17 knockdown on the worm lifespan and glucose metabolism were examine in WT animals and IIS pathway mutants, including *daf-2* (*e1370*), *age-1* (*hx546*), and *akt-1* (*mg144*). The knockdown of H17 expression did not affect the lifespan of any of the tested strains. The fact that H17 knockdown led to increase in glucose to fat conversion as well as glucose oxidation rate in the *daf-2* (*e1370*) suggested that this glucose transporter might play an important role in the insulin regulated glucose metabolism in *C. elegans*, particularly when the receptor for insulin-like peptides is non-functional.

The studies outlined above provide novel background information on *C. elegans* dependence on glucose transport that will eventually lead to further studies on the relationship between nutrient supply via transporters and hormonal control of nutrient use. These studies could aim to test new ideas concerning the metabolic role and significance of H17 in worms that have a deficiency to the *daf-2* pathway. Some approaches and new information that are needed for these further studies are suggested below.

6.2 Discussion

The initial goal of our study was to identify the GLUT4 ortholog in *C. elegans*. Because GLUT4 is the only insulin-regulated glucose transporter that is responsible for insulin-regulated glucose translocation into cells in mammals (Holman and Sandoval 2001). The identification of GLUT4 ortholog in *C. elegans* may provide

further understanding to the link between IIS- and CR-regulated lifespan extension in worm. However, the predicted GLUT4 ortholog in *C. elegans*, K09C4.1, did not have glucose affinity when being expressed in the *Xenopus* oocytes (detailed in section 4.2.2). It is possible that the glucose homeostasis in the lower organism, *C. elegans*, is relatively simple, therefore, the insulin responsive GLUT4-mediated glucose transport may not be necessary for the worms. There is also the possibility that the correct GLUT4 ortholog is not selected since the initial selection of the candidate putative transporters is not only based on the similarity to the mammalian GLUT super family but also based on the growth or metabolic RNAi phenotype of the worms. If there were no obvious RNAi phenotype for the worm GLUT-4 ortholog, the putative protein would not be selected for subsequent cloning. Despite the unsuccessful search of *C. elegans* GLUT4-like protein, a GLUT3 ortholog, H17B01.1 (H17) is identified. The two transcripts of H17 are high affinity glucose transporters and they are also capable of transporting trehalose. However, the affinity of H17 to trehalose still needs to be determined.

The *in vivo* functional characterization of H17 was carried out via RNAi techniques that involve feeding the worms with bacteria carrying the RNAi. Although RNAi by feeding is widely used in the functional study of the *C. elegans* genes, the results of the lifespan assay on H17 RNAi worms indicate that the effect of H17 knockdown on the worms' lifespan may be compromised either by the incomplete removal of the glucose supply, or by the presence of the bacteria food source (discussed in section 5.3). Hence in order to further investigate whether H17 is affecting the lifespan of the worms or not, a transgenic H17 worm strain could be constructed so that the glucose transport activity of H17 could be completely depleted without exposing the worms to RNAi bacteria food source. Since the HA tag insertion into the first exofacial loop of H17 completely disrupts the H17 mediated-glucose transport (detailed in section 4.2.2), it is possible to introduce the HA-tagged H17 into the *C. elegans* by microparticle bombardment method (Praitis 2006). Upon the successful introduction of the HA-tagged H17 into worm, the transgenic line could also be used in the study

of H17 mediated glucose metabolism in *C. elegans,* as well as the visualization of the *in vivo* expression and intracellular expression of H17 in *C. elegans* when combined with antibody labelling techniques.

Similar to the mammalian nutrient metabolic system, the carbohydrates and lipid metabolism in *C. elegans* are also regulated by IIS pathway (Braeckman, Houthoofd et al. 2009). Two models (the increase of glucose metabolic efficiency vs. the presence of compensatory glucose uptake process) are suggested in Chapter 5 to interpret the effect of H17 knockdown on the glucose metabolism in *daf-2* mutant worms (detailed in section 5.3). The major difference between the two models is whether the increase of the exogenous glucose derived fat content and glucose oxidation in *daf-2* mutants are induced by more efficient usage of the available glucose source or the activation of compensatory glucose uptake process due to the knockdown of H17. To distinguish which of the two models fits the results better, the total amount of glucose taken up during the experiment should be determined. This would involve measuring the radioactivity of the extracted fat content, the released CO_2, as well as the whole worm lysates. Decrease of total glucose uptake would not only indicate that the efficiency model accounts for the increased glucose metabolism caused by H17 knockdown in *daf-2* mutants, but also would suggest that H17 could be the major glucose transporter in *C. elegans*; whereas, increase of the total glucose uptake would indicate the presence of other glucose transporter(s), as well as the presence of the compensatory glucose uptake process. Since the total glucose uptake would be limited in the efficiency model, a decrease of carbohydrate storage, such as glycogen and trehalose would be expected in the efficiency model. However, the total amount of fat content might not be necessarily increased comparing the same WT or IIS mutation background worms with/without H17 knockdown. On the contrary, in the compensatory model, the glycogen level might not be significantly changed while the trehalose level would be increased as trehalose was the circulating sugar when the worms entered the anaerobic status (Braeckman, Houthoofd et al. 2009). An increase of total fat content level should also

be observed in this model. Moreover, an HA-tagged H17, *daf-2* mutant line could also be constructed so that the function of H17 can be completely suppressed during the starvation of the worms before the glucose metabolism assays.

To sum up*, C. elegans* is extensively used in the studies of the lifespan regulation mechanisms because of its completely sequenced genome, relatively short lifespan, as well as the conserved metabolic and signalling pathway, including the IIS pathway. The IIS pathway in *C. elegans* also plays an important role in the regulation of the nutrient homeostasis (Braeckman, Houthoofd et al. 2009) and, moreover, in the regulation of aging process (Porte, Baskin et al. 2005; Broughton and Partridge 2009) (detailed in section 1.1.1). Recent studies showed that glucose restriction extends the lifespan of *C. elegans* (Schulz, Zarse et al. 2007) while excessive glucose shortens the lifespan of the worms (Lee, Murphy et al. 2009) (detailed in section 5.1.1). However, the mechanism of this process remains largely unknown. The first identification of the glucose transporter in *C. elegans* and its IIS- and age-related functional studies described in this thesis may provide the beginning of a course of investigation that eventually leads to further understanding of the IIS-regulated nutrient homeostasis in worms, as well as the link between IIS- and CR-related lifespan extensions in *C. elegans*.

Reference list

Abramson, J., I. Smirnova, et al. (2003). "Structure and mechanism of the lactose permease of *Escherichia coli*." *Science* 301(5633): 610-615.

Accili, D., J. Drago, et al. (1996). "Early neonatal death in mice homozygous for a null allele of the insulin receptor gene." *Nat Genet* 12(1): 106-109.

Ahringer (ed.), J. (2006). Reverse genetics. *WormBook*. T. C. e. R. Community, WormBook.

Al-Hasani, H., C. S. Hinck, et al. (1998). "Endocytosis of the glucose transporter GLUT4 is mediated by the GTPase dynamin." *J Biol Chem* 273(28): 17504-17510.

Antebi, A. (2007). "Ageing: when less is more." *Nature* 447(7144): 536-537.

Apfeld, J., G. O'Connor, et al. (2004). "The AMP-activated protein kinase AAK-2 links energy levels and insulin-like signals to lifespan in C. elegans." *Genes Dev* 18(24): 3004-3009.

Asano, T., H. Katagiri, et al. (1991). "The role of N-glycosylation of GLUT1 for glucose transport activity." *J Biol Chem* 266(36): 24632-24636.

Asano, T., K. Takata, et al. (1993). "The role of N-glycosylation in the targeting and stability of GLUT1 glucose transporter." *FEBS Lett* 324(3): 258-261.

Ashrafi, K. (2007). Obesity and the regulation of fat metabolism. *WormBook*. T. C. e. R. Community, WormBook.

Augustin, R., M. O. Carayannopoulos, et al. (2004). "Identification and characterization of human glucose transporter-like protein-9 (GLUT9): alternative splicing alters trafficking." *J Biol Chem* 279(16): 16229-16236.

Baldwin, S. A. (1993). "Mammalian passive glucose transporters: members of an ubiquitous family of active and passive transport proteins." *Biochim Biophys Acta* 1154(1): 17-49.

Baldwin, S. A., J. M. Baldwin, et al. (1982). "Monosaccharide transporter of the human erythrocyte. Characterization of an improved preparation." *Biochemistry* 21(16): 3836-3842.

Barnell, W. O., K. C. Yi, et al. (1990). "Sequence and genetic organization of a Zymomonas mobilis gene cluster that encodes several enzymes of glucose metabolism." *J Bacteriol* 172(12): 7227-7240.

Bartke, A. (2008). "Insulin and aging." *Cell Cycle* 7(21): 3338-3343.

Behm, C. A. (1997). "The role of trehalose in the physiology of nematodes." *Int J Parasitol* 27(2): 215-229.

Bell, G. I., T. Kayano, et al. (1990). "Molecular biology of mammalian glucose transporters." *Diabetes Care* 13(3): 198-208.

Bergmeyer, H. U. a. B., E. (1974). *Methods of Enzymatic Analysis*. New York, Academic Press.

Bianchi, L. and M. Driscoll (2006). Heterologous expression of *C. elegans* ion channels in *Xenopus* oocytes. *WormBook*. T. C. e. R. Community, WormBook.

Bluher, M., B. B. Kahn, et al. (2003). "Extended longevity in mice lacking the insulin receptor in adipose tissue." *Science* 299(5606): 572-574.

Boily, G., E. L. Seifert, et al. (2008). "SirT1 regulates energy metabolism and response to caloric restriction in mice." *PLoS One* 3(3): e1759.

Boos, W. and H. Shuman (1998). "Maltose/maltodextrin system of *Escherichia coli*: transport, metabolism, and regulation." *Microbiol Mol Biol Rev* 62(1): 204-229.

Braeckman, B. P., K. Houthoofd, et al. (2001). "Insulin-like signaling, metabolism, stress resistance and aging in *Caenorhabditis elegans*." *Mech Ageing Dev* 122(7): 673-693.

Braeckman, B. P., K. Houthoofd, et al. (2002). "Assessing metabolic activity in aging *Caenorhabditis elegans*: concepts and controversies." *Aging Cell* 1(2): 82-88.

Braeckman, B. P., K. Houthoofd, et al. (2009). Intermediary metabolism. *WormBook*. T. C. e. R. Community, WormBook.

Bringaud, F. and T. Baltz (1992). "A potential hexose transporter gene expressed predominantly in the bloodstream form of *Trypanosoma brucei*." *Mol Biochem Parasitol* 52(1): 111-121.

Broughton, S. and L. Partridge (2009). "Insulin/IGF-like signalling, the central nervous system and aging." *Biochem J* 418(1): 1-12.

Brown-Borg, H. M., K. E. Borg, et al. (1996). "Dwarf mice and the ageing process." *Nature* 384(6604): 33.

Bryant, N. J., R. Govers, et al. (2002). "Regulated transport of the glucose transporter GLUT4." *Nat Rev Mol Cell Biol* 3(4): 267-277.

Buhr, A., G. A. Daniels, et al. (1992). "The glucose transporter of *Escherichia coli*. Mutants

with impaired translocation activity that retain phosphorylation activity." *J Biol Chem* 267(6): 3847-3851.

Burant, C. F., J. Takeda, et al. (1992). "Fructose transporter in human spermatozoa and small intestine is GLUT5." *J Biol Chem* 267(21): 14523-14526.

Burnell, A. M., K. Houthoofd, et al. (2005). "Alternate metabolism during the dauer stage of the nematode *Caenorhabditis elegans*." *Exp Gerontol* 40(11): 850-856.

Cairns, B. R., M. W. Collard, et al. (1989). "Developmentally regulated gene from *Leishmania* encodes a putative membrane transport protein." *Proc Natl Acad Sci U S A* 86(20): 7682-7686.

Canto, C. and J. Auwerx (2009). "Caloric restriction, SIRT1 and longevity." *Trends Endocrinol Metab* 20(7): 325-331.

Carayannopoulos, M. O., M. M. Chi, et al. (2000). "GLUT8 is a glucose transporter responsible for insulin-stimulated glucose uptake in the blastocyst." *Proc Natl Acad Sci U S A* 97(13): 7313-7318.

Carruthers, A. (1990). "Facilitated diffusion of glucose." *Physiol Rev* 70(4): 1135-1176.

Celenza, J. L., L. Marshall-Carlson, et al. (1988). "The yeast SNF3 gene encodes a glucose transporter homologous to the mammalian protein." *Proc Natl Acad Sci U S A* 85(7): 2130-2134.

Chandler, J. D., E. D. Williams, et al. (2003). "Expression and localization of GLUT1 and GLUT12 in prostate carcinoma." *Cancer* 97(8): 2035-2042.

Chang, L., S. H. Chiang, et al. (2004). "Insulin signaling and the regulation of glucose transport." *Mol Med* 10(7-12): 65-71.

Cheeseman, C. (2008). "GLUT7: a new intestinal facilitated hexose transporter." *Am J Physiol Endocrinol Metab* 295(2): E238-241.

Chen, D., J. Bruno, et al. (2008). "Tissue-specific regulation of SIRT1 by calorie restriction." *Genes Dev* 22(13): 1753-1757.

Cheng, C. H., T. Kikuchi, et al. (2009). "Mutations in the SLC2A10 gene cause arterial abnormalities in mice." *Cardiovasc Res* 81(2): 381-388.

Clancy, D. J., D. Gems, et al. (2002). "Dietary restriction in long-lived dwarf flies." *Science* 296(5566): 319.

Clancy, D. J., D. Gems, et al. (2001). "Extension of life-span by loss of CHICO, a *Drosophila* insulin receptor substrate protein." *Science* 292(5514): 104-106.

Cooper, A. F. and S. D. Van Gundy (1970). "Metabolism of Glycogen and Neutral Lipids by *Aphelenchus avenae* and *Caenorhabditis sp.* in Aerobic, Microaerobic and Anaerobic Environments." *J Nematol* 2(4): 305-315.

Dahlqvist, A. (1968). "Assay of intestinal disaccharidases." *Anal Biochem* 22(1): 99-107.

Dasgupta, S., L. Fernandez, et al. (1998). "Genetic uncoupling of the dsRNA-binding and RNA cleavage activities of the *Escherichia coli* endoribonuclease RNase III--the effect of dsRNA binding on gene expression." *Mol Microbiol* 28(3): 629-640.

Diez-Sampedro, A., B. A. Hirayama, et al. (2003). "A glucose sensor hiding in a family of transporters." *Proc Natl Acad Sci U S A* 100(20): 11753-11758.

Doblado, M. and K. H. Moley (2009). "Facilitative glucose transporter 9, a unique hexose and urate transporter." *Am J Physiol Endocrinol Metab* 297(4): E831-835.

Doege, H., A. Bocianski, et al. (2000). "Activity and genomic organization of human glucose transporter 9 (GLUT9), a novel member of the family of sugar-transport facilitators predominantly expressed in brain and leucocytes." *Biochem J* 350 Pt 3: 771-776.

Doege, H., A. Bocianski, et al. (2001). "Characterization of human glucose transporter (GLUT) 11 (encoded by SLC2A11), a novel sugar-transport facilitator specifically expressed in heart and skeletal muscle." *Biochem J* 359(Pt 2): 443-449.

Doege, H., A. Schurmann, et al. (2000). "GLUT8, a novel member of the sugar transport facilitator family with glucose transport activity." *J Biol Chem* 275(21): 16275-16280.

Dorman, J. B., B. Albinder, et al. (1995). "The *age-1* and *daf-2* genes function in a common pathway to control the lifespan of *Caenorhabditis elegans*." *Genetics* 141(4): 1399-1406.

Douard, V. and R. P. Ferraris (2008). "Regulation of the fructose transporter GLUT5 in health and disease." *Am J Physiol Endocrinol Metab* 295(2): E227-237.

Dugani, C. B. and A. Klip (2005). "Glucose transporter 4: cycling, compartments and controversies." *EMBO Rep* 6(12): 1137-1142.

Elbein, A. D. (1974). "The metabolism of alpha, alpha-trehalose." *Adv Carbohydr Chem Biochem* 30: 227-256.

Elbein, A. D., Y. T. Pan, et al. (2003). "New insights on trehalose: a multifunctional molecule." *Glycobiology* 13(4): 17R-27R.

Escher, S. A. and A. Rasmuson-Lestander (1999). "The *Drosophila* glucose transporter gene: cDNA sequence, phylogenetic comparisons, analysis of functional sites and secondary structures." *Hereditas* 130(2): 95-103.

Fielenbach, N. and A. Antebi (2008). "*C. elegans* dauer formation and the molecular basis of plasticity." *Genes Dev* 22(16): 2149-2165.

Finch, C. E. (1990). *Longevity, Senescence, and the Genome*. Chicago, The University of Chicago Press.

Fire, A., S. Xu, et al. (1998). "Potent and specific genetic interference by double-stranded RNA in *Caenorhabditis elegans*." *Nature* 391(6669): 806-811.

Fisher, T. L. and M. F. White (2004). "Signaling pathways: the benefits of good communication." *Curr Biol* 14(23): R1005-1007.

Forster, M. J., P. Morris, et al. (2003). "Genotype and age influence the effect of caloric intake on mortality in mice." *FASEB J* 17(6): 690-692.

Friedman, D. B. and T. E. Johnson (1988). "A mutation in the age-1 gene in *Caenorhabditis elegans* lengthens life and reduces hermaphrodite fertility." *Genetics* 118(1): 75-86.

Friedman, J. and K. Kaestner (2006). "The Foxa family of transcription factors in development and metabolism." *Cellular and Molecular Life Sciences (CMLS)* 63(19): 2317-2328.

Fukumoto, H., T. Kayano, et al. (1989). "Cloning and characterization of the major insulin-responsive glucose transporter expressed in human skeletal muscle and other insulin-responsive tissues." *J Biol Chem* 264(14): 7776-7779.

Fukumoto, H., S. Seino, et al. (1988). "Sequence, tissue distribution, and chromosomal localization of mRNA encoding a human glucose transporter-like protein." *Proc Natl Acad Sci U S A* 85(15): 5434-5438.

Gems, D., A. J. Sutton, et al. (1998). "Two pleiotropic classes of *daf-2* mutation affect larval arrest, adult behavior, reproduction and longevity in *Caenorhabditis elegans*." *Genetics* 150(1): 129-155.

Giannakou, M. E. and L. Partridge (2007). "Role of insulin-like signalling in *Drosophila* lifespan." *Trends Biochem Sci* 32(4): 180-188.

Golden, T. R. and S. Melov (2007). Gene expression changes associated with aging in *C. elegans*. *WormBook*, ed, The *C. elegans* Research Community. WormBook, doi/10.1895/wormbook.1.127.2, http://www.wormbook.org.

Gould, G. W. and G. D. Holman (1993). "The glucose transporter family: structure, function and tissue-specific expression." *Biochem J* 295 (Pt 2): 329-341.

Han, E. K., F. Cotty, et al. (1995). "Characterization of AGT1 encoding a general alpha-glucoside transporter from *Saccharomyces*." *Mol Microbiol* 17(6): 1093-1107.

Hanover, J. A., M. E. Forsythe, et al. (2005). "A *Caenorhabditis elegans* model of insulin resistance: altered macronutrient storage and dauer formation in an OGT-1 knockout." *Proc Natl Acad Sci U S A* 102(32): 11266-11271.

Hansen, M., A. L. Hsu, et al. (2005). "New genes tied to endocrine, metabolic, and dietary regulation of lifespan from a *Caenorhabditis elegans* genomic RNAi screen." *PLoS Genet* 1(1): 119-128.

Henderson, P. J. and M. C. Maiden (1990). "Homologous sugar transport proteins in *Escherichia coli* and their relatives in both prokaryotes and eukaryotes." *Philos Trans R Soc Lond B Biol Sci* 326(1236): 391-410.

Henderson, S. T. and T. E. Johnson (2001). "*daf-16* integrates developmental and environmental inputs to mediate aging in the nematode *Caenorhabditis elegans*." *Curr Biol* 11(24): 1975-1980.

Hertweck, M., C. Gobel, et al. (2004). "*C. elegans* SGK-1 is the critical component in the Akt/PKB kinase complex to control stress response and life span." *Dev Cell* 6(4): 577-588.

Hirokawa, T., S. Boon-Chieng, et al. (1998). "SOSUI: classification and secondary structure prediction system for membrane proteins." *Bioinformatics* 14(4): 378-379.

Holman, G. D. and I. V. Sandoval (2001). "Moving the insulin-regulated glucose transporter GLUT4 into and out of storage." *Trends Cell Biol* 11(4): 173-179.

Holt, S. J. and D. L. Riddle (2003). "SAGE surveys *C. elegans* carbohydrate metabolism: evidence for an anaerobic shift in the long-lived dauer larva." *Mech Ageing Dev* 124(7): 779-800.

Holzenberger, M., J. Dupont, et al. (2003). "IGF-1 receptor regulates lifespan and resistance to oxidative stress in mice." *Nature* 421(6919): 182-187.

Honda, Y., M. Tanaka, et al. (2010). "Trehalose extends longevity in the nematode *Caenorhabditis elegans*." *Aging Cell*.

Houthoofd, K., B. P. Braeckman, et al. (2003). "Life extension via dietary restriction is independent of the Ins/IGF-1 signalling pathway in *Caenorhabditis elegans*." *Exp Gerontol* 38(9): 947-954.

Hruz, P. W. and M. M. Mueckler (2001). Structural analysis of the GLUT1 facilitative glucose transporter, *Informa Healthcare*. 18: 183 - 193.

Huang, Y., M. J. Lemieux, et al. (2003). "Structure and mechanism of the glycerol-3-phosphate transporter from *Escherichia coli*." *Science* 301(5633): 616-620.

INTERPRO. (2009). "IPR005828 General substrate transporter." Retrieved 24-11-2009, 2009, from http://www.ebi.ac.uk/interpro/IEntry?ac=IPR005828.

Jiang, G. and B. B. Zhang (2003). "Glucagon and regulation of glucose metabolism." *Am J Physiol Endocrinol Metab* 284(4): E671-678.

Joost, H. G. and B. Thorens (2001). "The extended GLUT-family of sugar/polyol transport facilitators: nomenclature, sequence characteristics, and potential function of its novel members (review)." *Mol Membr Biol* 18(4): 247-256.

Kahn, B. B. (1992). "Facilitative glucose transporters: regulatory mechanisms and dysregulation in diabetes." *J Clin Invest* 89(5): 1367-1374.

Kaiser, N., G. Leibowitz, et al. (2003). "Glucotoxicity and beta-cell failure in type 2 diabetes mellitus." *J Pediatr Endocrinol Metab* 16(1): 5-22.

Kassi, E. and A. G. Papavassiliou (2008). "Could glucose be a proaging factor?" *Journal of Cellular and Molecular Medicine* 12(4): 1194-1198.

Katic, M. and C. R. Kahn (2005). "The role of insulin and IGF-1 signaling in longevity." *Cell Mol Life Sci* 62(3): 320-343.

Kayano, T., C. F. Burant, et al. (1990). "Human facilitative glucose transporters. Isolation, functional characterization, and gene localization of cDNAs encoding an isoform (GLUT5) expressed in small intestine, kidney, muscle, and adipose tissue and an unusual glucose transporter pseudogene-like sequence (GLUT6)." *J Biol Chem* 265(22): 13276-13282.

Kayano, T., H. Fukumoto, et al. (1988). "Evidence for a family of human glucose transporter-like proteins. Sequence and gene localization of a protein expressed in fetal skeletal muscle and other tissues." *J Biol Chem* 263(30): 15245-15248.

Kenyon, C. (2005). "The Plasticity of Aging: Insights from Long-Lived Mutants." *Cell* 120(4): 449.

Kenyon, C., J. Chang, et al. (1993). "A *C. elegans* mutant that lives twice as long as wild type." *Nature* 366(6454): 461-464.

Kikawada, T., A. Saito, et al. (2007). "Trehalose transporter 1, a facilitated and high-capacity

trehalose transporter, allows exogenous trehalose uptake into cells." *Proc Natl Acad Sci U S A* 104(28): 11585-11590.

Kimura, K. D., H. A. Tissenbaum, et al. (1997). "*daf-2*, an insulin receptor-like gene that regulates longevity and diapause in *Caenorhabditis elegans*." *Science* 277(5328): 942-946.

Kirkwood, T. B. (1977). "Evolution of ageing." *Nature* 270(5635): 301-304.

Kirkwood, T. B. and R. Holliday (1979). "The evolution of ageing and longevity." *Proc R Soc Lond B Biol Sci* 205(1161): 531-546.

Klass, M. R. (1983). "A method for the isolation of longevity mutants in the nematode *Caenorhabditis elegans* and initial results." *Mech Ageing Dev* 22(3-4): 279-286.

Kloting, N. and M. Bluher (2005). "Extended longevity and insulin signaling in adipose tissue." *Experimental Gerontology* 40(11): 878-883.

Koubova, J. and L. Guarente (2003). "How does calorie restriction work?" *Genes Dev* 17(3): 313-321.

Krebs, H. A. (1972). "The Pasteur effect and the relations between respiration and fermentation." *Essays Biochem* 8: 1-34.

Krieg, P. A. and D. A. Melton (1984). "Functional messenger RNAs are produced by SP6 in vitro transcription of cloned cDNAs." *Nucleic Acids Res* 12(18): 7057-7070.

Lakowski, B. and S. Hekimi (1998). "The genetics of caloric restriction in *Caenorhabditis elegans*." *Proc Natl Acad Sci U S A* 95(22): 13091-13096.

Lee, R. Y., J. Hench, et al. (2001). "Regulation of C. elegans DAF-16 and its human ortholog FKHRL1 by the *daf-2* insulin-like signaling pathway." *Curr Biol* 11(24): 1950-1957.

Lee, S. J., C. T. Murphy, et al. (2009). "Glucose shortens the life span of *C. elegans* by downregulating DAF-16/FOXO activity and aquaporin gene expression." *Cell Metab* 10(5): 379-391.

Li, J., M. Tewari, et al. (2007). "The 14-3-3 protein FTT-2 regulates DAF-16 in *Caenorhabditis elegans*." *Dev Biol* 301(1): 82-91.

Li, Q., A. Manolescu, et al. (2004). "Cloning and functional characterization of the human GLUT7 isoform SLC2A7 from the small intestine." *Am J Physiol Gastrointest Liver Physiol* 287(1): G236-242.

Lin, K., J. B. Dorman, et al. (1997). "*daf-16*: An HNF-3/forkhead family member that can

function to double the life-span of *Caenorhabditis elegans*." *Science* 278(5341): 1319-1322.

Lin, S. J., P. A. Defossez, et al. (2000). "Requirement of NAD and SIR2 for life-span extension by calorie restriction in *Saccharomyces cerevisiae*." *Science* 289(5487): 2126-2128.

Lin, S. J., E. Ford, et al. (2004). "Calorie restriction extends yeast life span by lowering the level of NADH." *Genes Dev* 18(1): 12-16.

Lin, S., S. Yang, et al. (1994). "lacZ expression in germline transgenic zebrafish can be detected in living embryos." *Dev Biol* 161(1): 77-83.

Linden, K. C., C. L. DeHaan, et al. (2006). "Renal expression and localization of the facilitative glucose transporters GLUT1 and GLUT12 in animal models of hypertension and diabetic nephropathy." *Am J Physiol Renal Physiol* 290(1): F205-213.

Lisinski, I., A. Schurmann, et al. (2001). "Targeting of GLUT6 (formerly GLUT9) and GLUT8 in rat adipose cells." *Biochem J* 358(Pt 2): 517-522.

Lizcano, J. M. and D. R. Alessi (2002). "The insulin signalling pathway." *Curr Biol* 12(7): R236-238.

Longo, V. D. and B. K. Kennedy (2006). "Sirtuins in aging and age-related disease." *Cell* 126(2): 257-268.

Lu, N. C., Goetsch, K.M. (1993). "Carbohydrate requirement of *Caenorhabditis elegans* and the final development of chemically defined medium." *Nematologica* 39: 303-311.

Lu, N. C., G. Hugenberg, et al. (1978). "The growth-promoting activity of several lipid-related compounds in the free-living nematode *Caenorhabditis briggsae*." *Proc Soc Exp Biol Med* 158(2): 187-191.

Lund, S., G. D. Holman, et al. (1995). "Contraction stimulates translocation of glucose transporter GLUT4 in skeletal muscle through a mechanism distinct from that of insulin." *Proc Natl Acad Sci U S A* 92(13): 5817-5821.

Macheda, M. L., D. J. Kelly, et al. (2002). "Expression during rat fetal development of GLUT12--a member of the class III hexose transporter family." *Anat Embryol (Berl)* 205(5-6): 441-452.

Maiden, M. C., M. C. Jones-Mortimer, et al. (1988). "The cloning, DNA sequence, and overexpression of the gene araE coding for arabinose-proton symport in *Escherichia coli* K12." *J Biol Chem* 263(17): 8003-8010.

Manolescu, A. R., K. Witkowska, et al. (2007). "Facilitated hexose transporters: new perspectives on form and function." *Physiology (Bethesda)* 22: 234-240.

McCarter, R., E. J. Masoro, et al. (1985). "Does food restriction retard aging by reducing the metabolic rate?" *Am J Physiol* 248(4 Pt 1): E488-490.

McCay, C. M., M. F. Crowell, et al. (1989). "The effect of retarded growth upon the length of life span and upon the ultimate body size. 1935." *Nutrition* 5(3): 155-171; discussion 172.

McElwee, J. J., E. Schuster, et al. (2004). "Shared transcriptional signature in *Caenorhabditis elegans* Dauer larvae and long-lived *daf-2* mutants implicates detoxification system in longevity assurance." *J Biol Chem* 279(43): 44533-44543.

McElwee, J. J., E. Schuster, et al. (2006). "Diapause-associated metabolic traits reiterated in long-lived *daf-2* mutants in the nematode *Caenorhabditis elegans*." *Mech Ageing Dev* 127(5): 458-472.

McVie-Wylie, A. J., D. R. Lamson, et al. (2001). "Molecular cloning of a novel member of the GLUT family of transporters, SLC2a10 (GLUT10), localized on chromosome 20q13.1: a candidate gene for NIDDM susceptibility." *Genomics* 72(1): 113-117.

Meissner, B., M. Boll, et al. (2004). Deletion of the Intestinal Peptide Transporter Affects Insulin and TOR Signaling in *Caenorhabditis elegans*. 279: 36739-36745.

Melvin, D. R., B. J. Marsh, et al. (1999). "Analysis of amino and carboxy terminal GLUT-4 targeting motifs in 3T3-L1 adipocytes using an endosomal ablation technique." *Biochemistry* 38(5): 1456-1462.

Moretti, S., F. Armougom, et al. (2007). "The M-Coffee web server: a meta-method for computing multiple sequence alignments by combining alternative alignment methods." *Nucleic Acids Res* 35(Web Server issue): W645-648.

Morris, J. Z., H. A. Tissenbaum, et al. (1996). "A phosphatidylinositol-3-OH kinase family member regulating longevity and diapause in *Caenorhabditis elegans*." *Nature* 382(6591): 536-539.

Mueckler, M. (1994). "Facilitative glucose transporters." *Eur J Biochem* 219(3): 713-725.

Mueckler, M., C. Caruso, et al. (1985). "Sequence and structure of a human glucose transporter." *Science* 229(4717): 941-945.

Mueckler, M. and C. Makepeace (2006). "Transmembrane segment 12 of the Glut1 glucose transporter is an outer helix and is not directly involved in the transport mechanism." *J Biol Chem* 281(48): 36993-36998.

Nishimura, H., F. V. Pallardo, et al. (1993). "Kinetics of GLUT1 and GLUT4 glucose transporters expressed in *Xenopus* oocytes." *J Biol Chem* 268(12): 8514-8520.

Notredame, C., D. G. Higgins, et al. (2000). "T-Coffee: A novel method for fast and accurate multiple sequence alignment." *J Mol Biol* 302(1): 205-217.

Ogg, S., S. Paradis, et al. (1997). "The Fork head transcription factor DAF-16 transduces insulin-like metabolic and longevity signals in *C. elegans*." *Nature* 389(6654): 994-999.

Olson, A. L. and J. E. Pessin (1996). "Structure, function, and regulation of the mammalian facilitative glucose transporter gene family." *Annu Rev Nutr* 16: 235-256.

Okada, C. Y. and M. Rechsteiner (1982). "Introduction of macromolecules into cultured mammalian cells by osmotic lysis of pinocytic vesicles." *Cell* 29(1): 33-41.

Olson, A. L. and J. E. Pessin (1996). "Structure, function, and regulation of the mammalian facilitative glucose transporter gene family." *Annu Rev Nutr* 16: 235-256.

Ozcan, S. and M. Johnston (1999). "Function and regulation of yeast hexose transporters." *Microbiol Mol Biol Rev* 63(3): 554-569.

Panowski, S. H. and A. Dillin (2009). "Signals of youth: endocrine regulation of aging in *Caenorhabditis elegans*." *Trends Endocrinol Metab* 20(6): 259-264.

Panowski, S. H., S. Wolff, et al. (2007). "PHA-4/Foxa mediates diet-restriction-induced longevity of *C. elegans*." *Nature* 447(7144): 550-555.

Paradis, S., M. Ailion, et al. (1999). "A PDK1 homolog is necessary and sufficient to transduce AGE-1 PI3 kinase signals that regulate diapause in *Caenorhabditis elegans*." *Genes Dev* 13(11): 1438-1452.

Paradis, S. and G. Ruvkun (1998). "*Caenorhabditis elegans* Akt/PKB transduces insulin receptor-like signals from AGE-1 PI3 kinase to the DAF-16 transcription factor." *Genes Dev* 12(16): 2488-2498.

Partridge, L., D. Gems, et al. (2005). "Sex and death: what is the connection?" *Cell* 120(4): 461-472.

Pellerone, F. I., S. K. Archer, et al. (2003). "Trehalose metabolism genes in *Caenorhabditis elegans* and filarial nematodes." *Int J Parasitol* 33(11): 1195-1206.

Perez, C. L. and M. R. Van Gilst (2008). "A 13C Isotope Labeling Strategy Reveals the Influence of Insulin Signaling on Lipogenesis in *C. elegans*." *Cell Metabolism* 8(3): 266-274.

Phay, J. E., H. B. Hussain, et al. (2000). "Cloning and expression analysis of a novel member of the facilitative glucose transporter family, SLC2A9 (GLUT9)." *Genomics* 66(2): 217-220.

Piper, M. D. and A. Bartke (2008). "Diet and aging." *Cell Metab* 8(2): 99-104.

Porte, D., Jr., D. G. Baskin, et al. (2005). "Insulin signaling in the central nervous system: a critical role in metabolic homeostasis and disease from *C. elegans* to humans." *Diabetes* 54(5): 1264-1276.

Praitis, V. (2006). Creation of Transgenic Lines Using Microparticle Bombardment Methods. 351: 93-107.

Quon, M. J., M. Guerre-Millo, et al. (1994). "Tyrosine Kinase-Deficient Mutant Human Insulin Receptors (Met1153 {rightarrow} Ile) Overexpressed in Transfected Rat Adipose Cells Fail to Mediate Translocation of Epitope-Tagged GLUT4." *PNAS* 91(12): 5587-5591.

Quon, M. J., M. J. Zarnowski, et al. (1993). "Transfection of DNA into isolated rat adipose cells by electroporation: evaluation of promoter activity in transfected adipose cells which are highly responsive to insulin after one day in culture." *Biochem Biophys Res Commun* 194(1): 338-346.

Quon, M. J., M. Guerre-Millo, et al. (1994). "Tyrosine Kinase-Deficient Mutant Human Insulin Receptors (Met1153 {rightarrow} Ile) Overexpressed in Transfected Rat Adipose Cells Fail to Mediate Translocation of Epitope-Tagged GLUT4." *PNAS* 91(12): 5587-5591.

Rogers, S., J. D. Chandler, et al. (2003). "Glucose transporter GLUT12-functional characterization in *Xenopus laevis* oocytes." *Biochem Biophys Res Commun* 308(3): 422-426.

Rogers, S., S. E. Docherty, et al. (2003). "Differential expression of GLUT12 in breast cancer and normal breast tissue." *Cancer Lett* 193(2): 225-233.

Rogina, B. and S. L. Helfand (2004). "Sir2 mediates longevity in the fly through a pathway related to calorie restriction." *Proc Natl Acad Sci U S A* 101(45): 15998-16003.

Rost, B., G. Yachdav, et al. (2004). "The PredictProtein server." *Nucleic Acids Res* 32(Web Server issue): W321-326.

Rulifson, E. J., S. K. Kim, et al. (2002). "Ablation of insulin-producing neurons in flies: growth and diabetic phenotypes." *Science* 296(5570): 1118-1120.

Sakamoto, K. and G. D. Holman (2008). "Emerging role for AS160/TBC1D4 and TBC1D1 in the regulation of GLUT4 traffic." *Am J Physiol Endocrinol Metab* 295(1): E29-37.

Salas-Burgos, A., P. Iserovich, et al. (2004). "Predicting the three-dimensional structure of the human facilitative glucose transporter glut1 by a novel evolutionary homology strategy: insights on the molecular mechanism of substrate migration, and binding sites for glucose and inhibitory molecules." *Biophys* J 87(5): 2990-2999.

Sasaki, T., S. Minoshima, et al. (2001). "Molecular cloning of a member of the facilitative glucose transporter gene family GLUT11 (SLC2A11) and identification of transcription variants." *Biochem Biophys Res Commun* 289(5): 1218-1224.

Sauer, N., K. Friedlander, et al. (1990). "Primary structure, genomic organization and heterologous expression of a glucose transporter from *Arabidopsis thaliana*." *EMBO J* 9(10): 3045-3050.

Sauer, N. and W. Tanner (1989). "The hexose carrier from Chlorella. cDNA cloning of a eucaryotic H^+-cotransporter." *FEBS Lett* 259(1): 43-46.

Scheepers, A., H. Joost, et al. (2004). "The glucose transporter families SGLT and GLUT: molecular basis of normal and aberrant function." *JPEN J Parenter Enteral Nutr* 28(5): 364-371.

Scheepers, A., H. G. Joost, et al. (2004). The glucose transporter families SGLT and GLUT: molecular basis of normal and aberrant function. 28: 364-371.

Schlotterer, A., G. Kukudov, et al. (2009). "*C. elegans* as model for the study of high glucose- mediated life span reduction." *Diabetes* 58(11): 2450-2456.

Schmidt, S., H. G. Joost, et al. (2009). "GLUT8, the enigmatic intracellular hexose transporter." *Am J Physiol Endocrinol Metab* 296(4): E614-618.

Schulz, T. J., K. Zarse, et al. (2007). "Glucose restriction extends *Caenorhabditis elegans* life span by inducing mitochondrial respiration and increasing oxidative stress." *Cell Metab* 6(4): 280-293.

Shanmugam, M., S. K. McBrayer, et al. (2009). "Targeting glucose consumption and autophagy in myeloma with the novel nucleoside analogue 8-aminoadenosine." *J Biol Chem* 284(39): 26816-26830.

Shaw, R. J., K. A. Lamia, et al. (2005). "The kinase LKB1 mediates glucose homeostasis in liver and therapeutic effects of metformin." *Science* 310(5754): 1642-1646.

Simpson, I. A., D. Dwyer, et al. (2008). "The facilitative glucose transporter GLUT3: 20 years of distinction." *Am J Physiol Endocrinol Metab* 295(2): E242-253.

Simpson, I. A., D. R. Yver, et al. (1983). "Insulin-stimulated translocation of glucose

transporters in the isolated rat adipose cells: characterization of subcellular fractions." *Biochim Biophys Acta* 763(4): 393-407.

Stambuk, B. U., M. A. da Silva, et al. (1999). "Active alpha-glucoside transport in *Saccharomyces cerevisiae*." *FEMS Microbiol Lett* 170(1): 105-110.

Stambuk, B. U., P. S. De Araujo, et al. (1996). "Kinetics and energetics of trehalose transport in *Saccharomyces cerevisiae*." *Eur J Biochem* 237(3): 876-881.

Stiernagle, T. (2006). Maintenance of *C. elegans*. *WormBook*. T. C. e. R. Community, WormBook.

Szkutnicka, K., J. F. Tschopp, et al. (1989). "Sequence and structure of the yeast galactose transporter." *J Bacteriol* 171(8): 4486-4493.

Tabara, H., A. Grishok, et al. (1998). "RNAi in *C. elegans*: soaking in the genome sequence." *Science* 282(5388): 430-431.

Taguchi, A., L. M. Wartschow, et al. (2007). "Brain IRS2 signaling coordinates life span and nutrient homeostasis." *Science* 317(5836): 369-372.

Taguchi, A. and M. F. White (2008). "Insulin-Like Signaling, Nutrient Homeostasis, and Life Span." *Annual Review of Physiology* 70(1): 191-212.

Takiff, H. E., S. M. Chen, et al. (1989). "Genetic analysis of the rnc operon of *Escherichia coli*." *J Bacteriol* 171(5): 2581-2590.

Tatar, M., A. Kopelman, et al. (2001). "A mutant *Drosophila* insulin receptor homolog that extends life-span and impairs neuroendocrine function." *Science* 292(5514): 107-110.

Taylor, L. P. and G. D. Holman (1981). "Symmetrical kinetic parameters for 3-O-methyl-D-glucose transport in adipocytes in the presence and in the absence of insulin." *Biochim Biophys Acta* 642(2): 325-335.

Timmons, L., D. L. Court, et al. (2001). "Ingestion of bacterially expressed dsRNAs can produce specific and potent genetic interference in *Caenorhabditis elegans*." *Gene* 263(1-2): 103-112.

Timmons, L. and A. Fire (1998). "Specific interference by ingested dsRNA." *Nature* 395(6705): 854.

Tissenbaum, H. A. and L. Guarente (2001). "Increased dosage of a sir-2 gene extends lifespan in *Caenorhabditis elegans*." *Nature* 410(6825): 227-230.

Toivonen, J. M. and L. Partridge (2009). "Endocrine regulation of aging and reproduction in *Drosophila*." *Mol Cell Endocrinol* 299(1): 39-50.

Tusnady, G. E. and I. Simon (1998). "Principles governing amino acid composition of integral membrane proteins: application to topology prediction." *J Mol Biol* 283(2): 489-506.

Uldry, M., M. Ibberson, et al. (2001). "Identification of a mammalian H($^{+}$)-myo-inositol symporter expressed predominantly in the brain." *EMBO J* 20(16): 4467-4477.

Uldry, M., M. Ibberson, et al. (2002). "GLUT2 is a high affinity glucosamine transporter." *FEBS Lett* 524(1-3): 199-203.

Utsugi, T., T. Ohno, et al. (2000). "Decreased insulin production and increased insulin sensitivity in the klotho mutant mouse, a novel animal model for human aging." *Metabolism* 49(9): 1118-1123.

Van Voorhies, W. A. and S. Ward (1999). "Genetic and environmental conditions that increase longevity in *Caenorhabditis elegans* decrease metabolic rate." *Proc Natl Acad Sci U S A* 96(20): 11399-11403.

Wang, S., N. Tulina, et al. (2007). "The origin of islet-like cells in *Drosophila* identifies parallels to the vertebrate endocrine axis." *Proc Natl Acad Sci U S A* 104(50): 19873-19878.

Wang, Y., S. W. Oh, et al. (2006). "*C. elegans* 14-3-3 proteins regulate life span and interact with SIR-2.1 and DAF-16/FOXO." *Mech Ageing Dev* 127(9): 741-747.

Wang, Y. and H. A. Tissenbaum (2006). "Overlapping and distinct functions for a *Caenorhabditis elegans* SIR2 and DAF-16/FOXO." *Mech Ageing Dev* 127(1): 48-56.

Watson, R. T. and J. E. Pessin (2006). "Bridging the GAP between insulin signaling and GLUT4 translocation." *Trends in Biochemical Sciences* In Press, Corrected Proof.

Watson, R. T., M. Kanzaki, et al. (2004). Regulated Membrane Trafficking of the Insulin-Responsive Glucose Transporter 4 in Adipocytes. 25: 177-204.

Williams, G. C. (1957). "Pleiotropy, natural selection and the evolution of senescence." *Evolution* 11: 398–411.

Wolf, G. (2006). "Calorie restriction increases life span: a molecular mechanism." *Nutr Rev* 64(2 Pt 1): 89-92.

Wolff, S. and A. Dillin (2006). "The trifecta of aging in *Caenorhabditis elegans*." *Experimental Gerontology* 41(10): 894-903.

Wood, I. S. and P. Trayhurn (2003). "Glucose transporters (GLUT and SGLT): expanded families of sugar transport proteins." *Br J Nutr* 89(1): 3-9.

Wood, J. G., B. Rogina, et al. (2004). "Sirtuin activators mimic caloric restriction and delay ageing in metazoans." *Nature* 430(7000): 686-689.

WormBase. (2009). "Gene Summary for H17B01.1." Retrieved 9, Dec, 2009, 2009, from http://www.wormbase.org/db/gene/gene?name=WBGene00019207;class=Gene.

Wright, E. M. (2001). "Renal Na^+-glucose cotransporters." *Am J Physiol Renal Physiol* 280(1): F10-18.

Wu, X. and H. H. Freeze (2002). "GLUT14, a duplicon of GLUT3, is specifically expressed in testis as alternative splice forms." *Genomics* 80(6): 553-557.

Wullschleger, S., R. Loewith, et al. (2006). "TOR signaling in growth and metabolism." *Cell* 124(3): 471-484.

Zaidi, S. H., S. Meyer, et al. (2009). "A novel non-sense mutation in the SLC2A10 gene of an arterial tortuosity syndrome patient of Kurdish origin." *Eur J Pediatr* 168(7): 867-870.

Zhang, C. C., M. C. Durand, et al. (1989). "Molecular and genetical analysis of the fructose-glucose transport system in the cyanobacterium Synechocystis PCC6803." *Mol Microbiol* 3(9): 1221-1229.

Zhao, F. Q. and A. F. Keating (2007). "Functional properties and genomics of glucose transporters." *Curr Genomics* 8(2): 113-128.

Appendix

1) Buffer compositions

Name of buffer	Composition
General buffers	
PBS	154 mM NaCl, 12.5 mM $Na_2HPO_4 \cdot 12H_2O$, pH7.2
TBS	10 mM Tris, pH 7.4, 154 mM NaCl
TBS-Tween 20	10 mM Tris, pH 7.4, 154 mM NaCl, 0.1% (v/v) Tween-20
SDS Sample buffer	2% (w/v) SDS, 62.5 mM Tris HCl pH6.8, 0.01% (w/v) bromophenol blue, and 10% (v/v) glycerol
Resolving gel buffer	1.5 M Tris-HCl, pH 8.9, 0.4 % (w/v) SDS
Stacking gel buffer	0.5 M Tris-HCl, pH6.8, 0.4% (w/v) SDS
Electrophoresis running buffer	25 mM Tris-HCl, pH6.3, 0.1% (w/v) SDS, 0.2 M Glycine
Transfer buffer	48 mM Tris, 39 mM glycine, 0.0375% SDS (w/v), 20% (v/v) methanol, pH8.8 without adjusting
Ponceau S stain	0.1% (w/v)Ponceau S, 3% (w/v) TCA
BCA Reagent B	4% (w/v) $CuSO_4 \cdot 5H_2O$
TAE	40 mM Tris-acetate, 1 mM EDTA, pH 8.5
TFB1 buffer	100 mM RbCl, 50 mM $MnCl_2$, 30 mM Potassium acetate, 10 mM $CaCl_2$, 15% glycerol (v/v), pH 5.8
TFB2 buffer	10 mM RbCl, 10 mM MOPS, 75 mM $CaCl_2$, 15% glycerol (v/v), pH 6.5
LB	1% (w/v) Bacto™ Tryptone, 0.5% (w/v) Bacto™ Yeast Extract, 0.5% NaCl, pH 7.5, autoclaved
LB Agar plates	1% (w/v) Bacto™ Tryptone, 0.5% (w/v) Bacto™ Yeast Extract, 0.5% NaCl, pH 7.5, 1.5% agar, autoclaved
Worm buffers	
M9 buffer	22 mM KH_2PO_4, 22 mM Na_2HPO_4, 85 mM NaCl, 1 mM $MgSO_4$
NGM	0.3% (w/v) NaCl, 0.25% (w/v) peptone, 1mM KPO_4 buffer pH 6.0, 1 mM $MgSO_4$, autocalved; 5 μg/ml cholesterol (added after autoclave)
***Xenopus* oocyte buffers**	
Ca^{2+} free	82.5 mM NaCl, 2.5 mM KCl, 1 mM $NaHPO_4$, 1 mM $MgCl_2$,

OR-2 buffer	5 mM HEPES, pH 7.5
ND96 buffer	96 mM NaCl, 2 mM KCl, 1 mM $MgCl_2$, 1.8 mM $CaCl_2$, 5 mM HEPES pH 7.5, 2.5 pyruvic acid
complete ND96 buffer	96 mM NaCl, 2 mM KCl, 1 mM $MgCl_2$, 1.8 mM $CaCl_2$, 5 mM HEPES pH 7.5, 2.5 pyruvic acid, 1% FBS
Rat adipocytes buffers	
KRH buffer	140 mM NaCl, 4.7 mM KCl, 2.5 mM $CaCl_2$, 1.25 mM $MgSO_4$, 0.2 mM NaH_2PO_4, 10 mM HEPES, 200 nM adenosine, pH 7.4
Adipocyte digestion buffer	3.5% (w/v) BSA in KRH supplemented with 5 mM glucose and 500 µg/ml Collagenase type 1 from *Clostridium histolyticum*

2) Sequence alignment of the putative glucose transporters with human GLUT1 and GLUT4 (T08 excepted)

```
C35A11.4  MV----------EAPSFR--MICVAVITSIAGSFHFGFNLVLTNPSQEAFLNFMNQTLAKRFD----GGLSDNTLQNIWSFVVAILFLGALAGSFSIR
GLUT1     M-----------EPSSKKLTGRLMLAVGGAVLGSLQFGYNTGVINAPQKVIEEFYNQTWVHRYG----ESILPTTLTTLWSLSVAIFSVGGMIGSFSVG
GLUT4     MPSGFQQIGSEDGEPPQQRVTGTLVLAVFSAVLGSLQFGYNIGVINAPQKVIEQSYNETWLGRQGPEGPSSIPPGTLTTLWALSVAIFSVGGMISSFLIG
          *          *.... :    : :**  :: **::***:*  : *..*:.: :  *:*   * .      .:   **  .:*:: ***: :*.: .** :

C35A11.4  LIADWIGRKNGLYISIAVGVLAGGMSIASKFIPLFELYIASRIVMGWSVSVSLGLSALFLSEASPKQNRGAIGMMTGTCVQLGTVCGSVIAMPQIFGTED
GLUT1     LFVNRFGRRNSMLMMNLLAFVSAVLMGFSKLGKSFEMLILGRFIIGVYCGLITGFVPMYVGEVSPTAFRGALGTLHQLGIVVGILIAQVFGLDSIMGNKD
GLUT4     IISQWLGRKRAMLVNNVLAVLGGSLMGLANAAASYEMLILGRFLIGAYSGLTSGLVPMYVGEIAPTHLRGALGTLNQLAIVIGILIAQVLGLESLLGTAS
          :: : :**:..: :   :...:.. :   ::   :*: * .*:::*   .:: *: .:::.* :*.  ***:* :    : :* : ..*:.: .::*. .

C35A11.4  LWWLIYATEIGIMLFFGAALPFFPESPGFLIQRGATEAAIKSIAYYYNCEIDEAEKHLNEIKEEQKNS--TKNFKMMDIVRKKKSLRDKAFIGVVVTFAMS
GLUT1     LWPLLLSIIFIPALLQCIVLPFCPESPRFLLINRNEENRAKSVLKKLRGTAD-VTHDLQEMKEESRQMMREKKVTILELFRSPAYRQPILIAVVLQLSQQ
GLUT4     LWPLLLGLTVLPALLQLVLLPFCPESPRYLYIIQNLEGPARKSLKRLTGWAD-VSGVLAELKDEKRKLERERPLSLLQLLGSRTHRQPLIIAVVLQLSQQ
          ** *: .  .   *:   *** **** :*     *  ::.          * .  * *:*:*.::    : ..:::::. . : *:  :*.**: :: .

C35A11.4  FSGVAVINAFAFDILKDTGLKVLEASLANDAISVVSMISSIVAAVIVDRNGRRPLLLISFAGILVCNLIIFALMFTFYKFENHVLGFILICFICIFTFFF
GLUT1     LSGINAVFYYSTSIFEKAGVQ--QPVYATIGSGIVNTAFTVVSLFVVERAGRRTLHLIGLAGMAGCAILMTIALALLEQL--PWMSYLSIVAIFGFVAFF
GLUT4     LSGINAVFYYSTSIFETAGVG--QPAYATIGAGVVNTVFTLVSVLLVERAGRRTLHLLGLAGMCGCAILMTVALLLLERV--PAMSYVSIVAIFGFVAFF
          :**: .:  :: .*:: :*:  :. *. . .:*.   ::*: .:*:* ***.* *:.:**:  * :::   :  : :.   :.:: *  * *. **

C35A11.4  ALGPGPLCYFINAELVGQAARSAAQSWASVIQMLSRFVIVTAFLPMKNQLGEAWSYLILFVAPVAASLVYLYFSLPETKNKNPFEVEEAIEDLPKFPLCG
GLUT1     EVGPGPIPWFIVAELFSQGPRPAAIAVAGFSNWTSNFIVGMCFQYVEQLCGP-YV-FIIFTVLVLFFIFTYFKVPETKGRTFDEIASGFRQGGAS----
GLUT4     EIGPGPIPWFIVAELFSQGPRPAAMAVAGFSNWTSNFIIGMGFQYVAEAMGP-YV-FLLFAVLLLGFFIFTFLRVPETRGRTFDQISAAFHRTPSL----
           :*****: :** ***..*..*.** : *.. :  *.*::   *  : :  *  :  :::*.. :   ::: :: :***:.:.  ::  .:.

C35A11.4  KNRVYDRKQSQEMVLSRQMQLVVDYGSIESLSYRL
GLUT1     ----------Q-SDKTPEELFH-------P-LGADSQV
GLUT4     ----------LEQEVKPSTELE-------Y-LGPDEND
                     .:   .  :.          . . .
```

```
F14E5.1         MS------------NRLWPVKQVCIFAL-IAFASNFNYGFSTTYINTSVDEFKTFLNTSLSRRH-----VIMTEEKYDLIWNVFLNCWFIGSFFGVWINS
GLUT1           ME------------PSSKKLTGRLMLAVGGAVLGSLQFGYNTGVINAPQKVIEEFYNQTWVHRYG----ESILPTTLTTLWSLSVAIFSVGGMIGSFSVG
GLUT4           MPSGFQQIGSEDGEPPQQRVTGTLVLAVFSAVLGSLQFGYNIGVINAPQKVIEQSYNETWLGRQGPEGPSSIPPGTLTTLWALSVAIFSVGGMISSFLIG
                *                  :.   ::*:  *. ..:::*:.   **:. . ::   * :   *       :   .   :* : :  : :*.::. :  .

F14E5.1         IFSERFGRRVGFLIGNSVAFISSILQCLSLIWYCPELLIVSRFITSICMAQSCILFLQECSPTHLRGSFSFLSEVSYSSMTMVGSFLGQDYIIGSHL
GLUT1           LFVNRFGRRNSMLMMNLLAFVSAVLMGFSKLGKSFEMLILGRFIIGVYCGGFVPMYVGEVSPTAFRGALGTLHQLGIVVGILIAQVFGLDSIMGNKD
GLUT4           IISQWLGRKRAMLVNNVLAVLGGSLMGLANAAASYEMLILGRFLIGAYSGGLVPMYVGEIAPTHLRGALGTLNQLAIVIGILIAQVLGLESLLGTAS
                :: : :**: .:*: * :*.:.. *  ::    . *:**:.**: .   .    ::: * :** :**::. * ::.     ::...:* : ::*.

F14E5.1         FWLCFF---VVPFCLFFTLILFILPETPKFLLISKDEEEEAIKSVKYYHGDGTDAKQVLEDIRKEAECEQDSSKSTTFQKMKELFTERHLRMALILSVSA
GLUT1           LWPLLLSIIFIPA-LLQCIVLPFCPESPRFLLINRNEENRAKSVLKKLRGT-ADVTHDLQEMKEESRQMMREKKVTILELFRSPAYRQPILIAVVLQLSQ
GLUT4           LWPLLLGLTVLPA-LLQLVLLPFCPESPRYLYIIQNLEGPARKSLKRLTGW-ADVSGVLAELKDEKRKLERERPLSLLQLLGSRTHRQPLIIAVVLQLSQ
                :*  ::   .:*  *:  ::* : **:*::* * :: *  * . :*   *  :*..  * :::.* .    .   : :: : .   .: : :*::*.:*

F14E5.1         LTNTVGLWALLLSSTFFLENANVESEIAEWSTTAMGLAYVSGTITGGIVIEKVGRRKLLLL-FTFLNNLALIAFVFFAKIRILIDPMKYGCLVALIIYGY
GLUT1           --QLSGINAVFYYSTSIFEKAGVQQPV--YATIGSGIVNTAFTVVSLFVVERAGRRTLHLIGLAGMAGCAILMTIALALLE-QLPWMSYLSIVAIFGFVA
GLUT4           --QLSGINAVFYYSTSIFETAGVGQPA--YATIGAGVVNTVFTLVSVLLVERAGRRTLHLLGLAGMCGCAILMTVALLLLE-RVPAMSYVSIVAIFGFVA
                  :  *: *::  ** ::*.*.* .    ::* . *:. .  *:.. :::*:.***.* *: :: : . *::  : :  :.  :  *.* .:**:: :

F14E5.1         TYGTGVGPISWFISSELVPQKHRSIAQSVAYSMNTVMVVISTFTVLPLYSVIGSYAFLILYSIPSFISMLILFRYLPETKGREIHDIVNELKK-------
GLUT1           FFEVGPGPIPWFIVAELFSQGPRPAAIAVAGFSNWTSNFIVGMCFQYVEQLCGPYVFIIF-TVLLVLFFIFTYFKVPETKGRTFDEIASGFRQGG-ASQS
GLUT4           FFEIGPGPIPWFIVAELFSQGPRPAAMAVAGFSNWTSNFIIGMGFQYVAEAMGPYVFLLF-AVLLLGFFIFTFLRVPETRGRTFDQISAAFHRTPSLLEQ
                 :  * ***.*** :**..*  *. * :**   * .  .*  : .  : .  *.*.*::: ::  .  ::: :  :***:** :.:*   :::

F14E5.1         ----------------K
GLUT1           DKTPEELFHPLGADSQV
GLUT4           EVKPSTELEYLGPDEND
```

```
F48E3.2         M----------------QKLNWKLLILSAVLAITAIFQMGYTNAYPNTAIGSFRIFLNESANE------PYTLSNSEFEWAWSAMLAIYFIGFAAGSVIS
GLUT1           M------------EPSSKKLTG-RLMLAVGGAVLGSLQFGYNTGVINAPQKVIEEFYNQTWVHRYG----ESILPTTLTTLWSLSVAIFSVGGMIGSFSV
GLUT4           MPSGFQQIGSEDGEPPQQRVTG-TLVLAVFSAVLGSLQFGYNIGVINAPQKVIEQSYNETWLGRQGPEGPSSIPPGTLTTLWALSVAIFSVGGMISSFLI
                *               :::.   *:*:.  *: . :*:**. .  *:.   :.   *::           ::    :   *:  :**: :*   .*.

F48E3.2         AGVADRIGRKWTLFLGTCGSLLSSLIALFAIILKMPLMFGFSRLVMSLSAAISMNGLILLFQESSPSHMRGLISFNAEMAFVITNLIGGLFGMQSILGQN
GLUT1           GLFVNRFGRRNSMLMMNLLAFVSAVLMGFSKLGKSFEMLILGRFIIGVYCGLTTGFVPMYVGEVSPTAFRGALGTLHQLGIVVGILIAQVFGLDSIMGNK
GLUT4           GIISQWLGRKRAMLVNNVLAVLGGSLMGLANAAASYEMLILGRFLIGAYSGLTSGLVPMYVGEIAPTHLRGALGTLNQLAIVIGILIAQVLGLESLLGTA
                . . : :**: :::: .  :.:.. :  ::      *: :.*:::.  ..:: . : : . * :*: :** :.   ::.:*:  **. ::*::*::*

F48E3.2         IVG--LIAVSIIPSSVACFLTVFLKESPKYLFLKKHDATEAGRALQFYQNIKDEEEKMNVLNDLKLEKEEMGHQKNGSLFDIMANQPVRRGFLLGLA--T
GLUT1           DLWPLLLSIIFIPALLQCIVLPFCPESPRFLLINRNEENRAKSVLK---KLRGTADVTHDLQEMKEESRQMMREKKVTILELFRSPAYRQPILIAVVLQL
GLUT4           SLWPLLLGLTVLPALLQLVLLPFCPESPRYLYIIQNLEGPARKSLK---RLTGWADVSGVLAELKDEKRKLERERPLSLLQLLGSRTHRQPLIIAVVLQL
                 :   *:.: .:*: :  .:  *  ***::* : ::    *   *:   .: .  :    * ::* *..:: :::  :::::: . . *: :::.:.

F48E3.2         MQLTASVWPVVFYSTDFLMDAGFSYELSESVSTGMLFLSSLSTIVGMFIVEKYSRKWL-LIGTASVNIAAILVFSLSAILSHYWTWIGYGCIICLILHGI
GLUT1           SQQLSGINAVFYYSTSIFEKAGVQQPVYATIGSGI--VNTAFTVVSLFVVERAGRRTLHLIGLAGMAGCAILM-TIALALLEQLPWMSYLSIVAIFGFVA
GLUT4           SQQLSGINAVFYYSTSIFETAGVGQPAYATIGAGV--VNTVFTLVSVLLVERAGRRTLHLLGLAGMCGCAILM-TVALLLLERVPAMSYVSIVAIFGFVA
                 *  :.: .*.:***.::  **.      ::.:*:  :.:  *:*.:::**: .*: * *:* *.:  .***: :::  * .  . :.* .*:.:: .

F48E3.2         SYSVAMGPIAWFITSELVPINFRAASQSLVLALNHTVALVLAFLTFPLYKTIGPITLVIFFVIPGILCIIMLILYLPETKDKHINVIVEQLRETKAKRKE
GLUT1           FFEVGPGPIPWFIVAELFSQGPRPAAIAVAGFSNWTSNFIVGMCFQYVEQLCGPYVFIIFTVLL-VLFFIFTYFKVPETKGRTFDEIASGFRQGGASQSD
GLUT4           FFEIGPGPIPWFIVAELFSQGPRPAAMAVAGFSNWTSNFIIGMGFQYVAEAMGPYVFLLFAVLL-LGFFIFTFLRVPETRGRTFDQISAAFHRTPSLLEQ
                 :.:. ***.***.:**.. . *.*: ::.   * *  :::.:    : :  ** .:::* *:  :  :*:  : :***:.: :: *   ::.  :  .:

F48E3.2         SQ-KLETEESIGMN-KL
GLUT1           KT-PEELFHPLGADSQV
GLUT4           EVKPSTELEYLGPDEND
                .       . :* : :
```


GLUT1 M----------EPSSKKLTGRLMLAVGGAVLGSLQFGYNTGVINAPQKVIEEFYNQTWVHRYGE-S---ILPTTLTTLWSLSVAIFSVGGMIGSFSVG
GLUT4 MPSGFQQIGSEDGEPPQQRVTGTLVLAVFSAVLGSLQFGYNIGVINAPQKVIEQSYNETWLGRQGPEGPSSIPPGTLTTLWALSVAIFSVGGMISSFLIG
K09C4.1 M----------K---FTVPRNILFMIFTFVLLDIVMQMQVLTFSALAELVNQMNNYTLSAHFGI-TPTETSVGV---LNSIFAVTHETGNALAIIFLL
GLUT1 LFVNRFGRRN-SMLMMNLLAFVSAVLMGFSKLGKSFEMLILGRFIIGVYCGLTTGFVPMYVGEVSPTAFRGALGTLHQLGIVVGILIAQVFGLDSIMGNK
GLUT4 IISQWLGRKR-AMLVNNVLAVLGGSLMGLANAAASYEMLILGRFLIGAYSGLTSGLVPMYVGEIAPTHLRGALGTLNQLAIVIGILIAQVLGLESLLGTA
K09C4.1 PVADSRGRKFMAVYLRFALLFLTGFFHLLATSFQAAEAYTLGQLFLGIQSPLHLLITPMYILECAPDNCRGFASTALIFSFSIGKLLMFSAASPTFLGTI
GLUT1 DLWPLLLSIIFIPALLQCIVLPFCPESPRFLLINRNEENRAKSVLKKLRGTADVTHDLQEMKEESRQMMREKKVTILELFRSPAYRQPILIAVVLQLSQQ
GLUT4 SLWPLLLGLTVLPALLQLVLLPFCPESPRYLYIIQNLEGPARKSLKRLTGWADVSGVLAELKDEKRKLERERPLSLLQLLGSRTHRQPLIIAVVLQLSQQ
K09C4.1 DSWFIIPLFEMVCSVMILCLMIHLPDSPKWL-IQQNKVKKAEDSIKFYYGKHFLDEVVTSLIKEK-NLTKDNRISLRQIWENDTLRESLKILFAVTVFLQ
GLUT1 LSGINAVFYYSTSIFEKAGVQQPVYATIGSGIVNTAF--TVVSLFVVERAGRRTLHLIGLAGMAGCAILMTIALALLEQLPWMSYLSIVAIFGFVAF---
GLUT4 LSGINAVFYYSTSIFETAGVGQPAYATIGAGVVNTVF--TLVSVLLVERAGRRTLHLLGLAGMCGCAILMTVALLLLERVPAMSYVSIVAIFGFVAF---
K09C4.1 FDTTTAQSVYTIDFHKTAGFTVQEALNINLILTTVLFPTKFIGTLFLDALGRRPA--MGVAGVMKYSKSM--LLLAFEILVFISGSSLITKIMYVAVELL
GLUT1 ----FEVGPGPIPWFIVAELFSQGPRPAAIAVAGFSNWTSNFIVGMCFQYVEQLCGPYVFIIFTVLLVLFFIFTYFKVPETKGRTFDEIASGFRQGGASQ
GLUT4 ----FEIGPGPIPWFIVAELFSQGPRPAAMAVAGFSNWTSNFIIGMGFQYVAEAMGPYVFLLFAVLLLGFFIFTFLRVPETRGRTFDQISAAFHRTPSLL
K09C4.1 TILVPVTGANSIRVLFVTELFPPSARTAVGQAMLFGSMAVNSPIVALYPIVNSIFPPIFFVPFVISQMIFGIYLYRHMPETRGRAVYDIIESLDRNVASR
GLUT1 S-DKTPEELFHPL----------GADSQV
GLUT4 EQEVKPSTELEYL----------GPDEND
K09C4.1 TA-SVTDE-NTPLFKDQTENRDGKWNSLLNTPRTRALTFEENSHSPN


GLUT1 M----------EPSSK--KLTGRLMLAVGGAVLGSLQFGYNTGVINAPQKVIEEFYNQTWVHRYGE----SILPTTLTTLWSLSVAIFSVGGMIGSFS
GLUT4 MPSGFQQIGSEDGEPPQQ--RVTGTLVLAVFSAVLGSLQFGYNIGVINAPQKVIEQSYNETWLGRQGPEGPSSIPPGTLTTLWALSVAIFSVGGMISSFL
K09C4.5 MLF---------NAPPNIIYMLLCFLLMDISNTVLM-LLF-------PTLADIINEMNNHTLSAHFGI----EPTIANVNVMNSMITGASTVGLFVSLFV
GLUT1 VGLFVNRFGRRNSMLMMN-LLAFVSAVLMGFSKLGKSFEMLILGRFIIGVYCGLTTGFVPMYVGEVSPTAFRGALGTLHQLGIVVGILIAQVFGLDSIMG
GLUT4 IGIISQWLGRKRAMLVNN-VLAVLGGSLMGLANAAASYEMLILGRFLIGAYSGLTSGLVPMYVGEIAPTHLRGALGTLNQLAIVIGILIAQVLGLESLLG
K09C4.5 LVPFAETKGRKYTVVYFRFIISVVSSLCIIMSALFQASEFFILGSAVNGLQLPMRMFVTMLFITECAPDKYRGFASTALIFSDVIGQVIMFSIATPNVLG
GLUT1 NKDLWPLLLSIIFIPALLQCIVLPFCPESPRFLLINRNEENRAKSVLKKLRGTADVTHDLQEMKEESRQMMREKKVTILELFRSPAYRQPILIAVVLQL-
GLUT4 TASLWPLLLGLTVLPALLQLVLLPFCPESPRYLYIIQNLEGPARKSLKRLTGWADVSGVLAELKDEKRKLERERPLSLLQLLGSRTHRQPLIIAVVLQL-
K09C4.5 RANTWVIFPLAVLMSSTVIFFMTLRLPESPKWLV-RQNKIEEASRAIEFYHGENCCLNEVVSSYIKEKNLTQEDQISLRQALKV-------LCSVSLFLV
GLUT1 --SQQLSGINAVFYYSTSIFEKAGVQQPVYATIGSGIVNTAFTVVSLFVVERAGRRTLHLIGLAGMAGCAILMTIALALLEQLPWMSYLSIVAIFGFVAF
GLUT4 --SQQLSGINAVFYYSTSIFETAGVGQPAYATIGAGVVNTVFTLVSVLLVERAGRRTLHLLGLAGMCGCAILMTVALLLLERVPAMSYVSIVAIFGFVAF
K09C4.5 LDSGVIQGVYTVLLHKTAGFT---VQEALNVNLVLVIIFLPTRFVGTYIIDHLGRRPVMLIA--GI---IVYSKTWLMLS--------------TQFIIY
GLUT1 FEVGPG----------PIPWFIVAELFSQGPRPAAIAVAGFSNWTSNFIVGMCFQYVEQLCGPYVFIIFTVLLVLFFIFTYFKVPET
GLUT4 FEIGPG----------PIPWFIVAELFSQGPRPAAMAVAGFSNWTSNFIIGMGFQYVAEAMGPYVFLLFAVLLLGFFIFTFLRVPET
K09C4.5 F-VGPSVLTKWLYIGVECLSESSLATGVTSLGILFISELFPPSARTCVAQALILVTMTINLPIISIFPIVYSFFGPGFFIIHVFSQFFFGAYLYRHMPET
GLUT1 KGRTFDEIASGFRQGG-ASQSDKTPEEL----------FHP-LGADSQV
GLUT4 RGRTFDQISAAFHRTPSLLEQEVKPSTE----------LEY-LGPDEND
K09C4.5 RGRAVYDIIESLDQEV-ASRTASFLEETTPLVRKRSSTLAYKRNSILNTSRTRALTFDHNLIPSGEWN


GLUT1 M----------EPSSK--KLTGRLMLAVGGAVLGSLQFGYNTGVINAPQKVIEEFYNQTWVHRYGE----SILPTTLTTLWSLSVAIFSVGGMIGSFS
GLUT4 MPSGFQQIGSEDGEPPQQ--RVTGTLVLAVFSAVLGSLQFGYNIGVINAPQKVIEQSYNETWLGRQGPEGPSSIPPGTLTTLWALSVAIFSVGGMISSFL
K09C4.5 MLF---------NAPPNIIYMLLCFLLMDISNTVLM-LLF-------PTLADIINEMNNHTLSAHFGI----EPTIANVNVMNSMITGASTVGLFVSLFV
GLUT1 VGLFVNRFGRRNSMLMMN-LLAFVSAVLMGFSKLGKSFEMLILGRFIIGVYCGLTTGFVPMYVGEVSPTAFRGALGTLHQLGIVVGILIAQVFGLDSIMG
GLUT4 IGIISQWLGRKRAMLVNN-VLAVLGGSLMGLANAAASYEMLILGRFLIGAYSGLTSGLVPMYVGEIAPTHLRGALGTLNQLAIVIGILIAQVLGLESLLG
K09C4.5 LVPFAETKGRKYTVVYFRFIISVVSSLCIIMSALFQASEFFILGSAVNGLQLPMRMFVTMLFITECAPDKYRGFASTALIFSDVIGQVIMFSIATPNVLG
GLUT1 NKDLWPLLLSIIFIPALLQCIVLPFCPESPRFLLINRNEENRAKSVLKKLRGTADVTHDLQEMKEESRQMMREKKVTILELFRSPAYRQPILIAVVLQL-
GLUT4 TASLWPLLLGLTVLPALLQLVLLPFCPESPRYLYIIQNLEGPARKSLKRLTGWADVSGVLAELKDEKRKLERERPLSLLQLLGSRTHRQPLIIAVVLQL-
K09C4.5 RANTWVIFPLAVLMSSTVIFFMTLRLPESPKWLV-RQNKIEEASRAIEFYHGENCCLNEVVSSYIKEKNLTQEDQISLRQALKV-------LCSVSLFLV
GLUT1 --SQQLSGINAVFYYSTSIFEKAGVQQPVYATIGSGIVNTAFTVVSLFVVERAGRRTLHLIGLAGMAGCAILMTIALALLEQLPWMSYLSIVAIFGFVAF
GLUT4 --SQQLSGINAVFYYSTSIFETAGVGQPAYATIGAGVVNTVFTLVSVLLVERAGRRTLHLLGLAGMCGCAILMTVALLLLERVPAMSYVSIVAIFGFVAF
K09C4.5 LDSGVIQGVYTVLLHKTAGFT---VQEALNVNLVLVIIFLPTRFVGTYIIDHLGRRPVMLIA--GI---IVYSKTWLMLS--------------TQFIIY
GLUT1 FEVGPG----------PIPWFIVAELFSQGPRPAAIAVAGFSNWTSNFIVGMCFQYVEQLCGPYVFIIFTVLLVLFFIFTYFKVPET
GLUT4 FEIGPG----------PIPWFIVAELFSQGPRPAAMAVAGFSNWTSNFIIGMGFQYVAEAMGPYVFLLFAVLLLGFFIFTFLRVPET
K09C4.5 F-VGPSVLTKWLYIGVECLSESSLATGVTSLGILFISELFPPSARTCVAQALILVTMTINLPIISIFPIVYSFFGPGFFIIHVFSQFFFGAYLYRHMPET
GLUT1 KGRTFDEIASGFRQGG-ASQSDKTPEEL----------FHP-LGADSQV
GLUT4 RGRTFDQISAAFHRTPSLLEQEVKPSTE----------LEY-LGPDEND
K09C4.5 RGRAVYDIIESLDQEV-ASRTASFLEETTPLVRKRSSTLAYKRNSILNTSRTRALTFDHNLIPSGEWN


GLUT1 M----------EPSSKKLTGRLMLAVGGAVLGSLQFGYNTGVINAPQKVIEEFYNQTWVHRYGE----SILPTTLTTLWSLSVAIFSVGGMIGSFSVG
GLUT4 MPSGFQQIGSEDGEPPQQRVTGTLVLAVFSAVLGSLQFGYNIGVINAPQKVIEQSYNETWLGRQGPEGPSSIPPGTLTTLWALSVAIFSVGGMISSFLIG
Y39E4B.5 M----------RWQTIRLI--SIYAALSA-ITNFPSGFTNSSVNTAVEKLHKFI-ATSLRQPGV----PDDENTIALFQSATLNCWFVAQIFGAIMTP
GLUT1 LFVNRFGRRNSMLMMNLLAFVSAVLMGFSKLGKSFEMLILGRFIIGVYCGLTTGFVPMYVGEVSPTAFRGALGTLHQLGIVVGILIAQVFGLDSIMGNKD
GLUT4 IISQWLGRKRAMLVNNVLAVLGGSLMGLANAAASYEMLILGRFLIGAYSGLTSGLVPMYVGEIAPTHLRGALGTLNQLAIVIGILIAQVLGLESLLGTAS
Y39E4B.5 MISDGYGRKFGYIVCVTTTIFATFVQYFSICFYMPWGLILGRSLTALVSPLGDACLLLYVQETSPLEIRGMSSFLCEIGYGTMCVLGMVLGMKSVLGESL
GLUT1 LWPLLLSIIFIPALLQCIVLPFCPESPRFLLINRNEENRAKSVLKKLRGT-ADVTHDLQEMKEESRQMMREKKVTILELFRSPAYRQPILIAVVLQLSQQ
GLUT4 LWPLLLGLTVLPALLQLVLLPFCPESPRYLYIIQNLEGPARKSLKRLTGW-ADVSGVLAELKDEKRKLERERPLSLLQLLGSRTHRQPLIIAVVLQLSQQ
Y39E4B.5 SRLLLL--SLIPLFCSLCFIVRIPETPKFLMIMRNDREKALKSLEFFQGESSDNAYIMSEYQAEKMTDKLSQDSTFVDLLSKWHLRQAMRLALA-TLSLT
GLUT1 LSGINAVFYYSTSIFEKAGVQQPVYATIGS---GIVNTAFTVVSLFVVERAGRRTLHLIGLAGMAGC------AILMTIALALLEQLPWMSYLSIVAIFG
GLUT4 LSGINAVFYYSTSIFETAGVGQPAYATIGA---GVVNTVFTLVSVLLVERAGRRTLHLLGLAGMCGC------AILMTVALLLLERVPAMSYVSIVAIFG
Y39E4B.5 LSF-YPILQSSTYFLLESGVSVDM-AQICSTMAQVVLTLSSICGASIIDRFSRRKLLIT--FGILSNVLLVAFSFFSHLSATVVSPYSWPKYACLASLLA
GLUT1 FVAFFEVGPGPIPWFIVAELFSQGPRPAAI----AVAGFSNWTSNFIVGMCFQYVEQLCGPYVFIIFTVLLVLFFIFTYFKVPETKGRTF-DEIASGFRQ
GLUT4 FVAFFEIGPGPIPWFIVAELFSQGPRPAAM----AVAGFSNWTSNFIIGMGFQYVAEAMGPYVFLLFAVLLLGFFIFTFLRVPETRGRTF-DQISAAFHR
Y39E4B.5 YCISFGMVLGPLSWFVAPELVSQRHRCTIFSACFAIHNLLIALTDFATIPLFRIFGSMCFVFLFVV---PSFFCLCYIYLFMPETLGKSTLDIIHEMIDR
GLUT1 GG-----ASQSDKTPEELFHPL-------GADSQV
GLUT4 TPS----LLEQEVKPSTELEYL-------GPDEND
Y39E4B.5 GLHGSEHHLVNLDTPTLQIRPRMFSSNSDGHLRIY